Control of moving boundary parabolic partial differential equations (PDEs)

by

Mojtaba Izadi

A thesis submitted in partial fulfillment of the requirements for the degree of

Doctor of Philosophy

in

Process Control

Department of Chemical and Materials Engineering

University of Alberta

Abstract

Mathematical models of many transport processes are in the forms given by parabolic partial differential equations (PDEs). There are phenomena which may cause changes in shape and material properties of the process domain resulting in a moving boundary parabolic PDE model of the process. The focus of this thesis is to develop two control methods for parabolic PDE systems with time-dependent spatial domain.

The first approach uses the PDE backstepping tool for stabilization of a class of one-dimensional unstable parabolic PDEs. In this method, an integral transformation maps the PDE system to a suitably selected exponentially stable target system. The kernel of transformation is defined by the solution of the kernel PDE that is of higher-order in space. It is shown that the kernel PDE is well-posed and a numerical solution is provided with the error analysis to establish the accuracy. The stabilizing control law is shown in the form of state-feedback with the gain in terms of kernel function.

In addition, the backstepping-based observer design for state estimation of parabolic PDEs with time-dependent spatial domain is provided for a collocated boundary measurement and actuation. Specifically, the PDE system that describes the observation error dynamics is also transformed to the ex-

ponentially stable target system. The exponential stability of the closed-loop system with observer-based output-feedback controller is established by the use of a Lyapunov function. Finally, numerical solutions to the kernel PDEs and simulations are given to demonstrate successful stabilization of the unstable system.

Modal decomposition techniques have been extensively used for the order-reduction of dissipative systems. The second approach is the use of Karhunen-Loève (KL) decomposition to find the empirical eigenfunctions of the solution of moving boundary PDE systems. A mapping functional is obtained, which relates the evolution of the solution of the parabolic PDE with time-varying domain to a fixed reference configuration, while preserving space invariant properties of the initial solution ensemble. Subsequently, a low dimensional set of empirical eigenfunctions on the fixed domain is found and is mapped on the original time-varying domain resulting in the basis for the construction of the reduced-order model of the parabolic PDE system with time-varying domain. These modes are used as the basis set of functions in the Galerkin's method to find a reduced-order model for the optimal control design and state observation.

Preface

Chapter 2 of this thesis has been submitted for publication as M. Izadi, J. Abdollahi, S. Dubljevic, "PDE backstepping control of one-dimensional heat equation with time-varying domain," *Automatica*, 2013. I was responsible for the formulation, simulation and analysis as well as the manuscript composition. J. Abdollahi assisted in the mathematical formulation and S. Dubljevic was the supervisory author and was involved with concept formation and manuscript composition.

Chapter 3 of this thesis has been submitted for publication as M. Izadi, S. Dubljevic, "Backstepping output-feedback control of moving boundary parabolic PDEs," *European Journal of Control*, 2014. I was responsible for the formulation, simulation and analysis as well as the manuscript composition. S. Dubljevic was the supervisory author and was involved with concept formation and manuscript composition.

Chapter 4 of this thesis has been published as M. Izadi, S. Dubljevic, "Order-reduction of parabolic PDEs with time-varying domain using empirical eigenfunctions," *AIChE Journal*, vol. 59, issue 11, 4142-4150, 2013. I was responsible for the formulation, simulation and analysis as well as the manuscript composition. S. Dubljevic was the supervisory author and was

involved with concept formation and manuscript composition.

Chapter 5 of this thesis has been submitted for publication as M. Izadi, S. Dubljevic, "Low-order optimal regulation of parabolic PDEs with time-dependent domain," *AIChE Journal*, 2014. I was responsible for the formulation, simulation and analysis as well as the manuscript composition. S. Dubljevic was the supervisory author and was involved with concept formation and manuscript composition.

Acknowledgements

I would like to express my appreciation and thanks to my supervisor Dr. Stevan Dubljevic, who encouraged my research and guided me through all stages of this work. The many inspiring discussions we had over the years played an important role in shaping this research. I also want to thank my colleagues at Distributed Parameter Systems (DPS) Lab for their encouragement and helpful advice.

I acknowledge the continuous support and compassion of my in-laws, especially my mother in-law who devotedly accompanied us during a difficult stage of our life here in Canada.

Words cannot express how grateful I am to my parents for all of their encouragement, support, prayer, sacrifice and love. Without all of their patience and empathy, I would not have been able to start and finish this work. I would also like to thank my brothers for their support, specially Iman and Hossein who helped me not to feel homesick being thousands of kilometers away from home.

At the end I would like to express appreciation to my beloved wife Toktam for her unconditional understanding, love and faith. Her sacrifice, support and compassion was indeed what made this dissertation possible.

Contents

List of Figures

Chapter 1

Introduction

The states of many dynamical systems depend on spatial position in addition to time. These systems are called distributed parameter systems (DPSs) and they are mathematically described by partial differential equations (PDEs). The spatially distributed nature of their state is a distinguishing feature of process variables in contrast to those modelled by ordinary differential equations (ODEs) for which the process variables are represented by functions of time only.

Specifically, the models of transport-reaction processes are given as parabolic PDE systems in the science, engineering practice and industry. Examples of such processes includes tubular and plug-flow reactors in chemical engineering, fuel cells and modern batteries in energy management and power industry, phase transitions and thermal treatments in manufacturing, reservoir modeling in petroleum engineering and fabrication and processing of materials in material sciences.

1.1 Control methods of PDEs

Recent advancements in computing tools and numerical simulation of processes along with the available tools of classical and modern mathematical analysis have attracted many researchers in the control theory and engineering community to the analysis and control of DPSs.

Methods to control PDE systems fall into two categories (Ray, 1981): one common approach for control problems involving parabolic PDEs utilizes the so called early lumping methods through spatial discretization or modal decomposition to approximate the PDEs by finite-dimensional systems of ODEs, and subsequently enables the application of well developed finite-dimensional systems control theory. While this is straightforward to design a controller and readily implementable in industrial applications, there are limitations of the early lumping approach. The main disadvantage of early lumping technique is a mismatch in the dynamical properties of the original PDE and the approximated system. The reason is the intrinsic distributed nature of the PDE control problem which could not be completely accounted for through finite-dimensional approximations of the systems.

In the late lumping approach on the other hand, infinite-dimensional systems theory provided a viable methodology to capture the complete dynamics and analyze of the full PDE system for development of practical and implementable control schemes. It is only at the last stages of implementation or numerical integration that model equations are discretized. Specifically, the functional analytic formulation using semigroup theory and also PDE backstepping approach and related concepts have proven to be powerful tools for

system analysis and control design (Curtain and Zwart, 1995; Luo et al., 1999; Krstic and Smyshlyaev, 2008).

1.2 Moving boundary parabolic PDEs

The synthesis and treatment procedures in many processes such as chemical, petrochemical and pharmaceutical processes, lead to changes in the shape and material properties. This change can be characterized by transport phenomena associated with the material deformation, phase change mechanism, generation and consumption of chemical species through chemical reactions, heat and mass transfer. Mathematically, a broad collection of these processes are modelled by application of conservation laws and yield models in the form of moving boundary parabolic PDEs.

The occurrence of these changes introduce more complexities in the modelling, analysis and control of the process dynamics. It is established that parabolic PDE systems with time-varying domains are inherently nonautonomous (Kloeden et al., 2008) for which an analytic expression for the two-parameter semigroup describing the nonautonomous system behaviour can not be found in general. This fact prevents direct analysis and controller synthesis for such systems.

1.3 Thesis scope

Methods for control of linear parabolic PDEs have been extensively studied in the past and have mainly focused on process systems with fixed spatial domains

and boundary and/or distributed actuations. There are several contributions which formulate the solutions to nonautonomous parabolic PDE systems with fixed spatial domain, see the works of Lasiecka (1980); Pazy (1983); Acquistapace and Terreni (1987); Krstic and Smyshlyaev (2008); Meurer (2013). The objective of this research is the development of control method for parabolic PDE systems with time-dependent spatial domain. The formulations within this framework is provided using two general methodologies:

1. Falling in the category of late lumping methods, the first approach is the backstepping method emerging from nonlinear finite-dimensional control systems synthesis. In this formulation, a Volterra-type integral transformation is used to transform the PDE system to a suitably selected stable target system. The kernel of transformation is defined by the solution of the kernel PDE that is of higher-order in space, leading to a state-feedback control law.

2. Dissipative parabolic PDE systems have the property that the eigenspectrum of the spatial differential operator can be partitioned into a finite-dimensional slow subspace and the infinite-dimensional fast and stable complement. This fact implies that the dynamic behavior of such processes can be approximately described by finite-dimensional systems. The second approach in this research is an early lumping method which utilizes the well-known Karhunen-Loève (KL) decomposition to find the empirical eigenfunctions (modes) of an ensemble of solutions of the system. These modes are used as the basis set of functions in the Galerkin's method to find a reduced-order model for the optimal control design and

state observation.

The focus of this thesis is the feedback control of a class of moving boundary parabolic PDEs. The classes of problems considered are characterized by a variety of distinguishing features while the methodologies developed in this thesis are applicable to a broad number of different processes. In each case, the problem is formulated mathematically along with the required development and numerical realization within the following chapters.

Chapter 2 deals with the PDE backstepping boundary control of an unstable one-dimensional heat equation with time-varying domain. Initially, the stability of a selected target system is established by invoking a form of Poincaré inequality. Then, the PDE system is transformed to the target system through the Volterra-type integral transformation resulting the PDE describing the kernel of transformation. Subsequently, the well-posedness of the kernel PDE is given following a numerical solution which enables representation of explicit full state feedback control law. Appropriate simulations are given to demonstrate successful stabilization of the unstable system.

The formulation in Chapter 2 motivates the observer design of the boundary controlled parabolic PDEs with time-varying domain using backstepping approach which is the subject of Chapter 3. The PDE system that governs the observation error dynamics is transformed to an exponentially stable target system through the Volterra-type integral transformation to obtain the kernel PDE, which has time-dependent parameters and is defined on the 2D time-varying domain. Then, the separation principle is validated which provides the exponential stability of the observer-based output-feedback controller setup. Finally, numerical solutions to the kernel PDEs and various simulations are

given to demonstrate successful stabilization of the unstable system.

Chapter 4 provides a systematic approach to obtain a set of empirical eigenfunctions of a set of data given on a nontrivial spatially time-dependent domain that captures the most energy of the system's dynamics while preserving some physical invariant property. This methodology introduces transformations that map the time-varying domain of the PDE as well as the solutions to the PDE to a fixed reference configuration for all times during the evolution of the system. Then, KL decomposition is applied to extract a low-dimensional set of eigenfunctions. Different examples are provided in this Chapter to show the efficiency of the proposed methodology.

This method is extended in Chapter 5 for the boundary actuated PDE systems to be implementable for more realistic applications. The boundary input control problem is formulated as finding the appropriate state-space representation of the PDE system and the reduced order model is used to realize an observer and synthesize a linear optimal output tracking controller. Finally, numerical results are prepared for a 2D model of temperature distribution in the industrially relevant Czochralski (CZ) crystal growth process.

1.4 Czochralski crystal growth process

The prime example of relevant industrial transport process with time-varying domain is temperature distribution in Czochralski (CZ) crystal growth process which is the most important method for manufacturing large-scale crystals such as silicon, gallium arsenide, indium phosphide and cadmium telluride for use in the semiconductor, electronics and optics industry. In this method, the

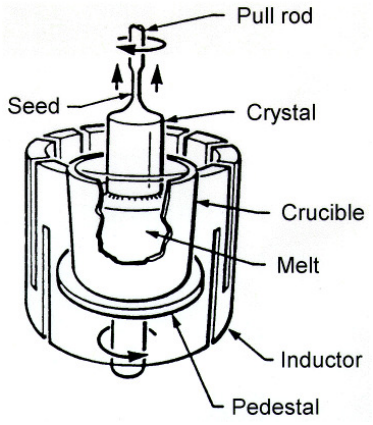

Figure 1.1: Czochralski crystal growth process setup (Sackinger et al. (1989) used with permission from John Wiley and Sons, Inc.)

crystal rod is pulled out vertically at the rate of a few centimeters per hour from the surface of a heated pool of melt contained in a crucible, as shown schematically in 1.1. The variation in thermal field in the grown crystal has significant effects on the crystalline structure and formation of micro-defects, which influence the quality and properties of the grown crystal.

The formulations in this research are typically applied to the CZ crystal temperature stabilization problem as an industrial application to utilize the theories provided.

References

Acquistapace, P., Terreni, B., 1987. A unified approach to abstract linear nonautonomous parabolic equations, in: Rendiconti del Seminario Matematico della Universita di Padova, pp. 47–107.

Curtain, R.F., Zwart, H., 1995. An introduction to infinite-dimensional linear systems theory. Springer-Verlag.

Kloeden, P., Marín-Rubio, P., Real, J., 2008. Pullback attractors for a semilinear heat equation in a non-cylindrical domain. Journal of Differential Equations 244, 2062–2090.

Krstic, M., Smyshlyaev, A., 2008. Boundary control of PDEs: A course on backstepping designs. SIAM, Philadelphia.

Lasiecka, I., 1980. Unified theory for abstract parabolic boundary problems–A semigroup approach. Applied Mathematics and Optimization 6, 287–333.

Luo, Z.H., Guo, B.Z., Morgül, Ö., 1999. Stability and stabilization of infinite-dimensional systems with applications. Springer.

Meurer, T., 2013. On the extended Luenberger-type observer for semilinear distributed-parameter systems. IEEE Transactions on Automatic Control 58, 1732–1743.

Pazy, A., 1983. Semigroups of linear operators and applications to partial differential equations. Springer-Verlag.

Ray, W.H., 1981. Advanced process control. McGraw-Hill New York.

Sackinger, P., Brown, R., Derby, J., 1989. A finite element method for analysis of fluid flow, heat transfer and free interfaces in Czochralski crystal growth. International journal for numerical methods in fluids 9, 453–492.

Chapter 2

PDE Backstepping Control of One-Dimensional Heat Equation with Time-Varying Domain

2.1 Introduction

The model of a wide variety of transport processes can be described in terms of partial differential equations (PDEs) based on the use of theoretical first-principles, experimental studies or system identification. In some applications, the shape of the PDE domain changes due to the phenomena such as phase change, generation and consumption of chemical species through the chemical reaction mechanism, heat and mass transfer. In addition to the time-dependent PDE parameters nature, the occurrence of these changes introduce more complexities in the modelling, analysis and control of the process dynamics. The representative case of theses systems is given by the Czochralski (CZ) crystal growth problem described by the one-dimensional heat parabolic PDE characterized by the presence of the grown crystal boundary velocity as a time-dependent coefficient associated with the first order advective transport

term (Derby et al., 1987).

Methods for control of linear parabolic PDEs with fixed spatial domain by boundary and/or distributed actuation setting are well established (Katō, 1995; Lasiecka, 1980; Curtain and Zwart, 1995; Krstic and Smyshlyaev, 2008). In this realm, there are several contributions which consider a time-varying parabolic PDE with fixed spatial domain (Acquistapace and Terreni, 1987; Pazy, 1983) where solutions to nonautonomous parabolic systems are formulated by two-parameter semigroups which resemble and inherit the properties of the standard one-parameter semigroup generated by time-invariant parabolic operators.

In a large number of cases an analytic expression for the two-parameter semigroup describing the nonautonomous system behaviour can not be found which prevents direct analysis and controller synthesis. In addition, only few results have been found when it comes to the study of parabolic PDEs with time-varying domain and these results are mainly centred on establishing existence and regularity properties of solution including the utilization of transformation, which maps the PDE onto a new time invariant spatial domain (Baconneau and Lunardi, 2004; Burdzy et al., 2004; Lunardi, 2004). Among few contributions along this line, Wang (1990) studied the stabilization and optimal control problem of such systems and later on, synthesized the linear optimal controller for thermal gradient regulation of crystal growth processes (Wang, 1995). To obtain a reduced-order model of nonlinear parabolic PDE systems with time-varying spatial domain, Armaou and Christofides (2001a) used a mathematical transformation to represent the PDE on a time-invariant spatial domain and applied Karhunen-Loève decomposition to find the set of

eigenfunctions on the fixed domain. In application, they used this approach in nonlinear feedback (Armaou and Christofides, 2001b) and robust (Armaou and Christofides, 2001c) control of one-dimensional reaction-diffusion systems based on the use of Galerkin's method.

In the last decade, the concept of backstepping emerging from nonlinear finite-dimensional control systems synthesis has been broadened to distributed parameter systems and provided a systematic approach for the boundary controlled linear parabolic PDEs. In the PDE backstepping methodology, a Volterra integral transformation is used to transform the PDE into a suitably selected stable target system. However, the kernel of this transformation is defined by the solution of the kernel PDE that is of a higher-order in space. Having the solution of the kernel PDE, the state-feedback control law which embeds desired transformation is obtained (Krstic and Smyshlyaev, 2008). The form of the hyperbolic kernel PDE is recognized in physics as Klein-Gordon equation. The powerful technique of backstepping synthesis provides a framework to handle a large class of distributed parameter systems controlled at the boundary. Namely, the stabilization of parabolic PDEs with spatially varying coefficients and advection-diffusion type of parabolic PDEs is easily realized by this method (Smyshlyaev and Krstic, 2004), as well as the boundary stabilization of the wave equation (Krstic et al., 2008). The introduction of the backstepping approach goes back to the works of Liu (2003) and Smyshlyaev and Krstic (2004) in the design of stabilizing state-feedback controllers, the reader is referred to Krstic and Smyshlyaev (2008) for the list.

The time-varying nature of PDE systems with moving boundaries introduces time-dependent parameters in the distributed system description. Along

this way, Smyshlyaev and Krstic (2005) studied the backstepping control of one-dimensional unstable heat equation with space-dependent diffusion and time-dependent reaction parameters. The form of the integral transformation obtained in the synthesis of an explicit controller that aims to stabilize parabolic PDEs with time-varying reaction term leads to the time-varying kernel PDE which is defined over fixed domain. In addition to this case, another instance of time-varying kernels incorporated in Volterra-type integral transformations is used in the stability analysis of time-varying input and state delays for nonlinear systems (Krstic, 2010; Bekiaris-Liberis and Krstic, 2012). Finally, the works of Meurer and Kugi (2009) on the design of a tracking controller and Meurer (2013) on the extension of Luenberger-type observers for semilinear PDEs broadened the PDE backstepping approach to the systems with time-dependent parameters.

The moving boundary aspect of the problem considered here suggests that not only time-varying parameters are associated with the characterization of the PDE system, but also the transformation kernel function is described on the time-varying domain. In the following, the formulation to the PDE backstepping boundary control of an unstable one-dimensional heat equation described on a domain with moving boundaries is presented. Initially, the stability of the target system by invoking a form of Poincaré inequality is established. Then, the PDE system is transformed to an exponentially stable target system through a Volterra-type integral transformation to obtain the PDE describing the transformation kernel. The time-varying kernel PDE defined on a moving boundary domain is analyzed and subsequently, a numerical solution is presented. An explicit full state feedback control law is provided

and appropriate simulations are given to demonstrate successful stabilization of the unstable system.

2.2 The control problem

Consider the linear one-dimensional parabolic PDE system of the form:

$$\partial_t \bar{x}(\xi, t) = \alpha \partial_\xi^2 \bar{x}(\xi, t) - \dot{h}(t) \partial_\xi \bar{x}(\xi, t) + \lambda_0 \bar{x}(\xi, t) \tag{2.1}$$

where $\bar{x}(\xi, t)$ is the state variable, $\mathbb{D}(t) = [0, h(t)] \subset \mathbb{R}$ is the time-varying domain of the definition of PDE, $\xi \in \mathbb{D}(t)$ is the spatial coordinate, $h(t) \in \mathbb{R}^+$ is the smooth time-dependent function describing the length of the domain, $\dot{h}(t)$ is its bounded time derivative, and $t \in [0, \infty)$ is the time. $\alpha > 0$ and λ_0 are process parameters and the advection term appearing in (2.1) is due to the moving boundaries of the PDE domain (Derby et al., 1987; Izadi and Dubljevic, 2013). The j-th partial derivative of a multivariable function ϕ with respect to the variable ζ is denoted by $\partial_\zeta^j \phi$, for the first derivative the superscript is dropped for simplicity. The temperature distribution in the crystal of the Czochralski process or the shrinkage of a catalyst in a chemical process are two typical examples of the models that can be approximated by this PDE system. Although this approach can be generalized for standard types of boundary conditions, the following boundary setting is assumed for the PDE system which is applicable to the temperature stabilization in the

Czochralski crystal growth process:

$$\begin{aligned} \bar{x}(0,t) &= 0 \\ \partial_\xi \bar{x}(h(t),t) &= U(t) \end{aligned} \tag{2.2}$$

Here $U(t)$ is the control applied at the boundary $\xi = h(t)$ to stabilize the system state.

In order to study the stability of the target system and specify boundedness and differentiability of the kernel function, the following assumption is required.

Assumption 2.1. The function $h(t)$ is analytic, or alternatively, there exists a real positive constant $\bar{D}$ such that for every non-negative integer j the following bound holds:

$$|\partial_t^j h(t)| \leq \bar{D}^{j+1} j! \tag{2.3}$$

In the subsequent sections, the plant (2.1-2.2) will be transformed to the target system:

$$\partial_t w(\xi,t) = \alpha \partial_\xi^2 w(\xi,t) - c w(\xi,t) \tag{2.4}$$

$$\begin{cases} w(0,t) = 0 \\ \partial_\xi w(h(t),t) = -\frac{\dot{h}(t)}{2\alpha} w(h(t),t) \end{cases} \tag{2.5}$$

with constant $c \geq 0$. The well-posedness of PDEs of this type with any initial condition $w(\xi,0) = w_0(\xi) \in L_2(\mathbb{D}(0))$ is shown by Ng and Dubljevic (2012). To show the stability of this system, first the following Lemma is required.

Lemma 2.1. *The following conservative form of Poincaré inequality holds for the time-varying space* $\mathbb{D}(t)$*:*

$$\int_0^{h(t)} w^2(\xi,t)d\xi \leq 2h(t)w^2(0,t) + 4h^2(t)\int_0^{h(t)} \left(\partial_\xi w(\xi,t)\right)^2 d\xi \tag{2.6}$$

Proof. We start with the following relation:

$$w^2(\xi,t) = -\partial_\xi[(h(t)-\xi)w^2(\xi,t)] + 2(h(t)-\xi)w(\xi,t)\partial_\xi w(\xi,t)$$

By integrating both sides of this equation with respect to ξ from 0 to $h(t)$ one obtains:

$$\begin{aligned}
&\int_0^{h(t)} w^2(\xi,t)d\xi = h(t)w^2(0,t) + 2\int_0^{h(t)} (h(t)-\xi)w(\xi,t)\partial_\xi w(\xi,t)d\xi \\
&\leq h(t)w^2(0,t) + \left(\int_0^{h(t)} w^2(\xi,t)d\xi\right)^{\frac{1}{2}} \left(\int_0^{h(t)} 4(h(t)-\xi)^2\left(\partial_\xi w(\xi,t)\right)^2 d\xi\right)^{\frac{1}{2}} \\
&\leq h(t)w^2(0,t) + \frac{1}{2}\int_0^{h(t)} w^2(\xi,t)d\xi + 2\int_0^{h(t)} (h(t)-\xi)^2\left(\partial_\xi w(\xi,t)\right)^2 d\xi
\end{aligned} \tag{2.7}$$

where Cauchy-Schwartz and Young's inequalities are used, respectively. One can readily show that these inequalities hold for the case of moving boundary space. The last integral in (2.7) is majorized by

$$\left[\sup_{\xi\in\mathbb{D}(t)} (h(t)-\xi)^2\right]\int_0^{h(t)} \left(\partial_\xi w(\xi,t)\right)^2 d\xi = h^2(t)\int_0^{h(t)} \left(\partial_\xi w(\xi,t)\right)^2 d\xi$$

resulting in the inequality (2.6). □

Now define the L_2-norm on the time-varying space $\mathbb{D}(t)$ as:

$$\|w(\xi,t)\| = \left(\int_0^{h(t)} w^2(\xi,t)d\xi\right)^{\frac{1}{2}} \tag{2.8}$$

The stability of the target system is explored in the following lemma.

Lemma 2.2. *The PDE system (2.4-2.5) is exponentially stable in the sense of the L_2-norm.*

Proof. Consider the Lyapunov function $V(t) = \frac{1}{2}\|w(\xi,t)\|^2$, its time derivative is:

$$\begin{aligned}
\dot{V}(t) &= \int_0^{h(t)} w(\xi,t)\partial_t w(\xi,t)d\xi + \frac{1}{2}\dot{h}(t)w^2(h(t),t) \\
&= \int_0^{h(t)} (\alpha w(\xi,t)\partial_\xi^2 w(\xi,t) - cw^2(\xi,t))d\xi + \frac{1}{2}\dot{h}(t)w^2(h(t),t) \\
&= -\alpha w(0,t)\partial_\xi w(0,t) + \alpha w(h(t),t)\partial_\xi w(h(t),t) \\
&\quad + \int_0^{h(t)} [-\alpha(\partial_\xi w(\xi,t))^2 - cw^2(\xi,t)]d\xi + \frac{1}{2}\dot{h}(t)w^2(h(t),t)
\end{aligned}$$

The first term vanishes from the first boundary condition in (2.5) and the second and last terms cancel out from the second boundary condition, leading to the following:

$$\dot{V}(t) = -\alpha\int_0^{h(t)} (\partial_\xi w(\xi,t))^2 d\xi - c\int_0^{h(t)} w^2(\xi,t)d\xi$$

Imposing bound $h(t) \leq \bar{D}$ from Assumption 2.1 to the Poincaré inequality

(2.6), one has:

$$\dot{V}(t) \leq -\left(\frac{\alpha}{4\bar{D}^2} + c\right) \int_0^{h(t)} w^2(\xi, t) d\xi = -\left(\frac{\alpha}{2\bar{D}^2} + 2c\right) V(t) \tag{2.9}$$

which implies the exponential stability of the target system in L_2-norm. □

2.3 Mathematical transformations

To eliminate advection term in (2.1), the transformation

$$\bar{x}(\xi, t) = x(\xi, t) e^{\int_0^\xi \frac{\dot{h}(t)}{2\alpha} d\eta} = x(\xi, t) e^{\frac{\xi \dot{h}(t)}{2\alpha}} \tag{2.10}$$

is used, which yields to the following plant

$$\partial_t x(\xi, t) = \alpha \partial_\xi^2 x(\xi, t) + \lambda(\xi, t) x(\xi, t) \tag{2.11}$$

$$\begin{cases} x(0, t) = 0 \\ \left[\partial_\xi x(h(t), t) + \frac{\dot{h}(t)}{2\alpha} x(h(t), t)\right] e^{\frac{h(t)\dot{h}(t)}{2\alpha}} = U(t) \end{cases} \tag{2.12}$$

where

$$\lambda(\xi, t) = \lambda_0 - \frac{\dot{h}^2(t) + 2\xi \ddot{h}(t)}{4\alpha}$$

Note that the stability of $x(\xi, t)$ in the L_2-norm implies the stability of $\bar{x}(\xi, t)$ since the norm $\|e^{\frac{\xi \dot{h}(t)}{2\alpha}}\|$ is bounded for all t.

The moving boundary characteristic of the PDE system imposes the use of the Volterra integral transformation given as follows:

$$w(\xi, t) = x(\xi, t) - \int_0^\xi k(\xi, \eta, t) x(\eta, t) d\eta \tag{2.13}$$

which maps (2.11-2.12) into the stable target system (2.4-2.5) with a free parameter c to manipulate the system's response. Substitution of (2.13) into (2.4-2.5) and use of (2.11-2.12) yields to the following time-varying PDE for the kernel function $k(\xi, \eta, t)$:

$$\partial_t k(\xi,\eta,t) = \alpha(\partial_\xi^2 k(\xi,\eta,t) - \partial_\eta^2 k(\xi,\eta,t)) - (\lambda(\eta,t)+c)k(\xi,\eta,t) \tag{2.14}$$

$$\begin{cases} k(\xi,0,t) = 0 \\ k(\xi,\xi,t) = -\frac{1}{2\alpha}\int_0^\xi (\lambda(\eta,t)+c)d\eta \end{cases} \tag{2.15}$$

defined on the time-varying domain $\mathbb{S}(t) = \{(\xi,\eta)|0 \leq \eta \leq \xi \leq h(t)\} \subset \mathbb{R}^2$ shown in Fig. 2.1a. Hence, the control problem (2.1-2.2) is now reduced to finding the solution of (2.14-2.15). Also, the control action can be found in the form of a state-feedback as:

$$\begin{aligned} U(t) = \Bigg(\int_0^{h(t)} \left[\frac{\dot{h}(t)}{2\alpha} k(h(t),\eta,t) + \partial_\xi k(h(t),\eta,t) \right] x(\eta,t) d\eta \\ + k(h(t),h(t),t)x(h(t),t) \Bigg) e^{\frac{h(t)\dot{h}(t)}{2\alpha}} \end{aligned} \tag{2.16}$$

Finding the solution to (2.14-2.15) on the time-dependent domain $\mathbb{S}(t)$ is not straight forward. However, the following transformation will map $\mathbb{S}(t)$ to the fixed domain $\bar{\mathbb{S}} = \{(\rho,\sigma)|0 \leq \sigma \leq \rho \leq 2-\sigma\} \subset \mathbb{R}^2$ (see Fig. 2.1b):

$$\rho = \frac{\xi+\eta}{h(t)}, \quad \sigma = \frac{\xi-\eta}{h(t)} \tag{2.17}$$

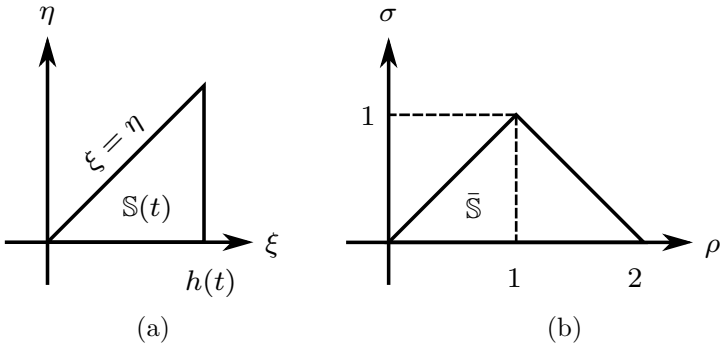

Figure 2.1: (a) Time-dependent domain $\mathbb{S}(t)$ of the kernel function $k(\xi, \eta, t)$ and (b) fixed domain $\bar{\mathbb{S}}$ of the kernel function $k(\rho, \sigma, t)$.

Using (2.17), the kernel PDE for $k(\rho, \sigma, t)$ takes the form:

$$\partial_t k(\rho,\sigma,t) = \frac{4\alpha}{h^2(t)}\partial_\rho\partial_\sigma k(\rho,\sigma,t) + \frac{\dot{h}(t)}{h(t)}\left[\rho\partial_\rho k(\rho,\sigma,t) + \sigma\partial_\sigma k(\rho,\sigma,t)\right] - \bar{\lambda}(\rho,\sigma,t)k(\rho,\sigma,t) \tag{2.18}$$

$$\begin{cases} k(\rho,\rho,t) = 0 \\ k(\rho,0,t) = f(\rho,t) \end{cases} \tag{2.19}$$

where

$$\bar{\lambda}(\rho,\sigma,t) = \lambda((\rho-\sigma)\frac{h(t)}{2},t) + c = -\frac{\dot{h}^2(t) + (\rho-\sigma)h(t)\ddot{h}(t)}{4\alpha} + \lambda_0 + c \tag{2.20}$$

$$f(\rho,t) = \frac{\rho h(t)}{4\alpha}\left[\frac{2\dot{h}^2(t) + \rho h(t)\ddot{h}(t)}{8\alpha} - (\lambda_0 + c)\right] \tag{2.21}$$

2.4 Analysis of the kernel PDE

In general, the solution to the kernel PDE (2.18-2.19) is found by means of successive integration. Although this method is computationally rather expen-

sive except for special cases, it is a useful tool to analyze the well-posedness of the kernel PDE. To follow this method, integrate (2.18) with respect to σ from 0 to σ and then with respect to ρ from σ to ρ and use boundary conditions (2.19) and integration by-parts for the terms with the first-order derivative to transform the kernel PDE (2.18-2.19) into the following integral equation:

$$\begin{aligned}
&\int_\sigma^\rho \int_0^\sigma \left[\partial_t k(\mu,\nu,t) + \left(2\frac{\dot{h}(t)}{h(t)} + \bar{\lambda}(\mu,\nu,t)\right) k(\mu,\nu,t)\right] d\nu d\mu \\
&- \frac{\dot{h}(t)}{h(t)}\left(\rho\int_0^\sigma k(\rho,\nu,t)d\nu + \sigma\int_\sigma^\rho k(\mu,\sigma,t)d\mu\right) \\
&- \frac{4\alpha}{h^2(t)}\left[k(\rho,\sigma,t) - f(\rho,t) + f(\sigma,t)\right] = 0
\end{aligned} \tag{2.22}$$

that is rewritten as:

$$k(\rho,\sigma,t) = K_1(\rho,\sigma,t) + \mathcal{G}k(\rho,\sigma,t) \tag{2.23}$$

where

$$\begin{aligned}
K_1(\rho,\sigma,t) =& f(\rho,t) - f(\sigma,t) \\
\mathcal{G}k(\rho,\sigma,t) =& \frac{h^2(t)}{4\alpha}\int_\sigma^\rho\int_0^\sigma \partial_t k(\mu,\nu,t)d\nu d\mu \\
&+ \int_\sigma^\rho\int_0^\sigma \left(\frac{h(t)\dot{h}(t)}{2\alpha} + \frac{h^2(t)\bar{\lambda}(\mu,\nu,t)}{4\alpha}\right) k(\mu,\nu,t)d\nu d\mu \\
&- \frac{h(t)\dot{h}(t)}{4\alpha}\left(\rho\int_0^\sigma k(\rho,\nu,t)d\nu + \sigma\int_\sigma^\rho k(\mu,\sigma,t)d\mu\right)
\end{aligned} \tag{2.24}$$

The method of successive integration suggests that the solution to the integral equation (2.22) is given by the series

$$k(\rho,\sigma,t)=\sum_{n=1}^{\infty}K_n(\rho,\sigma,t) \tag{2.25}$$

$$K_{n+1}(\rho,\sigma,t)=\mathcal{G}K_n(\rho,\sigma,t) \tag{2.26}$$

with $K_1(\rho,\sigma,t)$ given in (2.24). The convergence of this series and hence, the existence of a solution for (2.22) is given by the following theorem:

Theorem 2.1. *The j-th time-derivative of K_n is bounded by*

$$\sup_t\left|\partial_t^j K_n(\rho,\sigma,t)\right|\leq\frac{3^{n+1}\gamma_{j,n}D^{j+2n}(j+n-1)!}{(n-1)!(n-1)!n!}(\rho\sigma)^{n-1} \tag{2.27}$$

where $D\geq 1$ is a real constant and

$$\gamma_{j,n}=\frac{\Gamma(\frac{4n+j}{3}+1)}{\Gamma(\frac{n+j}{3}+1)} \tag{2.28}$$

with $\Gamma(\zeta)$ being the gamma function. Moreover, the series (2.25) is absolutely convergent.

Proof. The proof to this theorem follows the same methodology as given by Meurer and Kugi (2009) along with Assumption 2.1 from which it is concluded that all the functions $\frac{h(t)\dot{h}^2(t)}{16\alpha^2}$, $\frac{h^2(t)\ddot{h}(t)}{32\alpha^2}$, $\frac{h(t)(\lambda_0+c)}{4\alpha}$, $\frac{h^2(t)}{4\alpha}$, $\frac{h(t)\dot{h}(t)}{2\alpha}+\frac{h^2(t)\bar{\lambda}(\rho,\sigma,t)}{4\alpha}$ are analytic as well. Hence, there exists real constant $D\geq 1$ such that the j-th time-derivative of these functions is bounded by $D^{j+1}j!$ for $j=0,1,2,\cdots$.

Because of the appearance of the time-derivative of $K_n(\rho,\sigma,t)$, the convergence analysis of series (2.25) requires to find a bound for $\left|\partial_t^j K_n(\rho,\sigma,t)\right|$,

which is given in (2.27) and is proved here by induction. For $n = 1$:

$$\begin{aligned}
\sup_t \left|\partial_t^j K_1(\rho,\sigma,t)\right| &= \sup_t \left|\partial_t^j \left[f(\rho,t) - f(\sigma,t)\right]\right| \\
&= \sup_t \left|\partial_t^j \left[\frac{h(t)\dot{h}^2(t)}{16\alpha^2}(\rho-\sigma) + \frac{h^2(t)\ddot{h}(t)}{32\alpha^2}(\rho^2-\sigma^2) - \frac{h(t)(\lambda_0+c)}{4\alpha}(\rho-\sigma)\right]\right| \\
&\leq D^{j+1} j! \left(|\rho-\sigma| + \left|\rho^2-\sigma^2\right| + |\rho-\sigma|\right) \leq 8D^{j+1} j! \leq 9\gamma_{j,1} D^{j+2} j!
\end{aligned}$$

which is equal to the right-hand side of (2.27) for $n = 1$. Assuming (2.27) holds for all $n = 1, 2, \cdots, N$, the upper bound of $\left|\partial_t^j K_{N+1}(\rho,\sigma,t)\right|$ can be determined as

$$\begin{aligned}
\sup_t \left|\partial_t^j K_{N+1}(\rho,\sigma,t)\right| &\leq \sup_t \left|\partial_t^j \mathcal{G} K_N(\rho,\sigma,t)\right| \\
&\leq \sup_t \left|\sum_{i=0}^{j} \binom{j}{i} \partial_t^{j-i} \left(\frac{h^2(t)}{4\alpha}\right) \int_\sigma^\rho \int_0^\sigma \partial_t^{i+1} K_N(\mu,\nu,t) d\nu d\mu\right| + \\
&\quad \sup_t \left|\sum_{i=0}^{j} \binom{j}{i} \int_\sigma^\rho \int_0^\sigma \partial_t^{j-i} \left(\frac{h(t)\dot{h}(t)}{2\alpha} + \frac{h^2(t)\bar{\lambda}(\mu,\nu,t)}{4\alpha}\right) \partial_t^i K_N(\mu,\nu,t) d\nu d\mu\right| + \\
&\quad \sup_t \left|\sum_{i=0}^{j} \binom{j}{i} \partial_t^{j-i} \left(\frac{h(t)\dot{h}(t)}{4\alpha}\right) \rho \int_0^\sigma \partial_t^i K_N(\rho,\nu,t) d\nu\right| + \\
&\quad \sup_t \left|\sum_{i=0}^{j} \binom{j}{i} \partial_t^{j-i} \left(\frac{h(t)\dot{h}(t)}{4\alpha}\right) \sigma \int_\sigma^\rho \partial_t^i K_N(\mu,\sigma,t) d\mu\right|
\end{aligned}$$

$$
\begin{aligned}
&\leq \sum_{i=0}^{j} \binom{j}{i} D^{j-i+1}(j-i)! \frac{3^{N+1}\gamma_{i+1,N} D^{i+2N+1}(i+N)!}{(N-1)!(N-1)!N!} \left| \int_\sigma^\rho \int_0^\sigma (\mu\nu)^{N-1} d\nu d\mu \right| + \\
&\quad \sum_{i=0}^{j} \binom{j}{i} D^{j-i+1}(j-i)! \frac{3^{N+1}\gamma_{i,N} D^{i+2N}(i+N-1)!}{(N-1)!(N-1)!N!} \left| \int_\sigma^\rho \int_0^\sigma (\mu\nu)^{N-1} d\nu d\mu \right| + \\
&\quad \sum_{i=0}^{j} \binom{j}{i} D^{j-i+1}(j-i)! \frac{3^{N+1}\gamma_{i,N} D^{i+2N}(i+N-1)!}{(N-1)!(N-1)!N!} \left| \rho \int_0^\sigma (\rho\nu)^{N-1} d\nu \right| + \\
&\quad \sum_{i=0}^{j} \binom{j}{i} D^{j-i+1}(j-i)! \frac{3^{N+1}\gamma_{i,N} D^{i+2N}(i+N-1)!}{(N-1)!(N-1)!N!} \left| \sigma \int_\sigma^\rho (\mu\sigma)^{N-1} d\mu \right| \\
&\leq \frac{3^{N+1}\gamma_{j+1,N} D^{j+2N+2}}{(N-1)!(N-1)!N!} \frac{(\rho\sigma)^N}{N^2} \sum_{i=0}^{j} \binom{j}{i} (j-i)!(i+N)! + \\
&\quad \frac{3^{N+1}\gamma_{j,N} D^{j+2N+1}}{(N-1)!(N-1)!N!} \frac{(\rho\sigma)^N}{N^2} \sum_{i=0}^{j} \binom{j}{i} (j-i)!(i+N-1)! + \\
&\quad \frac{3^{N+1}\gamma_{j,N} D^{j+2N+1}}{(N-1)!(N-1)!N!} \frac{(\rho\sigma)^N}{N} \sum_{i=0}^{j} \binom{j}{i} (j-i)!(i+N-1)! + \\
&\quad \frac{3^{N+1}\gamma_{j,N} D^{j+2N+1}}{(N-1)!(N-1)!N!} \frac{(\rho\sigma)^N}{N} \sum_{i=0}^{j} \binom{j}{i} (j-i)!(i+N-1)! \\
&\leq \frac{3^{N+1} D^{j+2N+2}(j+N)!}{(N-1)!N!N!} (\rho\sigma)^N \left[\frac{\gamma_{j+1,N}(j+N+1)}{N(N+1)} + \frac{\gamma_{j,N}}{N^2} + 2\frac{\gamma_{j,N}}{N} \right] \\
&\leq \frac{3^{N+1} D^{j+2N+2}(j+N)!}{N!N!N!} (\rho\sigma)^N \left[\frac{\gamma_{j+1,N}(j+N+1)}{N+1} + 3\gamma_{j+1,N} \right] \\
&= \frac{3^{N+1} D^{j+2N+2}(j+N)!}{N!N!(N+1)!} (\rho\sigma)^N \gamma_{j+1,N}(j+4N+4) \\
&= \frac{3^{N+2}\gamma_{j,N+1} D^{j+2N+2}(j+N)!}{N!N!(N+1)!} (\rho\sigma)^N
\end{aligned}
$$

which is identical to right-hand side of (2.27) for $n = N + 1$. This completes the proof of (2.27). In this sequence of inequalities, the following relations are

used for $(\rho,\sigma)\in\bar{\mathbb{S}}$, $j=0,1,2,\cdots$ and $n=1,2,\cdots$:

$$|\rho-\sigma|\le 2 \text{ and } \left|\rho^2-\sigma^2\right|\le 4$$
$$\int_\sigma^\rho\int_0^\sigma(\mu\nu)^{n-1}d\nu d\mu=\frac{\sigma^n(\rho^n-\sigma^n)}{n^2}\le\frac{(\rho\sigma)^n}{n^2}$$
$$\rho\int_0^\sigma(\rho\nu)^{n-1}d\nu=\frac{(\rho\sigma)^n}{n}$$
$$\sigma\int_\sigma^\rho(\mu\sigma)^{n-1}d\mu=\frac{\sigma^n(\rho^n-\sigma^n)}{n}\le\frac{(\rho\sigma)^n}{n}$$
$$\gamma_{j,1}=\frac{j+1}{3}+1\ge 1$$
$$\gamma_{i,n}\le\gamma_{j,n}\text{ for }i\le j$$
$$\gamma_{j+1,n}(4n+j+4)=3\frac{\Gamma(\frac{4n+j+1}{3}+1)}{\Gamma(\frac{n+j+1}{3}+1)}\frac{(4n+j+4)}{3}=3\frac{\Gamma(\frac{4n+j+4}{3}+1)}{\Gamma(\frac{n+j+1}{3}+1)}=3\gamma_{j,n+1}$$
$$\sum_{i=0}^{j}\binom{j}{i}(j-i)!(i+n)!=\frac{(j+n+1)!}{n+1}$$

Let $j=0$ in (2.27) to find $\sup_t|K_n(\rho,\sigma,t)|\le 3\frac{\left(3D^2\right)^n\gamma_{0,n}}{(n-1)!n!}(\rho\sigma)^{n-1}$ which provides the following bound for series (2.25):

$$|k(\rho,\sigma,t)|\le\sum_{n=1}^{\infty}|K_n(\rho,\sigma,t)|\le\sum_{n=1}^{\infty}3a_n(\rho,\sigma)$$

with $a_n(\rho,\sigma)=\frac{\left(3D^2\right)^n\gamma_{0,n}}{(n-1)!n!}(\rho\sigma)^{n-1}$. Hence, the ratio $|a_{n+1}(\rho,\sigma)/a_n(\rho,\sigma)|$ is

$$\frac{3D^2\rho\sigma}{n(n+1)}\frac{\gamma_{0,n+1}}{\gamma_{0,n}}$$

Having the limit

$$\lim_{n\to\infty}\frac{\gamma_{0,n+1}}{\gamma_{0,n}}=\lim_{n\to\infty}\frac{\Gamma\left(\frac{4n}{3}+\frac{7}{3}\right)\Gamma\left(\frac{n}{3}+1\right)}{\Gamma\left(\frac{4n}{3}+1\right)\Gamma\left(\frac{n}{3}+\frac{4}{3}\right)}=\lim_{n\to\infty}\frac{\Gamma\left(\frac{4n}{3}\right)\left(\frac{4n}{3}\right)^{\frac{7}{3}}\Gamma\left(\frac{n}{3}\right)\frac{n}{3}}{\Gamma\left(\frac{4n}{3}\right)\frac{4n}{3}\Gamma\left(\frac{n}{3}\right)\left(\frac{n}{3}\right)^{\frac{4}{3}}}$$
$$=\lim_{n\to\infty}\left(\frac{4n}{3}\right)^{\frac{4}{3}}\left(\frac{n}{3}\right)^{\frac{-1}{3}}=\lim_{n\to\infty}\frac{4\sqrt[3]{4}}{3}n$$

the series $\sum_{n=1}^{\infty}a_n(\rho,\sigma)$ is convergent since

$$\lim_{n\to\infty}|a_{n+1}(\rho,\sigma)/a_n(\rho,\sigma)|=\lim_{n\to\infty}\frac{4\sqrt[3]{4}D^2\rho\sigma}{n+1}=0<1$$

Therefore the series (2.25) is absolutely convergent by comparison. □

Note that $K_n(\rho,\sigma,t)$ is $C^2(\bar{\mathbb{S}}\times[0,\infty))$ which follows from (2.24, 2.26). Therefore, $k(\rho,\sigma,t)$ and $k(\xi,\eta,t)$ are also $C^2(\bar{\mathbb{S}}\times[0,\infty))$ and $C^2(\mathbb{S}\times[0,\infty))$, respectively, the latter is the result of the invertibility of transformation (2.17).

Lemma 2.3. *The control (2.16) given by the solution of (2.14-2.15) stabilizes the PDE system (2.11-2.12) in the L_2-norm.*

Proof. Consider the inverse backstepping transformation in terms of

$$x(\xi,t)=w(\xi,t)+\int_0^{\xi}q(\xi,\eta,t)w(\eta,t)d\eta \tag{2.29}$$

with the kernel $q(\xi,\eta,t)$. Substitution of (2.29) into (2.11-2.12) and use of

(2.4-2.5) results in the following PDE for the inverse kernel function:

$$\partial_t q(\xi, y, t) = \alpha(\partial_\xi^2 q(\xi, \eta, t) - \partial_\eta^2 q(\xi, \eta, t)) + (\lambda(\xi, t) + c)q(\xi, \eta, t) \tag{2.30}$$

$$\begin{cases} q(\xi, 0, t) = 0 \\ q(\xi, \xi, t) = -\frac{1}{2\alpha} \int_0^\xi (\lambda(\eta, t) + c) d\eta \end{cases} \tag{2.31}$$

This PDE is similar to (2.14-2.15) and Theorem 2.1 shows the existence of a solution. Hence, the transformation (2.13) is invertible and the stability of the target system (2.4-2.5) implies the stability of the closed-loop system (2.11-2.12). □

Theorem 2.2. *For any initial condition $x(\xi, 0) = x_0(\xi) \in L_2(\mathbb{D}(0))$ that satisfies (2.12) with $U(t)$ given in (2.16) for $t = 0$, the PDE system (2.11-2.12) with boundary control (2.16) has a unique solution.*

The proof to this theorem is given by Ng and Dubljevic (2012) where the closed-loop system (2.11-2.12) is represented as a nonautonomous parabolic evolution system with solutions given by a two-parameter evolution operator, following the boundedness and continuity of kernel function $k(\xi, \eta, t)$.

2.5 Numerical method

To find an approximate solution to the integral equation (2.22), the numerical method introduced in Jadachowski et al. (2012) is used. This approach is computationally tractable and is based on the approximation of integrals by the use of a composite trapezoidal rule. To this end, the triangular spatial domain is discretized in N^2 computational points on an equally-spaced square

grid as shown in Fig. 2.2. Hence, each continuous function $g(\rho, \sigma, t)$ is discretized and denoted by $g_{i,j}(t)$ at the coordinate (ρ_i, σ_j) or simply at the point $(i, j) \in \{(m, n) | 1 \leq n \leq m \leq 2N - n\} \subset \mathbb{N}^2$. Now, the integrals in (2.22) are approximated by using discrete values of their integrands evaluated at grid points through the application of the composite trapezoidal rule as:

$$\int_{\sigma_J}^{\rho_I} \int_{0}^{\sigma_I} g_{I,J}(t) d\nu d\mu \approx \frac{\Delta^2}{4} \sum_{i=J}^{I-1} \sum_{j=1}^{J-1} \left[g_{i,j}(t) + g_{i+1,j}(t) + g_{i,j+1}(t) + g_{i+1,j+1}(t) \right] \tag{2.32}$$

where $\Delta = 1/(N-1)$. To discretize (2.22), the integrals are replaced by composite trapezoidal rule as in (2.32) to obtain:

$$\begin{aligned}
&\frac{\Delta^2}{4} \sum_{i=J}^{I-1} \sum_{j=1}^{J-1} \left(\dot{\bar{k}}_{i,j} + \dot{\bar{k}}_{i+1,j} + \dot{\bar{k}}_{i,j+1} + \dot{\bar{k}}_{i+1,j+1} \right) \\
&+ \frac{\Delta^2}{4} \left(2 \frac{\dot{h}(t)}{h(t)} + c \right) \sum_{i=J}^{I-1} \sum_{j=1}^{J-1} \left(\bar{k}_{i,j} + \bar{k}_{i+1,j} + \bar{k}_{i,j+1} + \bar{k}_{i+1,j+1} \right) \\
&+ \frac{\Delta^2}{4} \sum_{i=J}^{I-1} \sum_{j=1}^{J-1} \left(\bar{\lambda}_{i,j} \bar{k}_{i,j} + \bar{\lambda}_{i+1,j} \bar{k}_{i+1,j} + \bar{\lambda}_{i,j+1} \bar{k}_{i,j+1} + \bar{\lambda}_{i+1,j+1} \bar{k}_{i+1,j+1} \right) \\
&- \frac{\Delta}{2} \frac{\dot{h}(t)}{h(t)} \left[\rho_I \sum_{j=1}^{J-1} \left(\bar{k}_{I,j} + \bar{k}_{I,j+1} \right) + \sigma_J \sum_{i=J}^{I-1} \left(\bar{k}_{i,J} + \bar{k}_{i+1,J} \right) \right] \\
&- \frac{4\alpha}{h^2(t)} \left[\bar{k}_{I,J} - f(\rho_I, t) + f(\sigma_J, t) \right] = 0
\end{aligned} \tag{2.33}$$

For each pair (I, J) with unknown $\bar{k}_{I,J}$ (i.e., the points that are not on the boundaries with known boundary conditions), (2.33) relates the kernel function and its time derivative of computational points in the form of an ODE. The new indexing $r = (2N - j)(j - 1) + i$ will vectorize the array $\bar{k}_{i,j}$ into κ_r and the set of $N^2 - 3N + 2$ ODE's can be written as the following

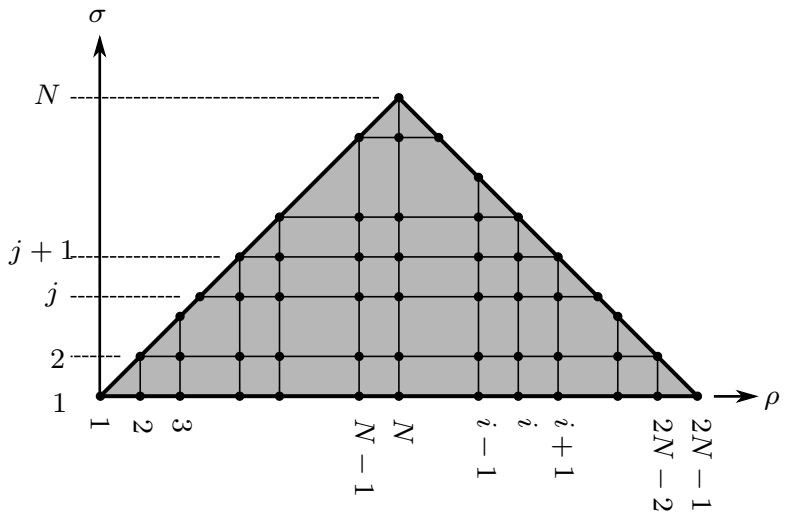

Figure 2.2: Discretization of the kernel PDE domain.

point-wise equation:

$$A\dot{\kappa}(t) + B(t)\kappa(t) + H(t) = 0 \tag{2.34}$$

where $H_r(t)$ is calculated from the values of the kernel function on boundaries with known boundary conditions as well as the term $\frac{4\alpha}{h^2(t)}\left[f(\rho_I, t) - f(\sigma_J, t)\right]$. Note that matrices A and $B(t)$ in (2.34) are in the lower triangular form. The initial condition $\kappa_0 = \kappa(0)$ for this equation is chosen as the stationary solution at $t = 0$:

$$\kappa(0) = -B(0)^{-1}H(0) \tag{2.35}$$

Equations (2.34-2.35) form an initial-value problem (IVP) as a set of linear time-varying ordinary differential equations and can be solved efficiently using available numerical methods. The over bar in $\bar{k}_{i,j}(t)$ indicates the approximated value of the kernel function.

2.6 Simulation results

For the special case $\alpha = 1, c = 0$ and fixed domain $h(t) = 1$, there is a closed-form solution for the kernel function (Krstic and Smyshlyaev, 2008) as:

$$k(\xi, \eta) = -\lambda_0 \eta \frac{I_1(\sqrt{\lambda_0(\xi^2 - \eta^2)})}{\sqrt{\lambda_0(\xi^2 - \eta^2)}} \tag{2.36}$$

where $I_1(\zeta)$ is the first-order modified Bessel function of the first kind. This solution can be used to validate and assess the accuracy of the numerical method used to solve the kernel PDE. Fig. 2.3 shows the approximated kernel function and associated numerical error of the solution as well as the numerical approximation of the kernel function $k(1, 0.5)$ and its derivative $\partial_\xi k(1, 0.5)$ for $\lambda_0 = 20$. The differentiation of the kernel function is performed by finite differencing and since the derivative term appears in the expression for control (2.16), it is included in the error analysis.

We choose the discretization associated with $N = 75$ for the error of order 0.01 for the kernel function derivative in the following simulations. The numerical approximation of the time-varying kernel function is used to stabilize the system given by (2.1-2.2) with $\alpha = 1$ and $\lambda_0 = 20$ on the time-varying domain $\mathbb{D}(t)$ shown in Fig. 2.4a. For these process parameters, the PDE system is unstable as depicted by the evolution of the norm of the system as given in Fig. 2.4b.

The evolution of approximate solution to the kernel PDE on the (ρ, σ)-domain for $c = 0$ is shown in Fig. 2.5. Figure 2.6a shows a closed-loop response of the system as the evolution of the state for an arbitrary chosen initial condition. Finally, control input and evolution of L_2-norm of the state

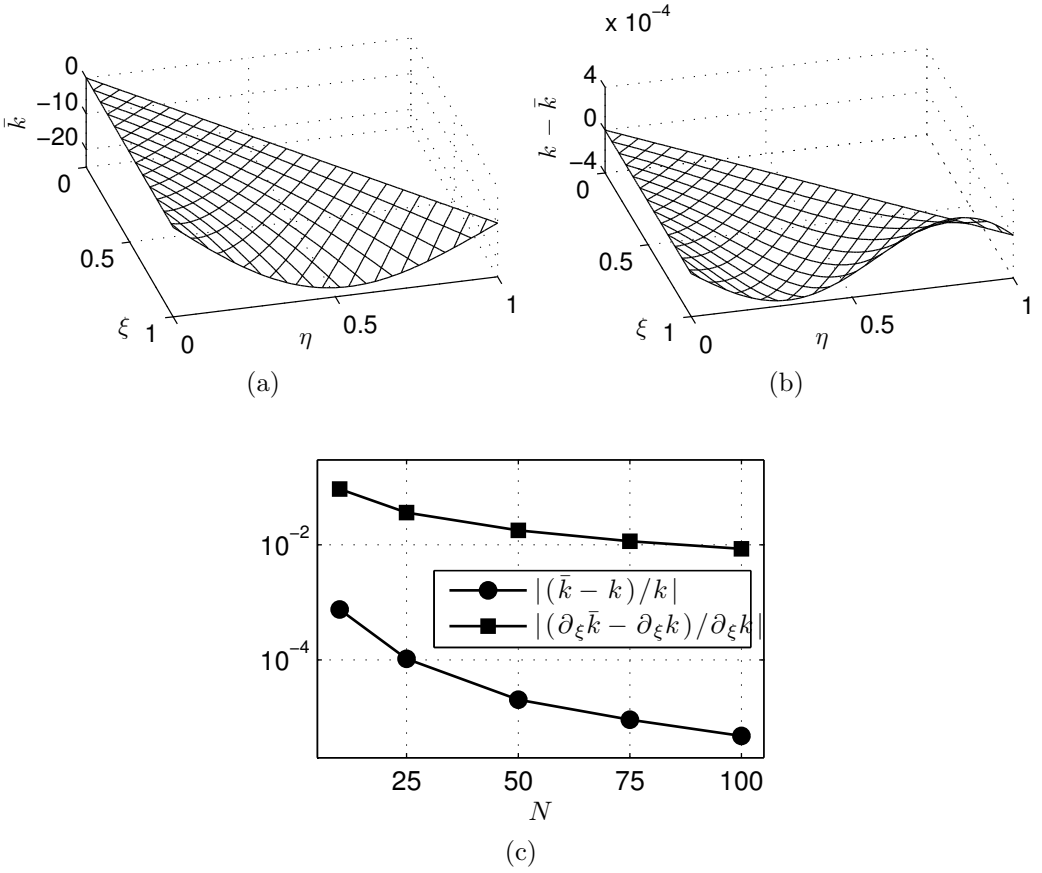

Figure 2.3: (a) Approximated solution to the kernel PDE for $h(t) = 1$ and (b) associated approximation error. (c) Numerical error of the kernel function and its derivative at $(\xi, \eta) = (1, 0.5)$ on the actuation boundary for different discretization levels defined by N.

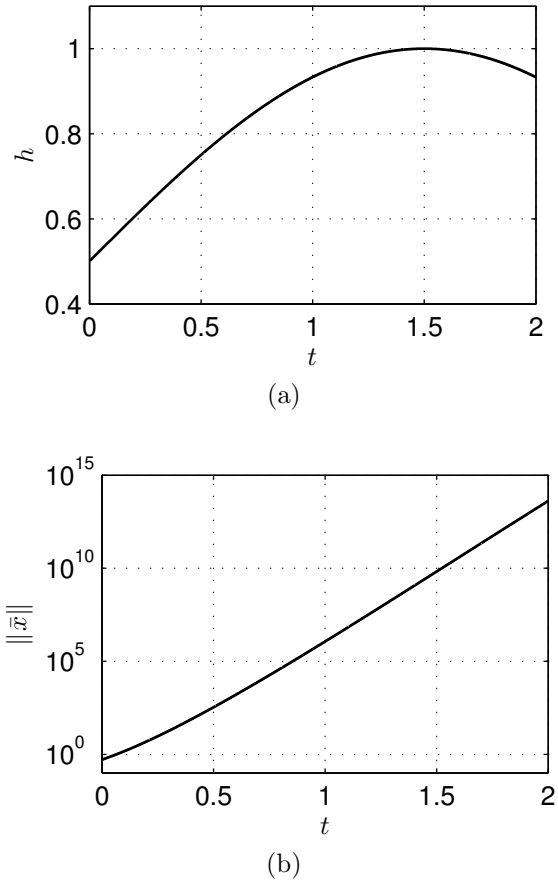

Figure 2.4: (a) Length $h(t)$ of the time-varying domain of the PDE system. (b) Norm of the state of the uncontrolled system for the given parameters.

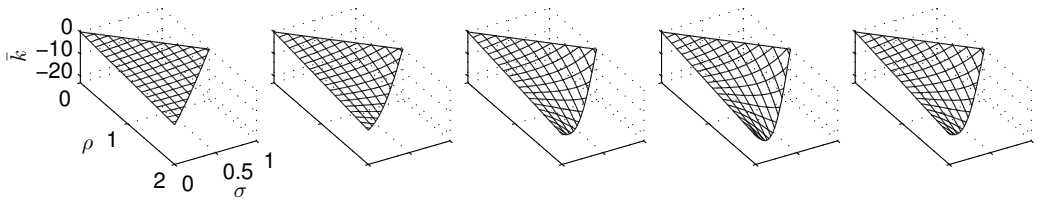

Figure 2.5: Approximated kernel function $\bar{k}(\rho, \sigma, t)$ at $t = 0, 0.5, 1, 1.5$ and 2.

are shown in Fig. 2.6b. The stabilization of the unstable PDE system is well provided in the simulations.

2.7 Summary

The PDE backstepping boundary control synthesis of one-dimensional heat equation on a time-varying domain is formulated in this Chapter. The PDE system is transformed to an exponentially stable target system through the invertible Volterra-type integral transformation resulting in the two-dimensional time-varying PDE with time-dependant domain describing the transformation kernel. Then, a numerical solution to the kernel PDE is provided and simulated to demonstrate stabilization of the unstable system with time-varying domain.

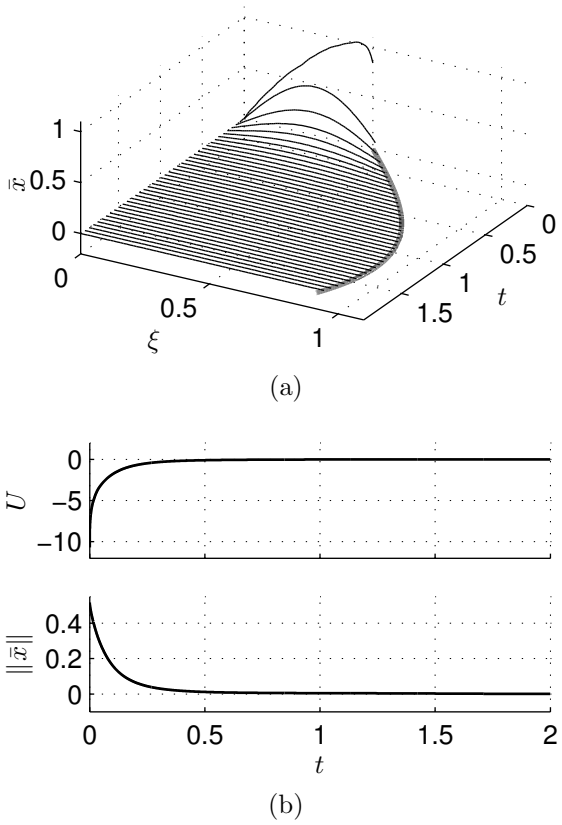

Figure 2.6: (a) Closed-loop profile of $\bar{x}(\xi, t)$. The thick grey line shows evolution of domain. (b) Control input and evolution of the norm of state.

References

Acquistapace, P., Terreni, B., 1987. A unified approach to abstract linear nonautonomous parabolic equations, in: Rendiconti del Seminario Matematico della Universita di Padova, pp. 47–107.

Armaou, A., Christofides, P.D., 2001a. Computation of empirical eigenfunctions and order reduction for nonlinear parabolic PDE systems with time-dependent spatial domains. Nonlinear Analysis: Theory, Methods and Applications 47, 2869–2874.

Armaou, A., Christofides, P.D., 2001b. Finite-dimensional control of nonlinear parabolic PDE systems with time-dependent spatial domains using empirical eigenfunctions. Applied Mathematics and Computer Science 11, 287–318.

Armaou, A., Christofides, P.D., 2001c. Robust control of parabolic PDE systems with time-dependent spatial domains. Automatica 37, 61–69.

Baconneau, O., Lunardi, A., 2004. Smooth solutions to a class of free boundary parabolic problems. Transactions of the American Mathematical Society 356, 987–1005.

Bekiaris-Liberis, N., Krstic, M., 2012. Compensation of time-varying input and state delays for nonlinear systems. Journal of Dynamic Systems, Measurement, and Control 134, 011009.

Burdzy, C., Chen, Z.Q., Sylvester, J., 2004. The heat equation in time dependent domains with insulated boundaries. Journal of mathematical analysis and applications 294, 581–595.

Curtain, R.F., Zwart, H., 1995. An introduction to infinite-dimensional linear systems theory. Springer-Verlag.

Derby, J., Atherton, L., Thomas, P., Brown, R., 1987. Finite-element methods for analysis of the dynamics and control of Czochralski crystal growth. Journal of Scientific Computing 2, 297–343.

Izadi, M., Dubljevic, S., 2013. Order-reduction of parabolic PDEs with time-varying domain using empirical eigenfunctions. AIChE Journal 59, 4142–4150.

Jadachowski, L., Meurer, T., Kugi, A., 2012. An efficient implementation of backstepping observers for time-varying parabolic PDEs, in: The Proceedings of 7th International Conference on Mathematical Modelling, pp. 798–803.

Katō, T., 1995. Perturbation theory for linear operators. Springer-Verlag.

Krstic, M., 2010. Lyapunov stability of linear predictor feedback for time-varying input delay. IEEE Transactions on Automatic Control 55, 554–559.

Krstic, M., Guo, B.Z., Balogh, A., Smyshlyaev, A., 2008. Output-feedback stabilization of an unstable wave equation. Automatica 44, 63–74.

Krstic, M., Smyshlyaev, A., 2008. Boundary control of PDEs: A course on backstepping designs. SIAM, Philadelphia.

Lasiecka, I., 1980. Unified theory for abstract parabolic boundary problems–A semigroup approach. Applied Mathematics and Optimization 6, 287–333.

Liu, W., 2003. Boundary feedback stabilization of an unstable heat equation. SIAM journal on control and optimization 42, 1033–1043.

Lunardi, A., 2004. An introduction to parabolic moving boundary problems, in: Iannelli, M., Nagel, R., Piazzera, S. (Eds.), Functional analytic methods for evolution equations. Springer. volume 1855, pp. 371–399.

Meurer, T., 2013. On the extended Luenberger-type observer for semilinear distributed-parameter systems. IEEE Transactions on Automatic Control 58, 1732–1743.

Meurer, T., Kugi, A., 2009. Tracking control for boundary controlled parabolic PDEs with varying parameters: Combining backstepping and differential flatness. Automatica 45, 1182–1194.

Ng, J., Dubljevic, S., 2012. Optimal boundary control of a diffusion-convection-reaction PDE model with time-dependent spatial domain: Czochralski crystal growth process. Chemical Engineering Science 67, 111–119.

Pazy, A., 1983. Semigroups of linear operators and applications to partial differential equations. Springer-Verlag.

Smyshlyaev, A., Krstic, M., 2004. Closed-form boundary state feedbacks for a class of 1-D partial integro-differential equations. IEEE Transactions on Automatic Control 49, 2185–2202.

Smyshlyaev, A., Krstic, M., 2005. On control design for PDEs with space-dependent diffusivity or time-dependent reactivity. Automatica 41, 1601–1608.

Wang, P.K.C., 1990. Stabilization and control of distributed systems with time-dependent spatial domains. Journal of Optimization Theory and Applications 65, 331–362.

Wang, P.K.C., 1995. Feedback control of a heat diffusion system with time-dependent spatial domain. Optimal control applications & methods 16, 305–320.

Chapter 3

Backstepping Output-Feedback Control of Moving Boundary Parabolic PDEs

3.1 Introduction

In the application of many control strategies, the knowledge of the state of system is essential, yet, in most cases this information is not fully available due to many reasons such as variables may not be measurable and using sensors may not be physically possible or economically beneficial. Herein, a part of design problem is the synthesis of state estimators (observers) that can generate an estimation of system states. Standard systematic techniques are available to design observers for the linear and nonlinear finite-dimensional systems. However, for infinite-dimensional (or distributed-parameter) systems governed by partial differential equations (PDEs) the state variables not only depend on time, but they also depend on another independent variable, usually spatial coordinate, and this imposes complexities and limitations to analysis and design.

One can address the observer (or controller) design problem for distributed parameter systems (DPSs) by using one of the two approaches: in the early-lumping method, at first the DPS is discretized by the use of suitable approximation techniques such as modal decomposition or Galerkin's method, into an approximate finite-dimensional model based on which state estimator is designed, see, e.g. Orner and Foster (1971); Kobayashi and Hitotsuya (1981). However, this approximation may change the system properties such as observability and loses physical features of the problem. Moreover, the stability of the closed-loop system cannot be established in general and the neglected dynamics may result in destabilization due to the observer spillover (Balas, 1978). In the late-lumping approach on the other hand, the designer takes the full advantage of the physical nature of the process and uses available DPSs theory to design an observer for the PDE model, then the resulting observer is lumped for implementation. The works of Kitamura et al. (1972); Gressang and Lamont (1975); Sakawa and Matsushita (1975); Nambu (1984); Curtain and Zwart (1995); Demetriou (2004); Nguyen (2008) are notable in the generalization of the finite-dimensional systems observer theory to infinite-dimensional systems, specifically the study of observability and detectability properties of DPSs. Along this line, several observer design methods are suggested in the literature including extension of the Luenberger-type observer to PDE systems (El Jai and Amouroux, 1988) and Lyapunov-based methods (Liu and Lapdus, 1976).

Another state estimation approach introduced by Smyshlyaev and Krstic (2005) is the use of backstepping concept for boundary observation of PDE systems. In this methodology, an invertible Volterra integral transformation

is used to transform the estimation error dynamics into a suitably selected stable distributed-parameter target system. The kernel of this transformation is defined by the solution of the so-called kernel PDE that is of a higher-order in space in the form of Klein-Gordon equation (Krstic and Smyshlyaev, 2008). Having the solution of the kernel PDE, the observer gains can be found to be afforded in the state estimator. From a theoretical point of view, the technique of PDE backstepping observer design is extended to the state estimation of unstable hyperbolic equations (Krstic et al., 2008), compensation of sensor dynamics and/or PDE-ODE cascades (Krstic, 2009b,a; Antonio Susto and Krstic, 2010), state estimation and output-feedback control for coupled PDE-ODE systems (Tang and Xie, 2011), linear parabolic PDEs with spatially- and time-varying reaction parameters (Jadachowski et al., 2012), parabolic PDEs with nonlinear reactive-convective terms (Jadachowski et al., 2013) and ultimately, observer design to semilinear parabolic PDEs (Meurer, 2013).

The shape of the domain of PDEs describing dynamics of a wide variety of transport processes may change due to different phenomena such as phase change, generation and consumption of chemical species, heat and mass transfer. The occurrence of these changes introduce more complexities in the modelling, analysis and control of these systems. Even if the process parameters are time-invariant, it is established that parabolic PDE systems with moving boundaries are inherently nonautonomous (Kloeden et al., 2008). The use of Galerkin's method in early-lumping approach of eigenfunctions-based observer design is studied in Abdollahi et al. (2014) for the boundary control of a 2D heat equation with time-dependent spatial domain. Considering such problems as infinite-dimensional systems, direct state estimation is not possible in

a large number of cases, because analytic expressions for the two-parameter semigroups describing the nonautonomous behaviour of the system can not be found.

The formulation of the state-feedback boundary control of parabolic PDEs with time-varying domain using backstepping approach in Chapter 2 motivates the observer design by the same method. In this Chapter, the formulation to the PDE backstepping observer design for an unstable 1D heat equation described on a domain with moving boundaries is presented. The PDE system that governs the observation error dynamics is transformed to an exponentially stable target system through the Volterra-type integral transformation to obtain the kernel PDE, which has time-dependent parameters and is defined on the 2D time-varying domain. Then, the separation principle is validated which provides the exponential stability of the observer-based output-feedback controller setup. Finally, numerical solutions to the kernel PDEs and various simulations are given to demonstrate successful stabilization of the unstable system.

3.2 Problem statement

Consider the linear 1D parabolic PDE system of the form:

$$\partial_t \bar{x}(\xi,t) = \alpha \partial_\xi^2 \bar{x}(\xi,t) - \dot{h}(t)\partial_\xi \bar{x}(\xi,t) + \lambda_0 \bar{x}(\xi,t) \tag{3.1}$$

where $\bar{x}(\xi,t)$ is the state variable, $\mathbb{D}(t) = [0,h(t)] \subset \mathbb{R}$ is the time-varying domain of the definition of PDE, $\xi \in \mathbb{D}(t)$ is the spatial coordinate, $h(t) \in \mathbb{R}^+$

is the time-dependent length of the domain and $\dot{h}(t)$ is its time derivative, and $t \in [0, \infty)$ is the time. α and λ_0 are process parameters and the advection term appearing in (3.1) is due to the moving boundaries of the PDE domain (Derby et al., 1987; Izadi and Dubljevic, 2013). The temperature distribution $\bar{x}(\xi, t)$ in the crystal of the Czochralski process or the shrinkage of a catalyst in a chemical process are two typical examples of the models that can be approximated by this PDE system. Although this approach can be generalized for any standard type of boundary conditions, the following boundary setting is assumed for the PDE system which is applicable to the temperature stabilization in the Czochralski crystal growth process:

$$\begin{aligned} \bar{x}(0, t) &= 0 \\ \partial_\xi \bar{x}(h(t), t) &= U(t) \end{aligned} \tag{3.2}$$

Here $U(t)$ is the control applied at the boundary $\xi = h(t)$ to stabilize the system state. For the design of the state observer, it is assumed that the output variable is given by:

$$\bar{y}(t) = \bar{x}(h(t), t) \tag{3.3}$$

which characterizes the collocated measurement and actuation.

For the later analysis regarding the stability of the closed-loop system and boundedness and differentiability of the solutions the following assumption is required.

Assumption 3.1. The function $h(t)$ is analytic, i.e., there exists a real positive

constant D such that for every non-negative integer j,

$$|\partial_t^j h(t)| \leq D^{j+1} j! \tag{3.4}$$

To eliminate advection term in (3.1), the PDE state is transformed as $\bar{x}(\xi,t) = x(\xi,t)e^{\xi\dot{h}(t)/2\alpha}$, which yields to the following PDE plant with associated boundary conditions:

$$\partial_t x(\xi,t) = \alpha\partial_\xi^2 x(\xi,t) + \lambda(\xi,t)x \tag{3.5}$$

$$\begin{cases} x(0,t) = 0 \\ \left[\partial_\xi x(h(t),t) + \frac{\dot{h}(t)}{2\alpha}x(h(t),t)\right] e^{\frac{h(t)\dot{h}(t)}{2\alpha}} = U(t) \end{cases} \tag{3.6}$$

where $\lambda(\xi,t) = \lambda_0 - (\dot{h}^2(t) + 2\xi\ddot{h}(t))/4\alpha$. The output variable is transformed as well:

$$y(t) = x(h(t),t) = \bar{y}(t)e^{-\frac{h(t)\dot{h}(t)}{2\alpha}} \tag{3.7}$$

Also, for the stability analysis of moving-boundary PDEs, it is essential to define the L_2-norm of function $w(\xi,t)$, $\xi \in \mathbb{D}(t)$ for the time-varying space $\mathbb{D}(t)$:

$$\|w(\xi,t)\| = \left(\int_0^{h(t)} w^2(\xi,t)d\xi\right)^{\frac{1}{2}} \tag{3.8}$$

3.3 Backstepping state-feedback controller

The backstepping state-feedback results of Chapter 2 are frequently used in this Chapter and they are briefly given in this section for easy reference.

The following state-feedback control law stabilizes the PDE system (3.5,3.6):

$$U(t) = \left(\int_0^{h(t)} \left[\frac{\dot{h}(t)}{2\alpha} k(h(t), \eta, t) + \partial_\xi k(\xi, \eta, t)|_{\xi = h(t)} \right] x(\eta, t) d\eta + k(h(t), h(t), t) x(h(t), t) \right) e^{\frac{h(t)\dot{h}(t)}{2\alpha}} \tag{3.9}$$

where the control gain function $k(\xi, \eta, t)$ is the kernel of the Volterra transformation

$$w(\xi, t) = x(\xi, t) - \int_0^\xi k(\xi, \eta, t) x(\eta, t) d\eta \tag{3.10}$$

that transforms (3.5,3.6) to the following exponentially stable (in the sense of L_2-norm) PDE system:

$$\partial_t w(\xi, t) = \alpha \partial_\xi^2 w(\xi, t) - c w(\xi, t) \tag{3.11}$$

$$\begin{cases} w(0, t) = 0 \\ \partial_\xi w(h(t), t) = -\frac{\dot{h}(t)}{2\alpha} w(h(t), t) \end{cases} \tag{3.12}$$

Based on the Assumption 3.1, the kernel function is the unique solution of the following kernel-PDE:

$$\partial_t k(\xi, \eta, t) = \alpha(\partial_\xi^2 k(\xi, \eta, t) - \partial_\eta^2 k(\xi, \eta, t)) - (\lambda(\eta, t) + c) k(\xi, \eta, t) \tag{3.13}$$

$$\begin{cases} k(\xi, 0, t) = 0 \\ k(\xi, \xi, t) = -\frac{1}{2\alpha} \int_0^\xi (\lambda(\eta, t) + c) d\eta \end{cases} \tag{3.14}$$

defined on the time-varying domain $\mathbb{S}_{\mathrm{C}}(t) = \{(\xi, \eta) | 0 \leq \eta \leq \xi \leq h(t)\} \subset \mathbb{R}^2$, see Fig. 3.1a. Exponential stability of target system (3.11,3.12) implies the exponential stability of closed-loop plant (3.5,3.6,3.9) since (3.10) is invertible.

3.4 Observer design

In the following, a distributed-parameter Luenberger-type observer is designed by modifying the PDE system (3.5,3.6) with corrector terms as:

$$\partial_t \hat{x}(\xi,t) = \alpha \partial_\xi^2 \hat{x}(\xi,t) + \lambda(\xi,t)\hat{x}(\xi,t) + l(\xi,t)\left[y(t) - \hat{x}(h(t),t)\right] \tag{3.15}$$

$$\begin{cases} \hat{x}(0,t) = 0 \\ \left[\partial_\xi \hat{x}(h(t),t) + \frac{\dot{h}(t)}{2\alpha}\hat{x}(h(t),t)\right] e^{\frac{h(t)\dot{h}(t)}{2\alpha}} = -l_0(t)\left[y(t) - \hat{x}(h(t),t)\right] + U(t) \end{cases} \tag{3.16}$$

where $l(x,t)$ and $l_0(t)$ are observer gain functions to be designed. The observer error $e(\xi,t) = x(\xi,t) - \hat{x}(\xi,t)$ satisfies the following PDE:

$$\partial_t e(\xi,t) = \alpha \partial_\xi^2 e(\xi,t) + \lambda(\xi,t)e(\xi,t) - l(\xi,t)e(h(t),t) \tag{3.17}$$

$$\begin{cases} e(0,t) = 0 \\ \left[\partial_\xi e(h(t),t) + \frac{\dot{h}(t)}{2\alpha}e(h(t),t)\right] e^{\frac{h(t)\dot{h}(t)}{2\alpha}} = l_0(t)e(h(t),t) \end{cases} \tag{3.18}$$

In the subsequent sections, we are looking for the integral transformation:

$$e(\xi,t) = \tilde{w}(\xi,t) - \int_\xi^{h(t)} q(\xi,\eta,t)\tilde{w}(\eta,t)d\eta \tag{3.19}$$

that transforms (3.17-3.18) into the following exponentially stable (in the sense

of the L_2-norm) target system:

$$\partial_t \tilde{w}(\xi,t) = \alpha \partial_\xi^2 \tilde{w}(\xi,t) - \tilde{c}\tilde{w}(\xi,t) \tag{3.20}$$

$$\begin{cases} \tilde{w}(0,t) = 0 \\ \partial_\xi \tilde{w}(h(t),t) = -\frac{\dot{h}(t)}{2\alpha}\tilde{w}(h(t),t) \end{cases} \tag{3.21}$$

with a free parameter $\tilde{c} \geq 0$ to manipulate the observer's convergence rate. Taking derivative of (3.19) with respect to space and time and substitution into (3.17, 3.18) and performing intermediate computations yield to the time-varying PDE for the kernel function $q(\xi,\eta,t)$

$$\partial_t q(\xi,\eta,t) = \alpha(\partial_\xi^2 q(\xi,\eta,t) - \partial_\eta^2 q(\xi,\eta,t)) + (\lambda(\xi,t) + \tilde{c})q(\xi,\eta,t) \tag{3.22}$$

$$\begin{cases} q(0,\eta,t) = 0 \\ q(\xi,\xi,t) = -\frac{1}{2\alpha}\int_0^\xi (\lambda(\eta,t) + \tilde{c})d\eta \end{cases} \tag{3.23}$$

and observer gains

$$\begin{aligned} l(\xi,t) &= \frac{\dot{h}(t)}{2} q(\xi,h(t),t) - \alpha \partial_\eta q(\xi,h(t),t) \\ l_0(t) &= q(h(t),h(t),t)e^{\frac{h(t)\dot{h}(t)}{2\alpha}} \end{aligned} \tag{3.24}$$

The kernel PDE (3.22,3.23) is defined on the time-varying domain $\mathbb{S}_{\mathrm{O}}(t) = \{(\xi,\eta)|0 \leq \xi \leq \eta \leq h(t)\} \subset \mathbb{R}^2$, see Fig. 3.1b. Note that the form of PDE (3.22,3.23) is similar to (3.13,3.14) and in Chapter 2 the existence of the bounded solution to this PDE is proven.

The inverse backstepping transformation of (3.19) in terms of

$$\tilde{w}(\xi,t) = e(\xi,t) + \int_{\xi}^{h(t)} q_1(\xi,\eta,t)e(\eta,t)d\eta \tag{3.25}$$

with the kernel $q_1(\xi,\eta,t)$ maps (3.20,3.21) to (3.17,3.18) and it is straightforward to show that the PDE for the inverse kernel function is similar to (3.22,3.23) with a unique solution. Therefore, the invertibility of transformation (3.19) implies the exponential stability of the error dynamics (3.17,3.18).

3.5 Output-feedback

The development of the exponentially convergent state estimator in previous section is independent of the control input. In this section the observer is combined with the backstepping control to explore the output-feedback controller and establish separation principle, i.e., the incorporation of a separately designed state-feedback controller and observer results in a stabilizing output-feedback controller.

Consider the PDE plant (3.5,3.6) controlled by the following input based on the state observer (3.15,3.16):

$$\begin{aligned} U(t) = \Bigg(\int_0^{h(t)} \left[\frac{\dot{h}(t)}{2\alpha} k(h(t),\eta,t) + \partial_\xi k(\xi,\eta,t)|_{\xi=h(t)} \right] \hat{x}(\eta,t)d\eta + \\ k(h(t),h(t),t)\hat{x}(h(t),t) \Bigg) e^{\frac{h(t)\dot{h}(t)}{2\alpha}} \end{aligned} \tag{3.26}$$

Transformations

$$\hat{w}(\xi,t) = \hat{x}(\xi,t) - \int_0^\xi k(\xi,\eta,t)\hat{x}(\eta,t)d\eta \tag{3.27}$$

and (3.19) map the closed-loop system consisting of the observer PDE (3.15,3.16) and observation error PDE (3.17,3.18) into target systems

$$\partial_t\hat{w}(\xi,t) = \alpha\partial_\xi^2\hat{w}(\xi,t) - \hat{c}\hat{w}(\xi,t) + \left[l(\xi,t) - \int_0^\xi k(\xi,\eta,t)l(\eta,t)d\eta\right]\tilde{w}(h(t),t) \tag{3.28}$$

$$\begin{cases} \hat{w}(0,t) = 0 \\ \partial_\xi\hat{w}(h(t),t) + \frac{\dot{h}(t)}{2\alpha}\hat{w}(h(t),t) = -l_0(t)\tilde{w}(h(t),t)e^{-\frac{h(t)\dot{h}(t)}{2\alpha}} \end{cases} \tag{3.29}$$

and (3.20,3.21), respectively.

Theorem 3.1. *The system $(\hat{w},\tilde{w})$ is exponentially stable in the sense of L_2-norm.*

Proof. Consider the following Lyapunov function candidate:

$$V(t) = \frac{1}{2}\left(\|\hat{w}(\xi,t)\|^2 + \beta\|\tilde{w}(\xi,t)\|^2\right) \tag{3.30}$$

where $\beta = \gamma_0^2 + \gamma^2 D$ with

$$\begin{aligned} \gamma_0 &= \alpha\sup_t\left(l_0(t)e^{-\frac{h(t)\dot{h}(t)}{2\alpha}}\right) \\ \gamma &= \sup_{(\xi,t)}\left(l(\xi,t) - \int_0^\xi k(\xi,\eta,t)l(\eta,t)d\eta\right) \end{aligned} \tag{3.31}$$

The fact that these functions are majorized by real constants γ and γ_0 is due

to the boundedness of the solution to (3.22,3.23). Taking the time derivative of (3.30) and replacing from (3.28,3.20) yields:

$$\begin{aligned}\dot{V}(t) = \int_0^{h(t)} \hat{w}(\xi,t)\Bigg[&\alpha\partial_\xi^2\hat{w}(\xi,t) - \hat{c}\hat{w}(\xi,t) \\ &+ \left(l(\xi,t) - \int_0^\xi k(\xi,\eta,t)l(\eta,t)d\eta\right)\tilde{w}(h(t),t)\Bigg]d\xi + \frac{\dot{h}(t)}{2}\hat{w}^2(h(t),t) \\ &+ \beta\int_0^{h(t)} \tilde{w}(\xi,t)\left[\alpha\partial_\xi^2\tilde{w}(\xi,t) - \tilde{c}\tilde{w}(\xi,t)\right]d\xi + \beta\frac{\dot{h}(t)}{2}\tilde{w}^2(h(t),t)\end{aligned}$$

Using integration by parts, applying boundary conditions (3.29,3.21) and imposing (3.31) results

$$\begin{aligned}\dot{V}(t) \leq &-\alpha\int_0^{h(t)}\left[\partial_\xi\hat{w}(\xi,t)\right]^2 d\xi - \hat{c}\int_0^{h(t)}\hat{w}^2(\xi,t)d\xi \\ &-\gamma_0\hat{w}(h(t),t)\tilde{w}(h(t),t) + \gamma\int_0^{h(t)}\hat{w}(\xi,t)\tilde{w}(h(t),t)d\xi \\ &-\beta\alpha\int_0^{h(t)}\left[\partial_\xi\tilde{w}(\xi,t)\right]^2 d\xi - \beta\tilde{c}\int_0^{h(t)}\tilde{w}^2(\xi,t)d\xi\end{aligned}$$

Note that Poincaré inequality takes the following forms for any function $v(\xi,t)$ defined on the time-varying space $\mathbb{D}(t)$:

$$\begin{aligned}\int_0^{h(t)} v^2(\xi,t)d\xi &\leq 2h(t)v^2(0,t) + 4h^2(t)\int_0^{h(t)}\left(\partial_\xi v(\xi,t)\right)^2 d\xi \\ \int_0^{h(t)} v^2(\xi,t)d\xi &\leq 2h(t)v^2(h(t),t) + 4h^2(t)\int_0^{h(t)}\left(\partial_\xi v(\xi,t)\right)^2 d\xi\end{aligned}$$

and one can show the following inequalities hold by the use of Young's, Poincaré

and Cauchy-Schwartz inequalities for $\hat{w}(0,t)=0$ and $\tilde{w}(0,t)=0$:

$$-\gamma_0\hat{w}(h(t),t)\tilde{w}(h(t),t) \leq \frac{1}{4}\int_0^{h(t)}\hat{w}^2(\xi,t)d\xi + \gamma_0^2 D\int_0^{h(t)}\left[\partial_\xi\tilde{w}(\xi,t)\right]^2 d\xi$$
$$\gamma\int_0^{h(t)}\hat{w}(\xi,t)\tilde{w}(h(t),t)d\xi \leq \frac{1}{4}\int_0^{h(t)}\hat{w}^2(\xi,t)d\xi + \gamma^2 D^2\int_0^{h(t)}\left[\partial_\xi\tilde{w}(\xi,t)\right]^2 d\xi$$

Therefore,

$$\begin{aligned}\dot{V}(t) \leq & -\alpha\int_0^{h(t)}\left[\partial_\xi\hat{w}(\xi,t)\right]^2 d\xi - \left(\hat{c}-\frac{1}{2}\right)\int_0^{h(t)}\hat{w}^2(\xi,t)d\xi \\ & -\left(\beta\alpha-\gamma_0^2 D-\gamma^2 D^2\right)\int_0^{h(t)}\left[\partial_\xi\tilde{w}(\xi,t)\right]^2 d\xi - \beta\tilde{c}\int_0^{h(t)}\tilde{w}^2(\xi,t)d\xi \\ \leq & -\left(\hat{c}-\frac{1}{2}+\frac{\alpha}{4D^2}\right)\int_0^{h(t)}\hat{w}^2(\xi,t)d\xi \\ & -\left(\beta\tilde{c}+\frac{\beta\alpha-\gamma_0^2 D-\gamma^2 D^2}{4D^2}\right)\int_0^{h(t)}\tilde{w}^2(\xi,t)d\xi\end{aligned}$$

Now choose $\hat{c}\geq 1-\alpha/4D^2$ and $\tilde{c}\geq 1/2-(\alpha-D)/4D^2$, hence

$$\dot{V}(t) \leq -\frac{1}{2}\int_0^{h(t)}\hat{w}^2(\xi,t)d\xi - \frac{\beta}{2}\int_0^{h(t)}\tilde{w}^2(\xi,t)d\xi = -V(t)$$

Hence, the system $(\hat{w},\tilde{w})$ is exponentially stable. □

The system $(\hat{x},e)$ is also exponentially stable since it is related to $(\hat{w},\tilde{w})$ by the invertible backstepping transformations (3.27) and (3.19). This proves that the closed-loop system consisting of the plant with backstepping controller and observer is exponentially stable.

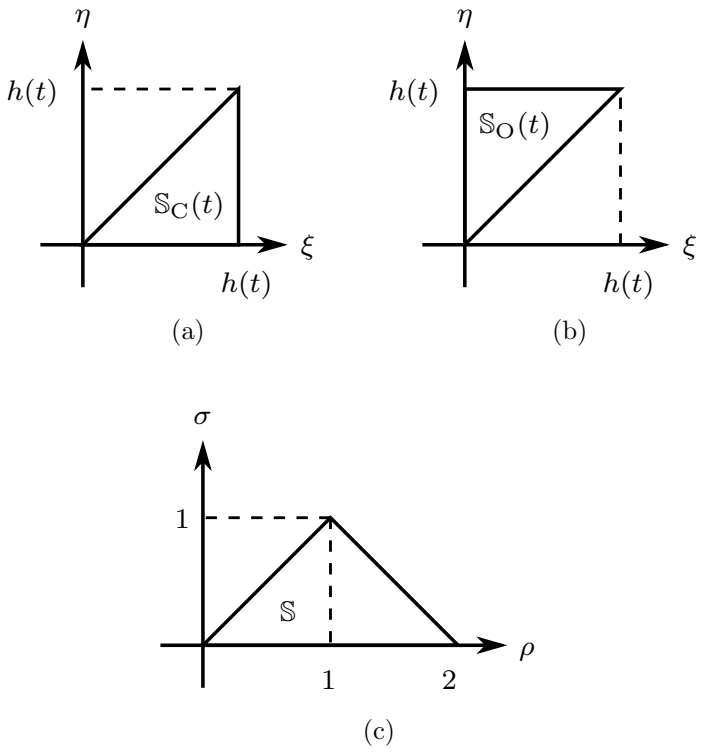

Figure 3.1: (a) Time-dependent domain $\mathbb{S}_{\mathrm{C}}(t)$ of the kernel function $k(\xi, \eta, t)$, (b) time-dependent domain $\mathbb{S}_{\mathrm{O}}(t)$ of the kernel function $q(\xi, \eta, t)$ and (c) fixed domain $\mathbb{S}$ of functions $k(\rho, \sigma, t)$ and $q(\rho, \sigma, t)$.

3.6 Numerical solution to the kernel PDEs

To apply the control (3.26), one should know control and observer gains given in terms of kernels $k(\xi,\eta,t)$ and $q(\xi,\eta,t)$ that are described by associated PDEs (3.13,3.14) and (3.22,3.23), respectively. However, finding the solution to these equations on the time-dependent domains $\mathbb{S}_{\mathrm{C}}(t)$ and $\mathbb{S}_{\mathrm{O}}(t)$ is not straight forward. In this section, these PDEs are transformed to fixed spatial domains and then they are solved numerically.

Consider the space $\mathbb{S} = \{(\rho,\sigma)|0 \leq \sigma \leq \rho \leq 2-\sigma\} \subset \mathbb{R}^2$ given in Fig. 3.1c. The transformations $\mathcal{T}_{\mathrm{C}}(t) : (\xi,\eta) \in \mathbb{S}_{\mathrm{C}} \mapsto (\rho,\sigma) \in \mathbb{S}$ given by

$$\rho = \frac{\xi+\eta}{h(t)}, \sigma = \frac{\xi-\eta}{h(t)} \tag{3.32}$$

and $\mathcal{T}_{\mathrm{O}}(t) : (\xi,\eta) \in \mathbb{S}_{\mathrm{O}} \mapsto (\rho,\sigma) \in \mathbb{S}$ given by

$$\rho = \frac{\xi+\eta}{h(t)}, \sigma = \frac{-\xi+\eta}{h(t)} \tag{3.33}$$

map time-dependent domains $\mathbb{S}_{\mathrm{C}}(t)$ and $\mathbb{S}_{\mathrm{O}}(t)$ to the time-invariant space $\mathbb{S}$, respectively. Using $\mathcal{T}_{\mathrm{C}}(t)$ and $\mathcal{T}_{\mathrm{O}}(t)$, the kernel PDEs for $k(\rho,\sigma,t)$ and $q(\rho,\sigma,t)$ take the form:

$$\begin{aligned}\partial_t g(\rho,\sigma,t) = \delta\frac{4\alpha}{h^2(t)}\partial_\rho\partial_\sigma g(\rho,\sigma,t) + \frac{\dot{h}(t)}{h(t)}\left(\rho\partial_\rho g(\rho,\sigma,t) + \sigma\partial_\sigma g(\rho,\sigma,t)\right)\\ - \delta\left(\lambda((\rho-\sigma)\frac{h(t)}{2},t) + \check{c}\right) g(\rho,\sigma,t)\end{aligned} \tag{3.34}$$

$$\begin{cases} g(\rho,\rho,t) = 0 \\ g(\rho,0,t) = f(\rho,t;\check{c}) \end{cases} \tag{3.35}$$

where $g(\rho,\sigma,t) = k(\rho,\sigma,t)$, $\delta = 1$ and $\check{c} = \hat{c}$ for (3.13,3.14) and $g(\rho,\sigma,t) = q(\rho,\sigma,t)$, $\delta = -1$ and $\check{c} = \tilde{c}$ for (3.22,3.23). Also,

$$f(\rho,t;\check{c}) = \frac{\rho h(t)}{4\alpha}\left[\frac{2\dot{h}^2(t) + \rho h(t)\ddot{h}(t)}{8\alpha} - (\lambda_0 + \check{c})\right] \tag{3.36}$$

To numerically realize the solution to (3.34,3.35), the method of successive integration is utilized followed by numerical integration (Jadachowski et al., 2012). To this end, integrate (3.34) with respect to σ from 0 to σ and then with respect to ρ from σ to ρ and use boundary conditions (3.35) and integration by-parts for the terms with the first-order derivative to deduce (3.34,3.35) to the following integral equation:

$$\begin{aligned}\int_\sigma^\rho \int_0^\sigma &\left[\partial_t g(\mu,\nu,t) + \left[2\frac{\dot{h}(t)}{h(t)} + \delta\left(\lambda((\mu-\nu)\frac{h(t)}{2},t) + \check{c}\right)\right] g(\mu,\nu,t)\right] d\nu d\mu \\ &- \frac{\dot{h}(t)}{h(t)}\left(\rho\int_0^\sigma g(\rho,\nu,t)d\nu + \sigma\int_\sigma^\rho g(\mu,\sigma,t)d\mu\right) \\ &- \delta\frac{4\alpha}{h^2(t)}\left[g(\rho,\sigma,t) - f(\rho,t;\check{c}) + f(\sigma,t;\check{c})\right] = 0\end{aligned} \tag{3.37}$$

To find an approximate solution to (3.37), the integrals are approximated by the use of a composite trapezoidal rule. The triangular spatial domain $\mathbb{S}$ is discretized in N^2 computational points on an equally-spaced square grid as shown in Fig. 3.2. Hence, the continuous function $g(\rho,\sigma,t)$ is spatially discretized and denoted by $g_{i,j}(t)$ at the coordinate (ρ_i,σ_j) or simply at the point $(i,j) \in \{(m,n)|1 \le n \le m \le 2N-n\} \subset \mathbb{N}^2$. Now, the integrals in (3.37) are approximated by using discrete values of their integrands evaluated at grid

points through the application of the composite trapezoidal rule to obtain:

$$\begin{aligned}
&\frac{\Delta^2}{4}\sum_{i=J}^{I-1}\sum_{j=1}^{J-1}\left[\dot{g}_{i,j}+\dot{g}_{i+1,j}+\dot{g}_{i,j+1}+\dot{g}_{i+1,j+1}\right] \\
&\quad+\frac{\Delta^2}{4}\left(2\frac{\dot{h}(t)}{h(t)}+\delta\check{c}\right)\sum_{i=J}^{I-1}\sum_{j=1}^{J-1}\left[g_{i,j}+g_{i+1,j}+g_{i,j+1}+g_{i+1,j+1}\right] \\
&\quad+\delta\frac{\Delta^2}{4}\sum_{i=J}^{I-1}\sum_{j=1}^{J-1}\left[\bar{\lambda}_{i,j}g_{i,j}+\bar{\lambda}_{i+1,j}g_{i+1,j}+\bar{\lambda}_{i,j+1}g_{i,j+1}+\bar{\lambda}_{i+1,j+1}g_{i+1,j+1}\right] \\
&\quad-\frac{\Delta}{2}\frac{\dot{h}(t)}{h(t)}\left(\rho_I\sum_{j=1}^{J-1}\left[g_{I,j}+g_{I,j+1}\right]+\sigma_J\sum_{i=J}^{I-1}\left[g_{i,J}+g_{i+1,J}\right]\right) \\
&\quad-\delta\frac{4\alpha}{h^2(t)}\left[g_{I,J}-f(\rho_I,t;\check{c})+f(\sigma_J,t;\check{c})\right]=0
\end{aligned} \tag{3.38}$$

where $\Delta = 1/(N-1)$ and $\bar{\lambda}_{i,j}(t) = \lambda((\rho_i - \sigma_j)h(t)/2, t)$. For each pair (I, J) with unknown $g_{I,J}(t)$ (i.e., the points that are not on the boundaries with known boundary conditions), (3.38) relates the kernel function and its time derivative at computational points in the form of an ordinary differential equation (ODE). The new indexing $r = (2N-j)(j-1)+i$ will bijectively vectorize the array $g_{i,j}(t)$ into κ_r and the set of (N^2-3N+2) ODEs can be written in the following point-wise equation:

$$A\dot{\kappa}(t) + B(t)\kappa(t) + H(t) = 0 \tag{3.39}$$

The initial condition $\kappa_0 = \kappa(0)$ for (3.39) is chosen as the stationary solution at $t = 0$:

$$\kappa(0) = -B(0)^{-1}H(0) \tag{3.40}$$

Equations (3.39,3.40) can be considered as an initial-value problem in the

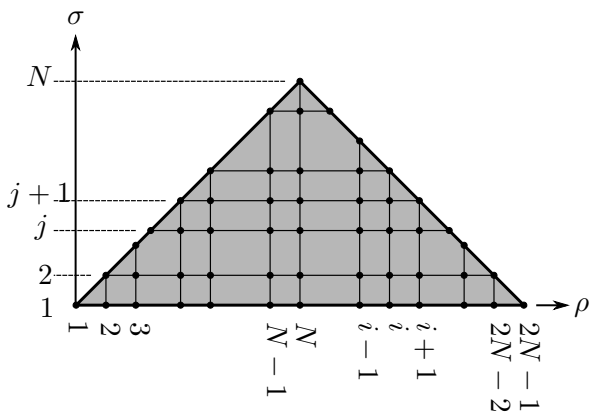

Figure 3.2: Spatial discretization of the domain $\mathbb{S}$ of transformed kernel PDEs.

form of a set of linear time-varying ODEs and can be solved efficiently using available numerical methods. Note that, the definition of the new index r results in matrices A and $B(t)$ being in the lower triangular form.

3.7 Simulation results

The given approach to output-feedback control of PDE system (3.5,3.6) is simulated and some results are shown in this section. Particularly, system parameters are $\alpha = 1$ and $\lambda_0 = 10$ and the change in the domain $h(t)$ is depicted in Fig. 3.3. The numerical discretization for the following simulations is obtained for $N = 80$. The set of ODE's (3.39) are numerically realized using a first-order implicit integration scheme with $dt = 10^{-4}$.

Figure 3.4 shows the numerical approximation of the time-varying observer kernel function $q(\rho, \sigma, t)$ on the computational domain $\mathbb{S}$ for $\hat{c} = \tilde{c} = 20$. The control gain kernel function $k(\rho, \sigma, t)$ has a very similar evolution profile. Observer gains $l(\xi, t)$ and $l_0(t)$ are computed numerically as given in (3.24)

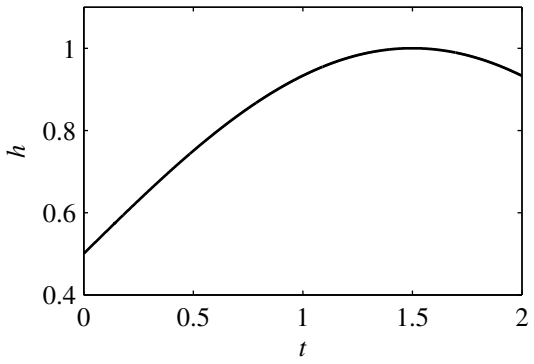

Figure 3.3: Length $h(t)$ of the time-varying domain $\mathbb{D}(t)$ of the PDE system.

and are shown in Fig. 3.5. The solution of plant and observer PDE's are obtained by application of finite-difference method for the same discretization level N. Figure 3.6 shows the norms of the PDE system state $x(\xi, t)$ and estimation error $e(\xi, t)$ for the open-loop system ($U(t) = 0$) with arbitrary different initial conditions for state $x(\xi, 0)$ and observer $\hat{x}(\xi, 0)$. It is seen that for the given parameters the open-loop system is unstable, however, observer converges exponentially to the plant.

The output-feedback control law (3.26) for the stabilization of the unstable PDE plant is shown in Fig. 3.7 where observer initial state is zero. The spike in the control close to $t = 0$ is due to the rather large estimation error at the initial time instances. Figure 3.8 shows the closed-loop evolution of the system state and L_2-norms of the state and estimation error. The exponentially convergence of the observer as well as the stabilization of the unstable PDE system is well provided in the simulation results.

In previous results, it is assumed that continuous measurements are available during the process evolution. This assumption does not hold in many applications and sensors generate discrete measurements with noise. Figure

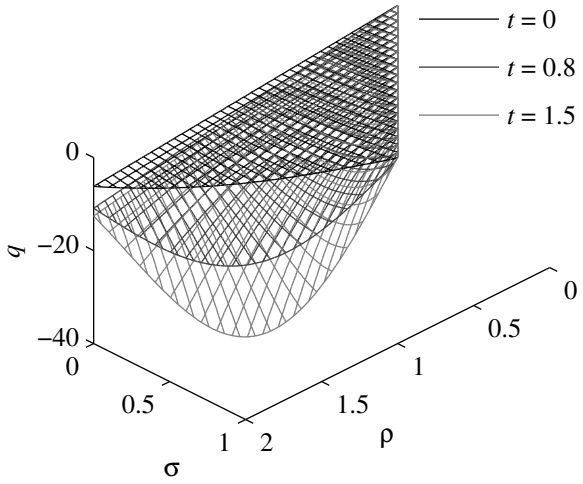

Figure 3.4: Evolution to the observer kernel function $q(\rho, \sigma, t)$ on the computational domain $\mathbb{S}$.

3.9 shows system evolution when measurement is available every 20 time steps of simulation and it is hold during this period. In this case, control action is highly sensitive to noisy measurement because of the collocated measurement and actuation. However, the stabilization of the unstable plant is achieved by using the observer-based output-feedback controller.

Finally, the simulation results of a reduced-order observer is presented, which will effectively reduce the computational cost. The low-order observer is designed by discretizing the observer PDE into the middle point at $\xi = \frac{h(t)}{2}$ and boundary points $\xi = 0$ and $\xi = h(t)$ at each time t. Then the estimated state $\hat{x}(\xi, t)$ is constructed by a quadratic function passing through the three computational points and evaluated at the original N grid points. Figure 3.10 shows the plant stabilization based on the reduced-order observer design and evolution of the system state and L_2-norms of the state and estimation error. The observer error exponentially approaches zero, but with a slower rate in

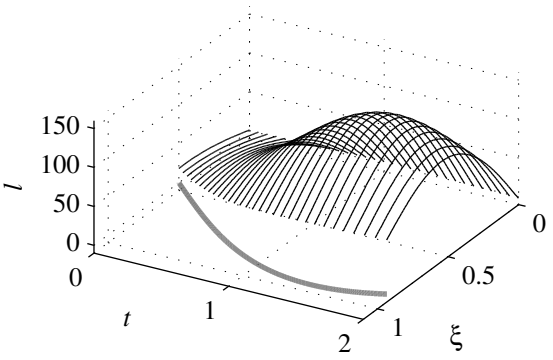

(a)

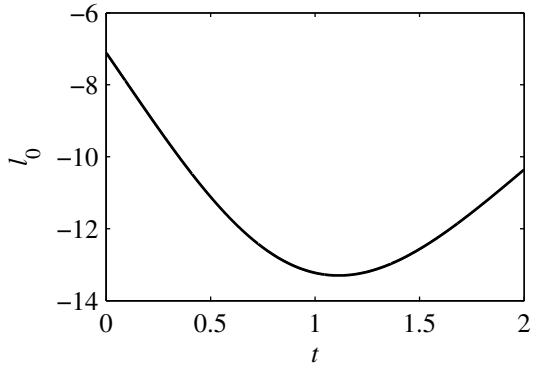

(b)

Figure 3.5: (a) Observer gains $l(\xi, t)$ (the thick grey line shows domain evolution) and (b) $l_0(t)$.

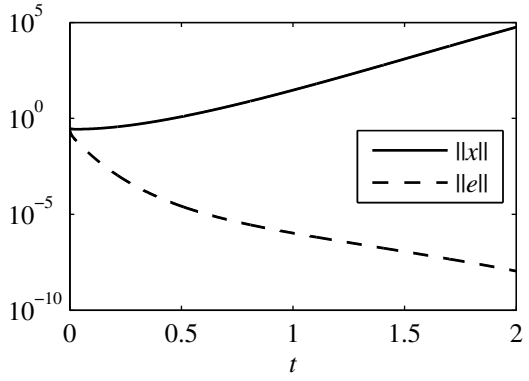

Figure 3.6: Norms of the state and estimation error for the open-loop system.

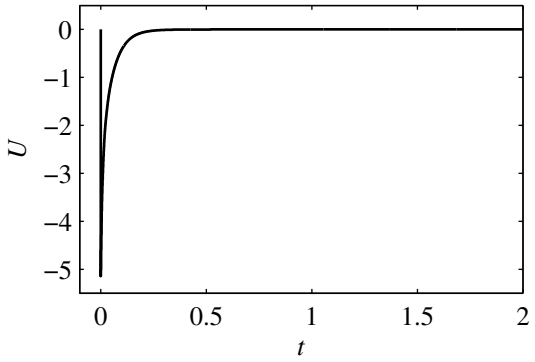

Figure 3.7: Stabilizing control input.

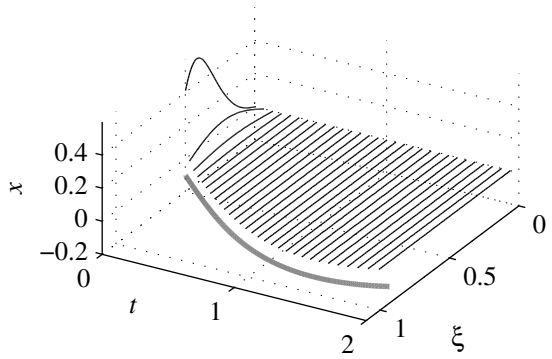

(a)

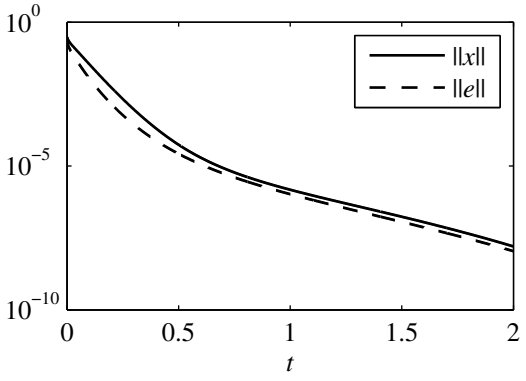

(b)

Figure 3.8: (a) Closed-loop PDE system state evolution. (b) Norms of the state and estimation error for the closed-loop system.

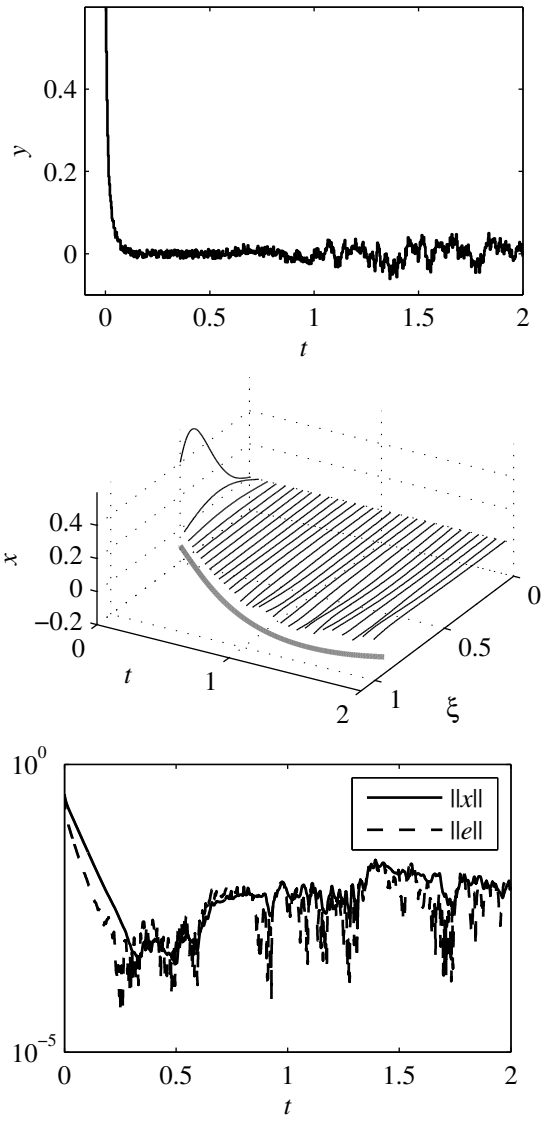

Figure 3.9: Noisy measurements and the resulting closed-loop PDE system evolution.

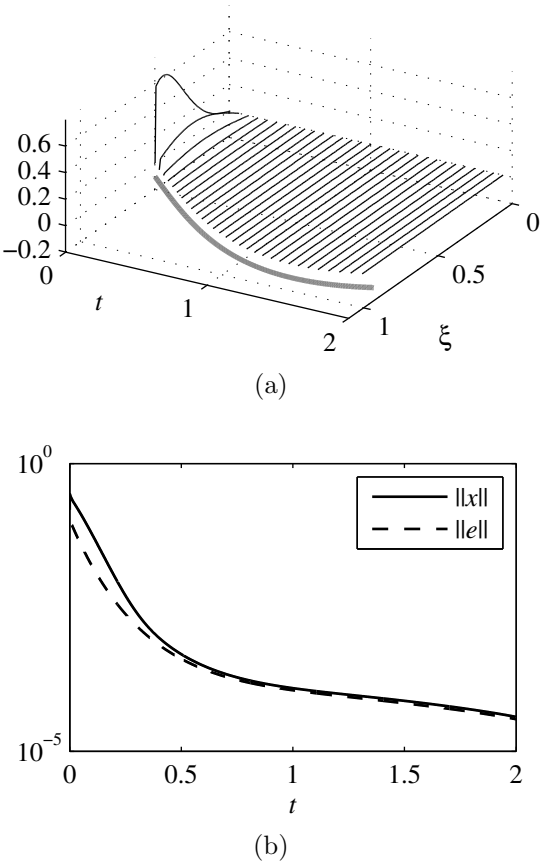

Figure 3.10: (a) Closed-loop PDE system state evolution with reduced-order observer and (b) norms of the resulting state and estimation error.

comparison to the higher-order observer given in Fig. 3.8 and the stabilization of the unstable PDE is accomplished.

3.8 Summary

The observer design of 1D unstable heat equation on a time-varying domain is formulated in this Chapter, where the observer gains are determined by the use of backstepping methodology. This includes a Volterra integral transformation

to transform the estimation error PDE to a prescribed exponentially stable target system. The kernel function of this transformation is described by a 2D time-varying PDE on a moving boundary domain. Then, the designed observer is incorporated with the backstepping control in an output-feedback controller and the exponential stability of the closed-loop system is shown by Lyapunov theorem. Finally, numerical solutions to the kernel PDEs are provided and the output-feedback boundary stabilization of the unstable system is simulated to demonstrate the successful performance of the state estimator.

References

Abdollahi, J., Izadi, M., Dubljevic, S., 2014. Temperature distribution reconstruction in Czochralski crystal growth process. AIChE Journal 60, 2839–2852.

Antonio Susto, G., Krstic, M., 2010. Control of PDE-ODE cascades with Neumann interconnections. Journal of the Franklin Institute 347, 284–314.

Balas, M.J., 1978. Active control of flexible systems. Journal of Optimization theory and Applications 25, 415–436.

Curtain, R.F., Zwart, H., 1995. An introduction to infinite-dimensional linear systems theory. Springer-Verlag.

Demetriou, M.A., 2004. Natural second-order observers for second-order distributed parameter systems. Systems & control letters 51, 225–234.

Derby, J., Atherton, L., Thomas, P., Brown, R., 1987. Finite-element methods for analysis of the dynamics and control of Czochralski crystal growth. Journal of Scientific Computing 2, 297–343.

El Jai, A., Amouroux, M., 1988. Sensors and observers in distributed parameter systems. International Journal of Control 47, 333–347.

Gressang, R.v., Lamont, G., 1975. Observers for systems characterized by semigroups. IEEE Transactions on Automatic Control 20, 523–528.

Izadi, M., Dubljevic, S., 2013. Order-reduction of parabolic PDEs with time-varying domain using empirical eigenfunctions. AIChE Journal 59, 4142–4150.

Jadachowski, L., Meurer, T., Kugi, A., 2012. An efficient implementation of backstepping observers for time-varying parabolic PDEs, in: The Proceedings of 7th International Conference on Mathematical Modelling, pp. 798–803.

Jadachowski, L., Meurer, T., Kugi, A., 2013. State estimation for parabolic pdes with reactive-convective non-linearities, in: The Proceedings of 12th European Control Conference (ECC), pp. 1603–1608.

Kitamura, S., Sakairi, S., Nishimura, M., 1972. Observer for distributed-parameter diffusion systems. Electrical engineering in Japan 92, 142–149.

Kloeden, P., Marín-Rubio, P., Real, J., 2008. Pullback attractors for a semilinear heat equation in a non-cylindrical domain. Journal of Differential Equations 244, 2062–2090.

Kobayashi, T., Hitotsuya, S., 1981. Observers and parameter determination for distributed parameter systems. International Journal of Control 33, 31–50.

Krstic, M., 2009a. Compensating a string PDE in the actuation or sensing path of an unstable ODE. IEEE Transactions on Automatic Control 54, 1362–1368.

Krstic, M., 2009b. Compensating actuator and sensor dynamics governed by diffusion PDEs. Systems & Control Letters 58, 372–377.

Krstic, M., Guo, B.Z., Balogh, A., Smyshlyaev, A., 2008. Output-feedback stabilization of an unstable wave equation. Automatica 44, 63–74.

Krstic, M., Smyshlyaev, A., 2008. Boundary control of PDEs: A course on backstepping designs. SIAM, Philadelphia.

Liu, Y., Lapdus, L., 1976. Observer theory for distributed-parameter systems. International Journal of Systems Science 7, 731–742.

Meurer, T., 2013. On the extended Luenberger-type observer for semilinear distributed-parameter systems. IEEE Transactions on Automatic Control 58, 1732–1743.

Nambu, T., 1984. On the stabilization of diffusion equations: boundary observation and feedback. Journal of differential equations 52, 204–233.

Nguyen, T.D., 2008. Second-order observers for second-order distributed parameter systems in R^2. Systems & Control Letters 57, 787–795.

Orner, P.A., Foster, A.M., 1971. A design procedure for a class of distributed parameter control systems. Journal of Dynamic Systems, Measurement, and Control 93, 86–92.

Sakawa, Y., Matsushita, T., 1975. Feedback stabilization of a class of distributed systems and construction of a state estimator. IEEE Transactions on Automatic Control 20, 748–753.

Smyshlyaev, A., Krstic, M., 2005. On control design for PDEs with space-dependent diffusivity or time-dependent reactivity. Automatica 41, 1601–1608.

Tang, S., Xie, C., 2011. State and output-feedback boundary control for a coupled PDE-ODE system. Systems & Control Letters 60, 540–545.

Chapter 4

Order-Reduction of Parabolic PDEs with Time-Varying Domain Using Empirical Eigenfunctions

4.1 Introduction

The modeling of a transport process is the most important issue in the process analysis and control design. It is currently addressed by phenomenological modeling arising from theoretical first-principles, experimental studies and/or with the help of the system identification theory. In many industries including chemical, petrochemical and pharmaceutical plants, model-based control has been very successful; in majority of them, the underlying plant model is low-dimensional and linear. In general, mathematical models of many industrial relevant transport processes are obtained from conservation laws, such as mass, momentum and/or energy, and yield the forms given by nonlinear partial differential equations (PDEs). In addition, many of these processes involve a change in shape and material properties which can be characterized

by phenomena associated with the phase change, generation and consumption of chemical species through the chemical reaction mechanism, heat and mass transfer.

In the past, dynamical analysis and control of parabolic PDEs with fixed spatial domain have been studied extensively, though, few investigations are available for the systems with time-dependent spatial domains. From the control point of view, main contributions include the works of Wang (1990, 1995) on the stabilization and optimal control problem of such systems and application in the synthesis of linear optimal controller for thermal gradient regulation in crystal growth processes, and the study of Ray and Seinfeld (1975) on the design of nonlinear distributed state estimators using stochastic methods. More recently, Ng and Dubljevic posed the time-varying optimal control problem (Ng and Dubljevic, 2011) and boundary control formulation (Ng and Dubljevic, 2012) for regulation of a parabolic PDE with time-varying domain by representing the PDE as an abstract evolution equation on an infinite-dimensional function space with non-autonomous parabolic operator which generates a two-parameter semigroup.

Low-dimensional model identification of distributed parameter systems governed by nonlinear PDEs attracted attention of a significant number of researchers in recent years. Among many, the most notable contributions came from Gay and Ray (1995); Chakravarti and Ray (1999); Park and Cho (1996); Christofides (2001); Armaou and Christofides (2002); Zheng and Hoo (2002, 2004). In these contributions, the common interpretation is that the dissipative distributed parameter systems could be modeled and reduced to a low finite-dimensional system representation which captures the dominant

dynamics, while the infinite-dimensional complement associated with the fast and stable dynamics can be neglected. The similar conceptual representation appears in the hydrodynamics where "coherent structures" are associated with the most dominant modes (Park and Lee, 1998, 2000).

In general, the model order-reduction can be achieved through the Galerkin's method which assumes the exact knowledge of the model and requires an analytic solution for the eigenvalue problem associated with the nonlinear spatial operator of a parabolic PDE. However, there is no general analytic solution to the operator eigenvalue problem, examples are the nonlinear spatial operator or problems with non-trivial geometric domain. In such cases, the exact description of the underlying distributed parameter system is not known, so the input-output model order-reduction approach has been proposed and explored (Gay and Ray, 1995). A well-known approach in the extraction of spatial characteristics (modes) of distributed parameter systems is the use of Karhunen-Loève (KL) expansion on an ensemble of solutions obtained from numerical or experimental resolution of the system (Park and Cho, 1996). These modes, known as empirical eigenfunctions, are used as the basis set of functions in the Galerkin's method. This approach is widely used in the derivation of accurate reduced-order approximations of many diffusion-reaction systems and fluid flows.

Bangia et al. (1997) used KL to find the eigenfunctions of accurate numerical solutions of the Navier-Stokes equations to study the bifurcation of incompressible flow in a model complex geometry. Park and Cho (1996) applied KL decomposition to a nonlinear two-dimensional heat conduction problem with a nontrivial domain to obtain the reduced-order model. In other

contributions, Park and coworkers used KL method to find basis functions for Galerkin's method to solve the inverse forced (Park and Lee, 1998) and natural (Park and Jung, 2001) convection problems. In the works of Shvartsman and Kevrekidis (1998); Theodoropoulou et al. (1999); Baker and Christofides (2000), low-dimensional models for specific diffusion-reaction systems are obtained using empirical eigenfunctions as basis functions in Galerkin's method, which is used to synthesize linear and nonlinear feedback controllers.

Other applications include, but are not limited to, the order-reduction of the sheet-forming processes (Arkun and Kayihan, 1998), order-reduction and control of multi-scale model of microstructure of materials during epitaxial growth (Raimondeau and Vlachos, 2000), optimal control of batch electrochemical reactor (Zhou et al., 2001), order-reduction of the nonlinear model of molten carbonate fuel cell (MCFC) (Mangold and Sheng, 2004), order-reduction and regulation of thermal transients in a microsystem models (Bleris and Kothare, 2005), order-reduction of multi-scale thermal model for electronic cabinets (Nie and Joshi, 2008), ground-water flow model reduction (McPhee and Yeh, 2008), order-reduction of low-voltage cascade electro-osmotic micropump model (Park and Lim, 2009).

Compared to the aforementioned extensive research efforts towards identification and model reduction of distributed parameter systems modeled by parabolic PDEs, there are only few studies to address order-reduction of parabolic PDE systems with spatial time-varying domain. In a series of works, Armaou and Christofides (2001a,b,c) used a mathematical transformation to represent the nonlinear parabolic PDE on a time-invariant spatial domain and applied KL decomposition to obtain the set of eigenfunctions on the fixed do-

main. In application, they used this method in the nonlinear feedback and robust control of one-dimensional reaction-diffusion systems. This approach cannot be used in general, since the mathematical transformation does not always have the analytical form, e.g. for nontrivial geometry. To obtain a reduced-order approximation of systems governed by PDEs that have a traveling wave solution, Glavaski et al. (1998) processed the available data set using a "centering" procedure prior to performing KL. This procedure involves giving an appropriate definition of the centre of a wave and moving it to a standard position. In the contribution by Fogleman et al. (2004) the proper orthogonal decomposition (POD) is applied to obtain the "phase invariant POD modes" of internal combustion engine flows. In their contribution, the velocity fields are stretched in one dimension to obtain data on a fixed grid such that the divergence-free (continuity) property of the original velocity field is preserved.

Following these ideas, a systematic approach is proposed in this Chapter to obtain a set of empirical eigenfunctions of a set of data given on an spatially time-dependent domain that captures the most energy of the system's dynamics while preserving some physical invariant property. We propose the following methodology which will be discussed in detail in the consecutive sections:

1. The solution to the parabolic PDE can be found as raw data by the experiments or high fidelity numerical simulations which describe the time evolution of dissipative distributed parameter system on a time-varying domain.

2. Geometrically, a mapping can be found by which the time-varying do-

main of the PDE is transformed to a fixed reference configuration for all times during the evolution of the solutions.

3. Having the set of solutions, the main idea is to transform them to the reference configuration and then use them with the KL decomposition. Among all transformations, the one that preserves the space-invariant property of the PDE solutions is selected. While this mapping transforms data, the mapping introduced in step 2 transforms geometry of the PDE domain.

4. Then, KL decomposition is applied on the mapped solutions to extract a low-dimensional set of eigenfunctions that contains most of the energy of the system on the fixed domain.

5. Using the inverse of the transformation found in step 3, these eigenfunctions are mapped on the time-varying domain. As a result, a set of time-varying empirical eigenfunctions are obtained and can be used as a tool for the reduced-order representation of the initially given distributed parameter system.

The focus of this Chapter is to explore this methodology and apply it to more realistic problems, and the examples provided here show the efficiency of the proposed methodology.

4.2 Mathematical Formulation

In this section, the mathematical aspects of the proposed method are reviewed. In particular, the mapping that transforms data from time-varying domain to

the reference geometry and preserves the properties of the data is derived. A brief essence of the Karhunen-Loève decomposition as the representation of a set of stochastic data with minimum number of degrees of freedom is given, as well.

4.2.1 Model Formulation of PDE systems with Time-Dependent Domain

This section is devoted to formulate the dynamics of a diffusion-reaction process with time-varying domain using continuum mechanics tools. In particular, we are interested in the model dynamics of an extensive property:

$$G(t) = \int_{\Omega(t)} \rho(\xi, t) C x(\xi, t) d\Omega$$

given by the intensive property $x(\xi, t)$ at each point $\xi \in \Omega(t) \subset \mathbb{R}^n$, where $\rho(\xi, t)$ is density and C is a constant.

Theorem 4.1. *Consider a continuous body $\Omega(t)$ that has the velocity $v(\xi, t)$. In addition, the boundary $\Gamma(t)$ of the body has the velocity $v_s(\xi|_{\Gamma(t)}, t)$ (see Fig.4.1). The differential form of a diffusion-reaction process dynamics in terms of the property $x(\xi, t)$ in the time-varying domain $\Omega(t)$ is given by*

$$\rho C \frac{\partial x}{\partial t} = \nabla \cdot (\kappa \nabla x) - \rho C v \cdot \nabla x + h + bu$$

where κ is diffusivity and $h(x(\xi, t), t)$ and $b(\xi, t)$ are smooth functions describing internal reaction/generation and distribution of the control action $u(t)$.

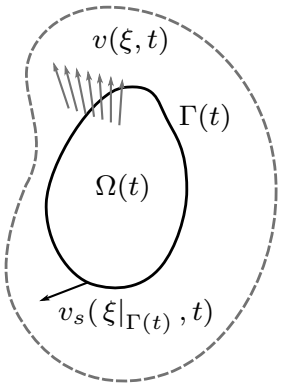

Figure 4.1: The control volume $\Omega(t)$ is a part of the body with velocity $v(\xi, t)$. The boundary $\Gamma(t)$ of the control volume has the velocity v_s.

Proof. The total change of $G(t)$ in the domain $\Omega(t)$ is given by the Leibniz integral rule for multi dimensions (Deen, 1998) as follows:

$$\frac{d}{dt}\int_{\Omega}\rho C x d\Omega = \int_{\Omega}\frac{\partial}{\partial t}\left(\rho C x\right)d\Omega + \int_{\Gamma} n \cdot v_s \rho C x d\Gamma \tag{4.1}$$

where n is the normal outward vector at each point on the Γ. On the other hand, conservation of the property $G(t)$ yields:

$$\frac{d}{dt}\int_{\Omega}\rho C x d\Omega = \int_{\Gamma} n \cdot \kappa \nabla x d\Gamma - \int_{\Gamma} n \cdot \left(v - v_s\right)\rho C x d\Gamma + \int_{\Omega}(h + bu) d\Omega \tag{4.2}$$

This equation states that the total change in the property $G(t)$ is given by the difference in the diffusive flux and mass transport from the boundary, in addition to internal generation and external input. Substituting Eq. (4.1) on the left-side of Eq. (4.2) and using divergence theorem leads to the following

differential form of the governing equation:

$$\frac{\partial}{\partial t}(\rho C x) = \nabla \cdot (\kappa \nabla x - v \rho C x) + h + bu$$

For $x = C = 1$ and the assumption of constant density, this equation reduces to the continuity as $\nabla \cdot v = 0$. Then, the differential form becomes:

$$\rho C \frac{\partial x}{\partial t} = \nabla \cdot (\kappa \nabla x) - \rho C v \cdot \nabla x + h + bu$$

□

Furthermore, it can be shown that the solution to this parabolic PDE is unique and sufficiently smooth for given boundary and initial conditions.

4.2.2 Geometry and Data Transformations

For later analysis and extraction of empirical eigenfunctions, the following Assumption is also required.

Assumption 4.1. Evolution of the domain $\Omega(t)$ is smooth and known *a priori*.

Note that the evolution of the time-varying domain can be easily measured in many process systems (e.g., phase change in the crystal growth processes).

In this section, it is intended to obtain a set of *time-varying* empirical eigenfunctions $\{\phi_j(\xi, t)\}$, $j = 1, 2, \cdots, M$ that capture the most energy of the ensemble of solutions (snapshots) $\{x(\xi, t_i)\}, i = 1, 2, \cdots, N \gg M$, of the parabolic PDE under consideration. The fact that eigenfunctions are inherently time-varying is due to their spatially time-dependent domain.

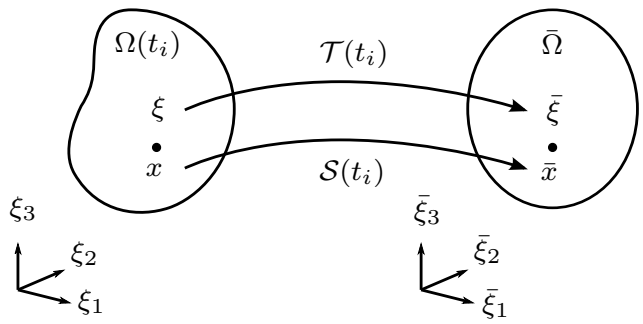

Figure 4.2: At each time instance t_i, $\mathcal{T}(t_i)$ maps time-varying domain Ω to fixed domain $\bar{\Omega}$. Also, the transformation $\mathcal{S}(t_i)$ maps the state $x(\xi, t_i)$ from time-varying domain to $\bar{x}_i(\xi)$ on the fixed domain

Lemma 4.1. *There exists invertible mapping $\mathcal{T}(t)$ which is smooth and preserves orientation of the coordinate system, that maps the domain $\Omega(t)$ to a fixed reference configuration $\bar{\Omega}$ as $\mathcal{T}(t) : \xi \in \Omega(t) \mapsto \bar{\xi} \in \bar{\Omega}$ at each time t as shown in Fig.4.2, with the coordinate transformation $\bar{\xi} = \bar{\xi}(\xi, t)$ and the Jacobian matrix $[J(t)] = \frac{\partial \bar{\xi}}{\partial \xi}$.*

Consider the extensive property:

$$G(t) = \int_{\Omega(t)} g(x(\xi, t)) d\Omega \tag{4.3}$$

Since the Karhunen-Loève decomposition deals with the ensemble of *snapshots* of solutions of the PDE, we restrict our derivation on the solutions $x(\xi, t_i)$ at time instances $t = t_i, i = 1, 2, \cdots, N$. In addition, the spatial integral in Eq. (4.3) allows to parameterize the independent variable time t and associate differential elements $d\Omega = J_i^{-1} d\bar{\Omega}$ at $t = t_i$, where J_i^{-1} is the determinant of the inverse of $[J(t_i)]$. Given the state $x(\xi, t_i)$, we are interested in a transformation thorough which the property $g(x)$ (e.g., thermal energy or density) is invariant

when transforming domain $\Omega(t)$ to $\bar{\Omega}$. This is given in the following Lemma.

Lemma 4.2. *The transformation $\mathcal{S}(t_i)$ that maps the state $x(\xi, t_i)$ on the time-varying domain to the state $\bar{x}_i(\bar{\xi})$ on the fixed reference domain given by*

$$\bar{x}_i(\bar{\xi}) = g^{-1}(g(x(\xi, t_i))J_i^{-1}) \tag{4.4}$$

preserves the property $g(x)$ by the following relation:

$$g(x(\xi, t_i))d\Omega = g(\bar{x}_i(\bar{\xi}))d\bar{\Omega} \tag{4.5}$$

Proof. Using the Jacobian of transformation,

$$g(x(\xi, t_i))d\Omega = g(x(\xi, t_i))J_i^{-1}d\bar{\Omega} \tag{4.6}$$

and comparing Eqs. (4.5) and (4.6):

$$g(x(\xi, t_i))J_i^{-1} = g(\bar{x}_i(\bar{\xi}))$$

which results in (4.4). □

Therefore, (4.4) can be regarded as the transformation $\mathcal{S}(t_i)$ that maps the state $x(\xi, t_i)$ on the time-varying domain to the state $\bar{x}_i(\bar{\xi})$ on the fixed reference domain preserving the invariant property $g(x)$. Note that, $\mathcal{T}(t_i)$ maps the domain (geometry) of interest at $t = t_i$, while $\mathcal{S}(t_i)$ maps the state (see Fig.4.2).

Remark 4.1. *The mapping transformation $\mathcal{T}(t_i)$ is required to be non-singular for all $\xi \in \Omega(t_i)$, that is, the Jacobian being non-zero. This notion comes from*

the topological characteristics of continuous transformation of domain from one configuration to another. If the transformation preserves the topology of the time-varying domain, the same approach can be used and numerically realized, see section 4.3.3. In the most general case when the time-varying domain contains holes, that is the case of a not simply connected domain, which is mapped into similar topological fixed domain with the holes, the expression given in Eqs. (4.6-4.4) holds. On the contrary, if the time-varying domain undergoes topological transformation which implies the change from non-simply connected to more complex connected region (the generation of holes within the domain by continuous transformation), the mapping into the fixed domain configuration will induce additional terms to be accounted for in Eqs. (4.6-4.4). In this Chapter we do not explore these complex cases, since the physical examples explored in our study do not show this type of the time-varying domain transformation.

4.2.3 Karhunen-Loève Decomposition

The Karhunen-Loève (KL) decomposition is a procedure for representation of an stochastic field with a minimum number of degrees of freedom (Loève, 1955; Sirovich and Park, 1990). In this subsection we briefly outline the KL procedure which is used to calculate the empirical eigenfunctions from the data on the fixed domain.

Consider the space of square integrable real-valued functions $\bar{x}(\bar{\xi})$ with inner product $\langle \bar{x}, \bar{y} \rangle$. Given an ensemble of states $\{\bar{x}_i(\bar{\xi})\}$, $i = 1, 2, \cdots, N$,

whose ensemble average is denoted by:

$$\widehat{\bar{x}_i(\bar{\xi})} = \frac{1}{N}\sum_{i=1}^{N} \bar{x}_i(\bar{\xi})$$

it is intended to obtain a function $\bar{\phi}(\bar{\xi})$ that maximizes $\widehat{\left\langle \bar{\phi}, \bar{x}_i \right\rangle}^2$, i.e., $\bar{\phi}(\bar{\xi})$ is closest to all $\bar{x}_i(\bar{\xi})$. This problem can be expressed as finding $\max_{\bar{\phi}(\bar{\xi})} \lambda$ where:

$$\lambda = \frac{\widehat{\left\langle \bar{\phi}, \bar{x}_i \right\rangle}^2}{\left\langle \bar{\phi}, \bar{\phi} \right\rangle} \tag{4.7}$$

Defining the two-point correlation function $K(\bar{\xi}, \bar{\eta}) = \widehat{\bar{x}_i(\bar{\xi})\bar{x}_i(\bar{\eta})}$ for $\bar{\xi}, \bar{\eta} \in \bar{\Omega}$ and the linear operator $\mathcal{R}$ as:

$$\mathcal{R}\bar{\phi} = \left\langle K(\bar{\xi}, \bar{\eta}), \bar{\phi}(\bar{\eta}) \right\rangle$$

equation (4.7) reduces to the following operator eigenvalue problem:

$$\mathcal{R}\bar{\phi} = \lambda\bar{\phi} \tag{4.8}$$

Equation (4.8) can be solved using the Schmidt-Hilbert technique or *the method of snapshots* (Sirovich, 1987). In this method, the eigenfunction $\bar{\phi}(\bar{\xi})$ is assumed to be a linear combination of ensemble elements as:

$$\bar{\phi}(\bar{\xi}) = \sum_{i=1}^{N} \alpha_i \bar{x}_i(\bar{\xi}) \tag{4.9}$$

Replacing 4.9 and introducing $P_{ij} = \frac{1}{N}\left\langle \bar{x}_i(\bar{\eta}), \bar{x}_j(\bar{\eta}) \right\rangle$, Eq. (4.8) takes the

following form:

$$\sum_{i=1}^{N}\sum_{j=1}^{N}\bar{x}_i(\bar{\xi})P_{ij}\alpha_j = \lambda\sum_{i=1}^{N}\alpha_i\bar{x}_i(\bar{\xi})$$

For this to hold, the coefficient of $x_i(\bar{\xi})$ on the left and right hand sides of this equation should be equal for all $i = 1, 2, \cdots, N$, that is:

$$\sum_{j=1}^{N}P_{ij}\alpha_j = \lambda\alpha_i$$

which is the eigenvalue problem of the matrix with elements P_{ij}. Finally, the set of eigenfunctions $\bar{\phi}_i(\bar{\xi}), i = 1, 2, \cdots, M$ associated with the M largest eigenvalues of $\mathcal{R}$ forms an optimal basis in the sense of $\bar{x}(\bar{\xi})$ representation in terms of $\bar{\phi}_i(\bar{\xi})$ with minimum error.

Remark 4.2. *The size of matrix P is as large as the number of snapshots of the PDE solution. On the other hand, for a set of eigenfunctions to be able to approximate the solutions accurately, the ensemble of solutions should contain adequate number of snapshots. Therefore, one faces the issue of a large matrix eigenvalue problem and numerical methods suitable for these problems should be chosen. In this Chapter, Arnoldi algorithm is used to solve the large matrix eigenvalue problem to reduce computational costs.*

4.2.4 Time-Varying Empirical Eigenfunctions

Once the set of M eigenfunctions $\bar{\phi}(\bar{\xi})$ are found, they can be transformed to the time-varying domain Ω at each time t_i using the inverse of $\mathcal{S}(t_i)$ (see Eq. (4.4)). Therefore, we have the basis of M time-varying eigenfunctions $\phi(\xi, t)$ which can be used to represent the state $x(\xi, t)$ on the time-varying domain

$\Omega(t)$.

4.3 Numerical Simulations

In this section, the proposed methodology is applied to three different PDE systems. For the first two process examples, the evolution of the systems is obtained as a solution of nonlinear parabolic PDEs by using the Galerkin's method, whereas for the third system, a moving-mesh finite element realization is developed. It is emphasized that domain evolution is known *a priori* in these simulation studies. In the subsequent numerical procedure, the eigenfunctions $\bar{\phi}_i(\bar{\xi})$ obtained from the method of snapshots are orthogonal and they are normalized to generate an orthonormal basis.

4.3.1 One-dimensional nonlinear reaction-diffusion system

Consider the one-dimensional reaction-diffusion system described by the following parabolic PDE:

$$\frac{\partial x(\xi,t)}{\partial t} = k\frac{\partial^2 x(\xi,t)}{\partial \xi^2} - \dot{l}(t)\frac{\partial x(\xi,t)}{\partial \xi} + h(x(\xi,t)) \tag{4.10}$$

on the time-varying domain $l(t) = \pi(1.4 - 0.4e^{-0.74t})$, $\dot{l}(t) = dl(t)/dt$, subject to Dirichlet boundary conditions:

$$x(0,t) = 0, \quad x(l(t),t) = 0$$

and initial condition $x(\xi, 0) = x_0(\xi)$. The process can be considered as the one-dimensional approximation of temperature evolution $x(\xi, t)$ in a catalytic rod. The reaction term is given by:

$$h(x) = \beta_1(e^{-\frac{\gamma}{1+x}} - e^{-\gamma}) - \beta_2 x \tag{4.11}$$

This example is adopted from Armaou and Christofides (2001b) where non-dimensional process parameters k and β_2 are functions of space ξ. For simplicity we averaged these parameters over domain and used $k = 0.4$, $\beta_1 = 45$, $\beta_2 = 2$ and $\gamma = 4$, however, the approach can be generalized for parameters depending on spatial coordinates.

To obtain an ensemble of solutions of (4.10), the Galerkin's method with the set of orthonormal basis functions:

$$\psi_i(\xi, t) = \sqrt{\frac{2}{l(t)}} \sin(\frac{i\pi\xi}{l(t)})$$

is used. An explicit Euler integration scheme is utilized to construct a higher-order resolution of the problem. Fig.4.3 shows the evolution of state of one-dimensional PDE using 10 modes of the Galerkin's method.

For this example, the reference configuration is simply a one-dimensional domain with constant length L_0 and the mapping $\mathcal{T}(t_i)$ is given by:

$$\bar{\xi} = \frac{L_0}{l(t_i)}\xi$$

If the state $x(\xi, t)$ represents the temperature at $\xi \in \Omega$, the invariant property of interest can be interpreted to be thermal energy $g(x(\xi, t_i)) = \rho c_p x(\xi, t_i)$ and

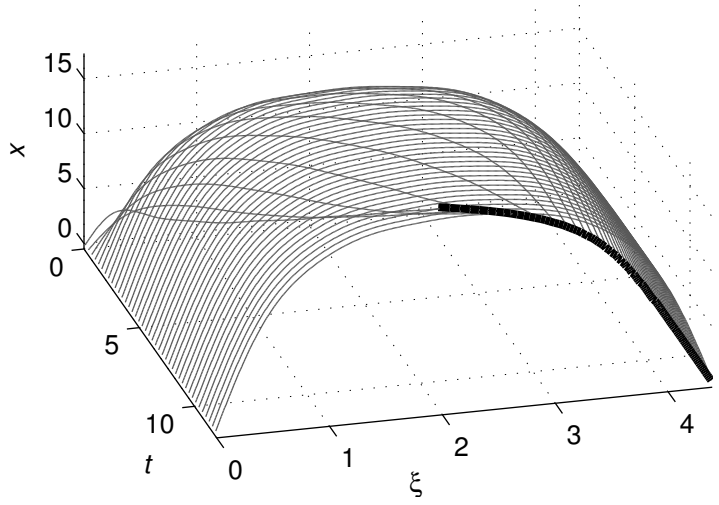

Figure 4.3: Evolution of the state of one-dimensional PDE given by Eqs. (4.10-4.11) obtained from Galerkin's method using 10th-order sinusoidal model. Thick black line shows domain evolution.

from Eq. (4.4), the mapping $\mathcal{S}(t_i)$ associated with is given as:

$$\bar{x}_i(\bar{\xi}) = \frac{1}{\rho c_p}\left(\rho c_p x(\xi, t_i) J_i^{-1}\right) = \frac{l(t_i)}{L_0} x(\xi, t_i)$$

Having the temperature distribution $\bar{x}_i(\bar{\xi})$ on the fixed domain $\bar{\Omega}$, one can perform KL decomposition to extract empirical eigenfunctions $\bar{\phi}_j(\bar{\xi})$, $j = 1, 2, \cdots, M$ of the data with inner product $\langle \bar{x}, \bar{y} \rangle = \int_0^{L_0} \bar{x}\bar{y} d\bar{\xi}$. Fig.4.4a shows the first three eigenfunctions on the fixed domain. Time-varying eigenfunctions are obtained by using the inverse mapping $\mathcal{S}^{-1}$ and the first two of them are shown in Fig.4.4b.

The set of time-varying eigenfunctions are used in the Galerkin's method to obtain the reduced-order model by replacing $x(\xi, t) = \sum_{i=1}^{M} a_i(t)\phi_i(\xi, t)$ in

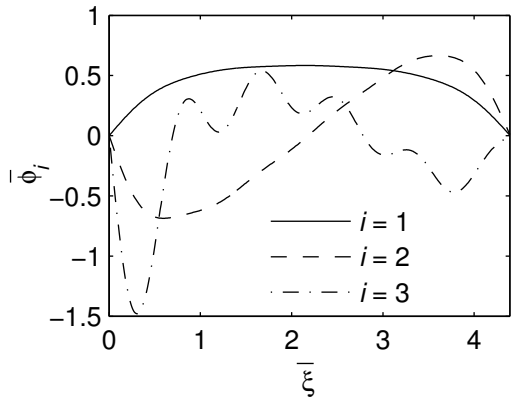

(a)

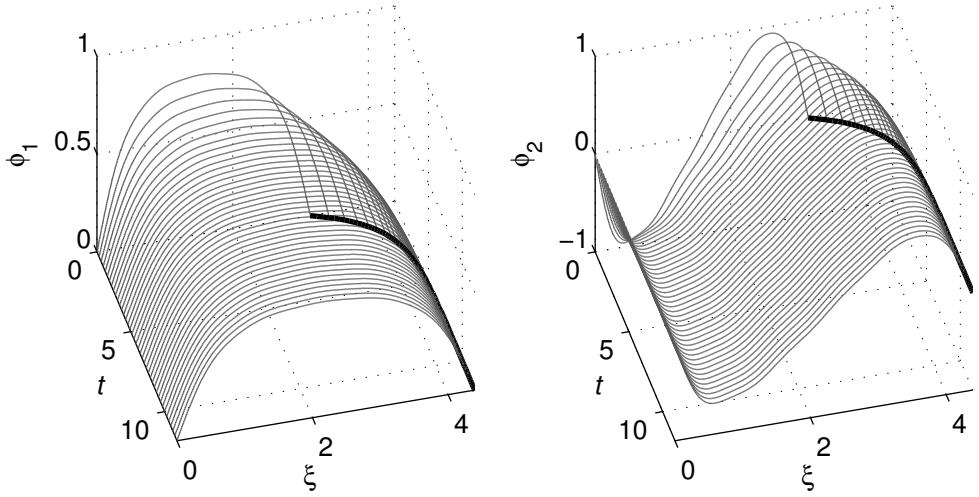

(b)

Figure 4.4: (a) The first three eigenfunctions extracted from the data mapped to the fixed domain. (b) The first two time-varying eigenfunctions.

(4.10) to get:

$$\sum_{i=1}^{M}\left(\dot{a}_i\phi_i + a_i\dot{\phi}_i\right) = \sum_{i=1}^{M}\left(ka_i\phi_i'' - \dot{l}a_i\phi_i'\right) + h\left(\sum_{i=1}^{M} a_i\phi_i\right)$$

where over dot and prime represent derivatives with respect to time and space, respectively. Projecting on the basis ϕ_j yields:

$$\dot{a}(t) = A(t)a(t) + \bar{h}(a(t), t) \tag{4.12}$$

where $a(t) = [a_1(t)\ a_2(t)\ \cdots a_M(t)]^T$, $A_{ij}(t) = \frac{\langle k\phi_i'' - \dot{l}\phi_i' - \dot{\phi}_i, \phi_j\rangle}{c(t)}$, $\bar{h}_j(a_i(t), t) = \frac{\langle h(\sum_{i=1}^{M} a_i\phi_i), \phi_j\rangle}{c(t)}$, and $c(t) = [L_0/l(t)]^2$.

Equation (4.12) represents the reduced-order model of the (4.10). Fig.4.5 compares the evolution of the norm of the states $\|x\| = \langle x, x\rangle^{1/2}$ for reconstruction of Fig.4.3 with three time-varying eigenfunctions used in (4.12). As it can be seen from Fig.4.5, the reduced-order model almost perfectly matches the profile obtained from the high-order fidelity simulation.

Remark 4.3. *The set of eigenfunctions ϕ_i in this example are orthogonal and $\langle\phi_i(\xi, t), \phi_j(\xi, t)\rangle = c(t)\delta_{ij}$ with δ_{ij} being Kronecker's delta. This is because the determinant of the Jacobian is not spatial-dependent. For general transformation in multi dimensions, this condition does not hold (see section 4.3.3).*

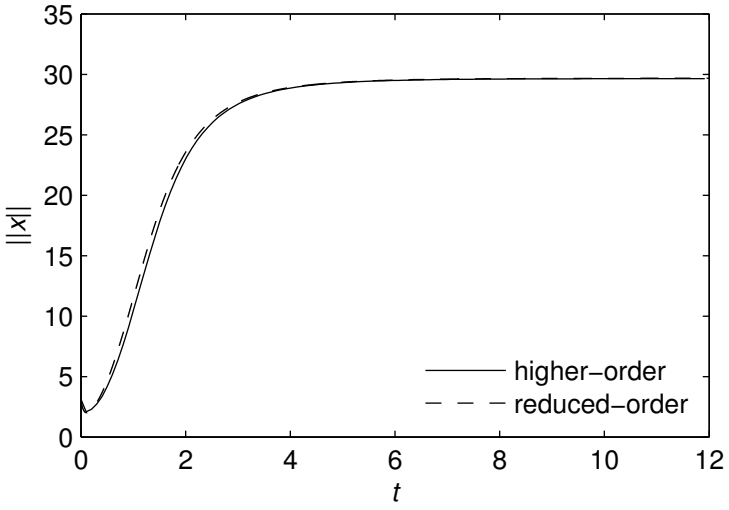

Figure 4.5: Comparison of the norm of the state for higher-order and reduced-order resolutions of the one-dimensional PDE.

4.3.2 Two-dimensional nonlinear reaction-diffusion system

The second example is the two-dimensional reaction-diffusion system governed by the nonlinear parabolic PDE given by:

$$\frac{\partial x(\xi_1, \xi_2, t)}{\partial t} = k\nabla^2 x(\xi_1, \xi_2, t) + h\left(x(\xi_1, \xi_2, t)\right) + u(t) \tag{4.13}$$

on the time-varying rectangular domain $L_1(t) \times L_2(t) \in \mathbb{R}^2$ subject to Dirichlet boundary conditions:

$$x(0, \xi_2, t) = x(L_1(t), \xi_2, t) = x(\xi_1, 0, t) = x(\xi_1, L_2(t), t) = 0$$

and initial condition $x(\xi_1, \xi_2, 0) = x_0(\xi_1, \xi_2)$, see Fig.4.6. The reaction term and process parameters are the same as in the previous example and $u(t)$ is

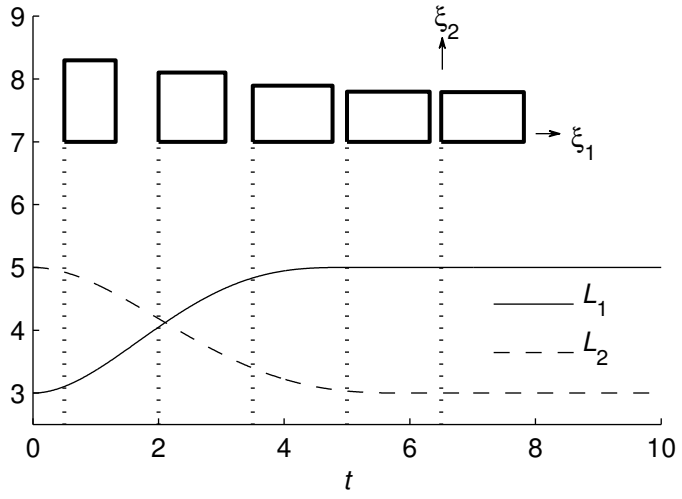

Figure 4.6: Two-dimensional time-varying domain of the nonlinear diffusion-reaction system.

the input. The ensemble of solutions of (4.13) subjected to the input shown in Fig.4.8a is obtained using the Galerkin's method with the set of orthogonal basis functions:

$$\psi_{ij}(\xi_1, \xi_2, t) = \sin(\frac{i\pi\xi_1}{l_1(t)}) \sin(\frac{j\pi\xi_2}{l_2(t)})$$

The reference fixed configuration $\bar{\Omega}$ on which the solutions of (4.13) are mapped is considered to be a square with lengths $L_0 = 4$, then the Jacobian matrix of transformation $\mathcal{T}(t_i)$ is:

$$J(t_i) = \begin{bmatrix} \frac{L_0}{L_1(t_i)} & 0 \\ 0 & \frac{L_0}{L_2(t_i)} \end{bmatrix}$$

Using the same energy function $g(x) = \rho c_p x$ as in the previous example, from (4.4) the ensemble of solutions is mapped to the fixed domain to obtain the data set for the KL decomposition. The first three extracted empirical eigen-

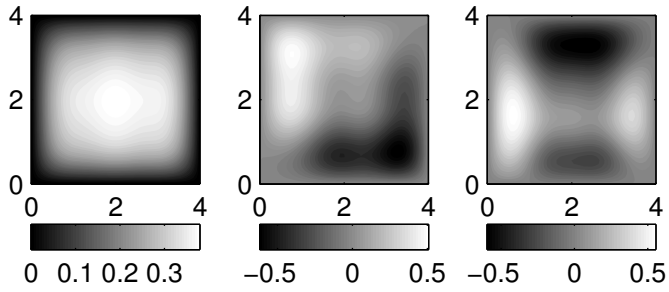

Figure 4.7: The first three eigenfunctions extracted from the data mapped to the fixed domain for the two-dimensional nonlinear PDE.

functions are shown in Fig.4.7.

These eigenfunctions are mapped on the time-varying domain at each time instance t_i to obtain the set of time-varying empirical eigenfunctions. Using this set in the Galerkin's method, the state evolution can be reconstructed. Fig.4.8b shows the evolution of the norm of states for simulations based on 25 sinusoidal function space basis and 3 empirical eigenfunctions.

4.3.3 Two-dimensional linear diffusive system with non-trivial geometry

In this section, the proposed methodology is applied to a diffusive process where the geometry of the time-varying domain is non-trivial. The Jacobian matrix of transformation in this case is not only time-dependent, but also it is space dependent, which implies that the Jacobian matrix needs to be computationally determined for each point within the deformable domain.

We consider the two-dimensional axisymmetric diffusive system described

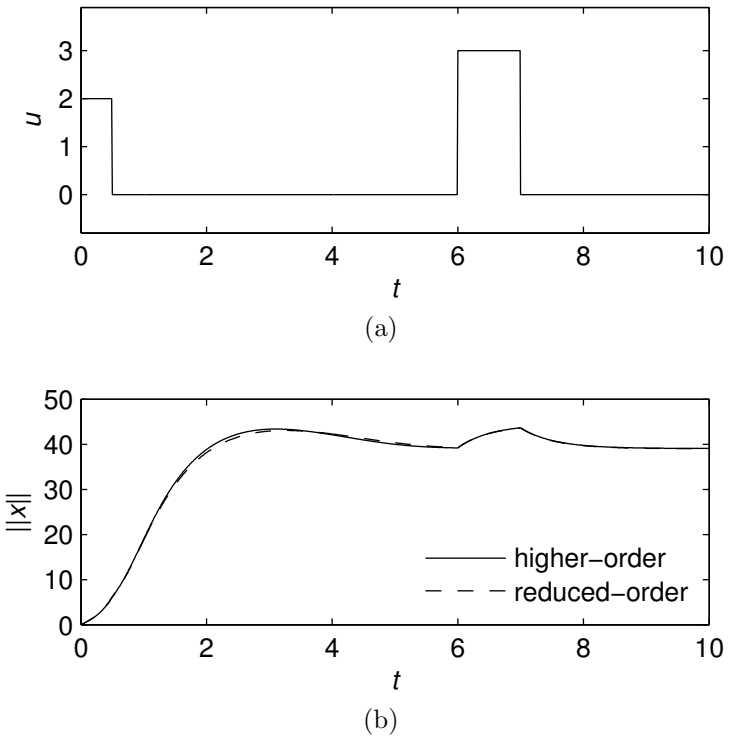

Figure 4.8: (a) Input to the two-dimensional reaction diffusion system. (b) Comparison of the norm of the state for higher-order and reduced-order resolutions of the two-dimensional PDE.

by the following parabolic PDE:

$$\frac{\partial x}{\partial t} = k\left[\frac{1}{r}\frac{\partial}{\partial r}\left(r\frac{\partial x}{\partial r}\right) + \frac{\partial^2 x}{\partial z^2}\right] - \dot{L}\frac{\partial x}{\partial z} + u \tag{4.14}$$

for $x(r, z, t)$ in the time-varying domain $\Omega(t)$ shown in Fig.4.9a, subject to boundary conditions:

$$\begin{aligned} &x(r, 0, t) = x(r, L(t), t) = 0 \\ &[kn \cdot \nabla x(r, z, t)]_{r=0} = [kn \cdot \nabla x(r, z, t)]_{r=\bar{R}(z)} = 0 \end{aligned} \tag{4.15}$$

with non-dimensional process parameter $k = 0.25$ and $\dot{L}(t)$ represents derivative of the length function $L(t)$ with respect to time. This system is a model that describes the non-dimensionalized crystal temperature distribution in the Czochralski crystal growth process. In this method, the crystal rod is pulled out vertically from the surface ($z = 0$) of a heated pool of melt contained in a crucible. A simplified radius control strategy arising from geometric model provides the domain evolution in terms of $L(t)$ and $R(t)$ as shown in Fig.4.9a, and $u(t)$ is the heat input to the parabolic PDE system.

The ensemble of solution of (4.14) is obtained using the finite element method. Since the geometry of domain is time-varying, a mesh moving scheme is used. Due to the fact that the evolution of the domain is not coupled with the PDE system (4.14) and is known, the Arbitrary Lagrangian Eulerian (ALE) method (Reddy and Gartling, 2010) is used to spatially discretize domain of interest as shown in Fig.4.10. The finite element mesh consists of 14×20 two-dimensional linear 4-node elements which discretizes spatial geometry to

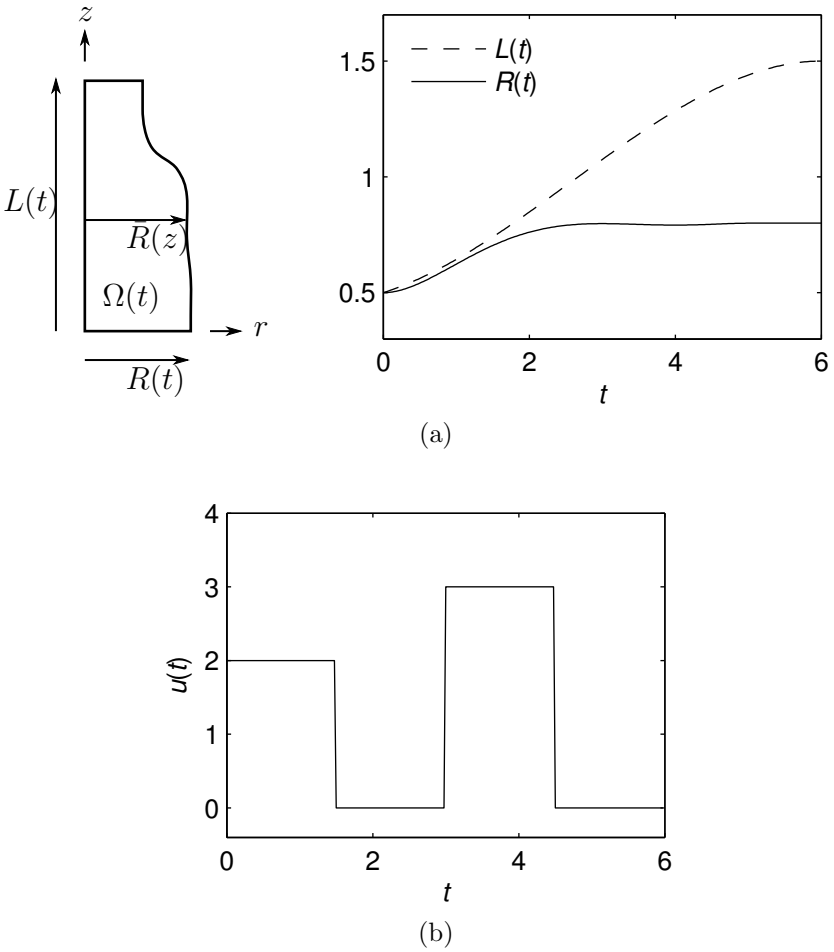

Figure 4.9: (a) Schematic representation of crystal growth in the 2D Czochralski process given by Eqs. (4.14, 4.15). $L(t)$ and $R(t)$ are the length and radius of crystal at time t. (b) The heat input to the Czochralski system.

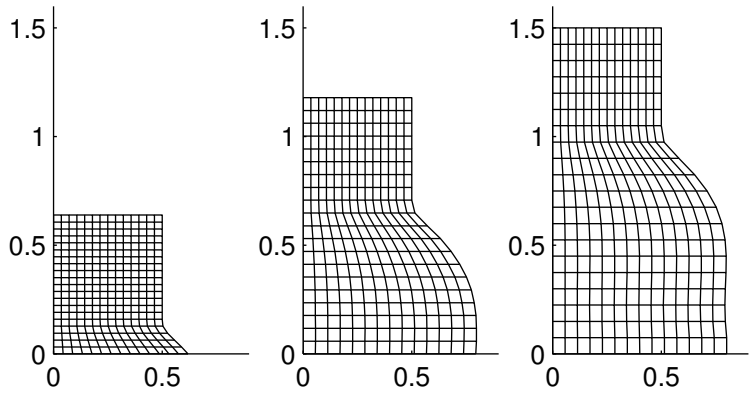

Figure 4.10: Finite element moving mesh at $t = 1, 3.5$, and, 6.

285 degrees of freedom. The evolution of the time-dependent set of ordinary differential equations obtained from the finite element discretization is realized by first-order implicit time integration with the time step $dt = 0.025$, while the heat input $u(t)$ is an arbitrary constructed function shown in Fig.4.9b.

To apply the proposed methodology, the reference configuration $\bar{\Omega}$ on which the solutions of (4.14) are mapped is considered to be a rectangular with dimensions $\bar{R} = 0.8$ and $\bar{L} = 1.5$. The mapping $\mathcal{T}(t_i)$ can be numerically constructed by introducing sets of computational grid points on both time-varying and fixed domains, as shown in Fig.4.11. Associating each grid point of the time-varying domain with one and only one grid point on the fixed-domain defines the one-to-one and onto (and hence invertible) mapping $\mathcal{T}(t_i)$. Note that, the coarse grid of 10×18 points is shown in Fig.4.11 for illustration and a 40×80 computational grid is used for calculation of the Jacobian. Also, it is important to emphasize that the Jacobian matrix of transformation in this case is space-dependant.

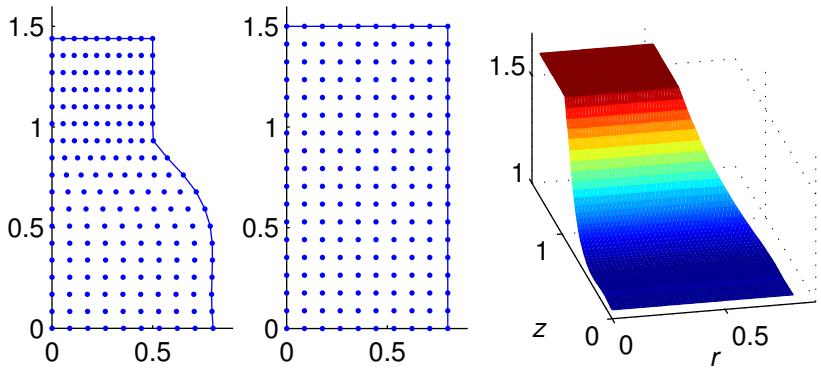

Figure 4.11: The sets of 10×18 grid points in time-varying domain at $t = 5$ (left panel) and in the fixed domain (middle panel). These computational grid points define the mapping $\mathcal{T}(t_i)$ by associating each point of the time-varying domain with one point in the fixed domain. Right panel shows $J_i^{-1}(r, z)$ at $t_i = 5$.

Considering the state $x(r, z, t)$ as temperature at $(r, z) \in \Omega(t)$, the invariant property $g(x(\xi, t_i))$ can be considered to be thermal energy as in previous examples and from (4.4), the map $\mathcal{S}(t_i)$ found as:

$$\bar{x}_i(\bar{r}, \bar{z}) = J_i^{-1} x(r, z, t_i)$$

Having the temperature distribution $\bar{x}_i(\bar{r}, \bar{z})$ on the fixed domain $\bar{\Omega}$, one can perform KL decomposition to extract empirical eigenfunctions $\bar{\phi}_j(\bar{r}, \bar{z}), j = 1, 2, \cdots, M$ of the data with inner product defined as:

$$\langle \bar{x}, \bar{y} \rangle = \int_{\bar{\Omega}} \bar{r} \bar{x} \bar{y} d\bar{r} d\bar{z}$$

Figure 4.12a shows the first 30 eigenvalues of the KL decomposition (see Eq. (4.8)), the first mode captures 99.2% of the energy solutions. Fig.4.12b

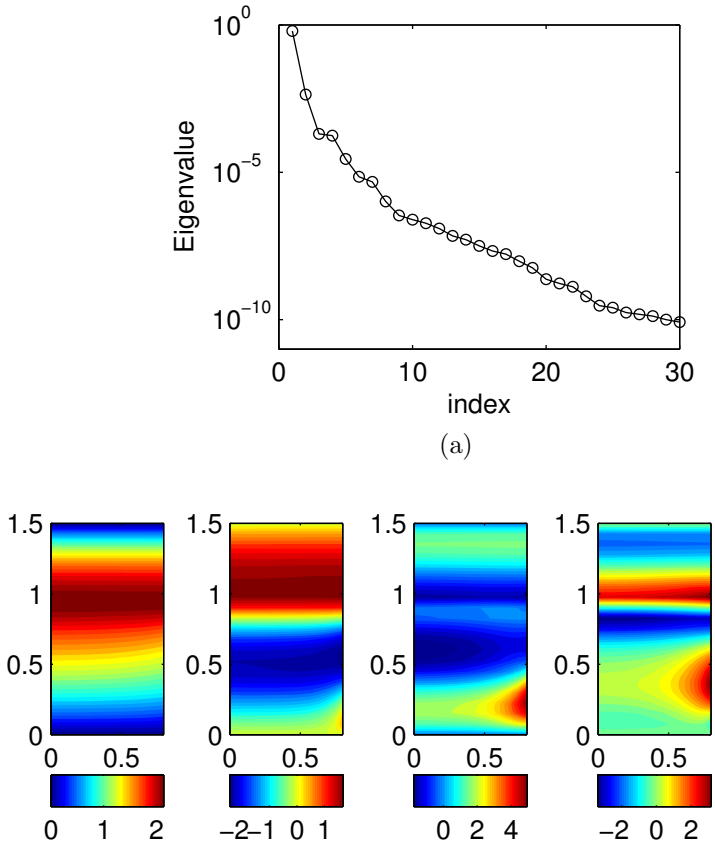

Figure 4.12: (a) The first 30 eigenvalues of the KL decomposition. (b) The first five eigenfunctions extracted from the data mapped to the fixed domain.

shows the first five eigenfunctions on the fixed domain.

The use of $\mathcal{S}^{-1}$ on eigenfunctions extracted from the data mapped to the reference configuration results in the time-varying eigenfunctions. Then, the Galerkin's method is used to obtain the reduced-order model by replacing $x(r,z,t) = \sum_{i=1}^{M} a_i(t)\phi_i(r,z,t)$ in (4.14) and projecting on the basis ϕ_j to get:

$$\dot{a}(t) = A(t)a(t) + B(t)u(t) \tag{4.16}$$

where

$$
\begin{aligned}
&a(t) = [a_1(t)\ a_2(t)\ \cdots a_M(t)]^T \\
&A(t) = C(t)^{-1}K(t), \quad B(t) = C(t)^{-1}F(t) \\
&C_{ij}(t) = \langle \phi_i, \phi_j \rangle \\
&K_{ij}(t) = \left\langle k\left[\frac{1}{r}\frac{\partial}{\partial r}\left(r\frac{\partial \phi_i}{\partial r}\right) + \frac{\partial^2 \phi_i}{\partial z^2}\right] - \dot{L}\frac{\partial \phi_i}{\partial z} - \frac{\partial \phi_i}{\partial t}, \phi_j \right\rangle \\
&F_i(t) = \langle 1, \phi_i \rangle
\end{aligned}
$$

Equation (4.16) represents the reduced-order form of (4.14).

Figure 4.13 compares the evolution of the norm of the states for reconstruction of the solutions of (4.14) with the same input with two time-varying eigenfunctions used in (4.16). As it can be seen the reduced-order model perfectly matches the profile obtained from the high-order simulation, the finite element model with order of 285 is reduced to a second-order system. Reconstructed states resulting from the reduced-order model are shown in Fig.4.14 against the finite element solutions.

4.4 Summary

In this Chapter, we proposed a method to obtain a set of time-varying empirical eigenfunctions of a set of data given on the spatially time-dependent domain. In this method the solutions of the PDE system on the time-varying domain are mapped to a fixed reference configuration in such a way that invariant properties of the data are preserved. Then, KL decomposition is applied on the mapped solutions to extract a small set of eigenfunctions that contains

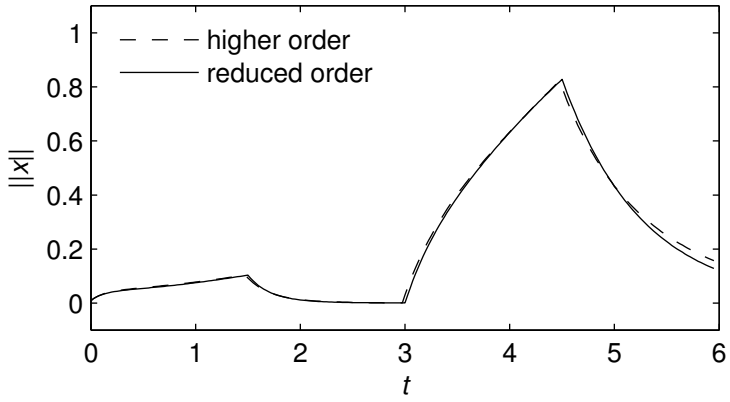

Figure 4.13: Comparison of the norm of the state for the higher-order finite element and reduced-order Galerkin's method resolutions of the parabolic PDE.

most of the energy of system on the fixed domain. These eigenfunctions are mapped back on the time-varying domain yielding a set of time-varying empirical eigenfunctions which are used to find the reduced-order representation of the main PDE system.

In the simulation part, the procedure is applied to two nonlinear reaction-diffusion systems with trivial domain, as well as a two-dimensional axisymmetric problem of temperature distribution of the Czochralski crystal growth process governed by parabolic PDE which represents time-varying domain with non-trivial geometry. The results show the capability of the method as a useful and efficient tool in representations of the reduced-order system with the time-varying domain.

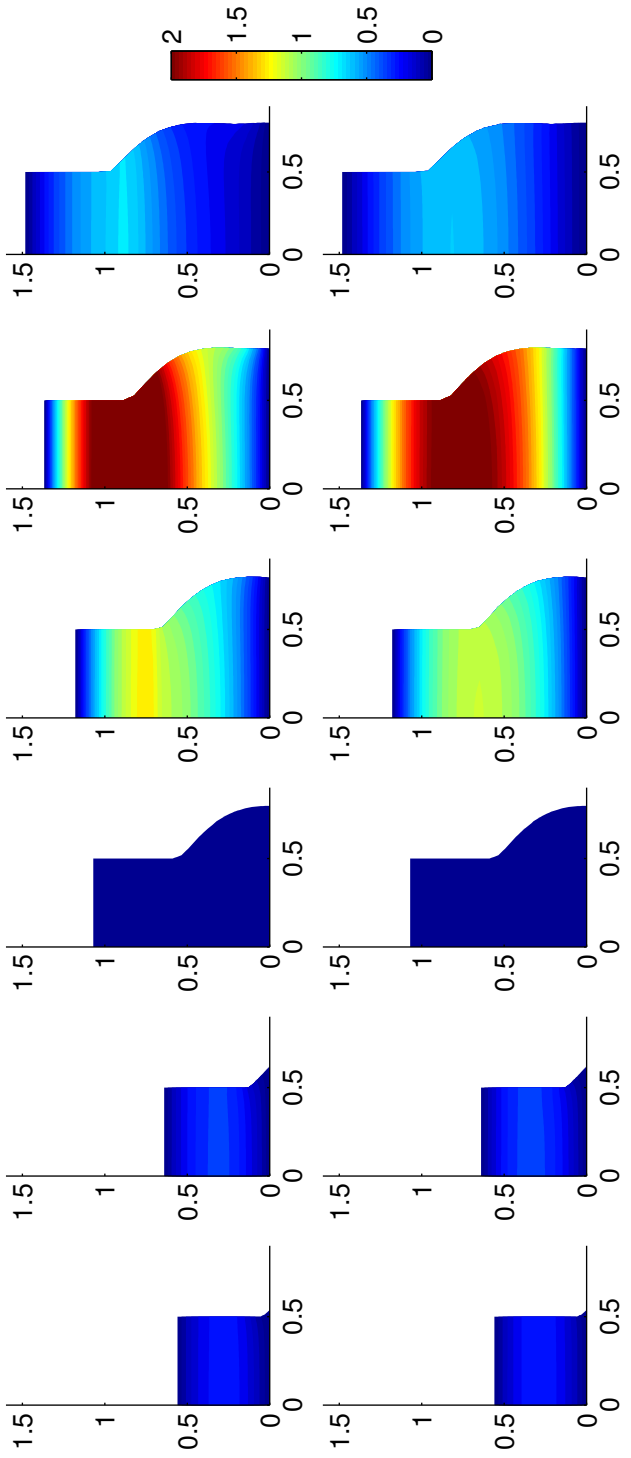

Figure 4.14: Solution of the two-dimensional diffusion-reaction system with the time-dependent spatial domain using the higher-order finite element (top) and reduced-order (bottom) model at $t = 0.5, 1, 3, 4, 4.5$, and 5.5.

References

Arkun, Y., Kayihan, F., 1998. A novel approach to full CD profile control of sheet-forming processes using adaptive PCA and reduced-order IMC design. Computers & Chemical Engineering 22, 945 – 962.

Armaou, A., Christofides, P.D., 2001a. Computation of empirical eigenfunctions and order reduction for nonlinear parabolic PDE systems with time-dependent spatial domains. Nonlinear Analysis: Theory, Methods and Applications 47, 2869–2874.

Armaou, A., Christofides, P.D., 2001b. Finite-dimensional control of nonlinear parabolic PDE systems with time-dependent spatial domains using empirical eigenfunctions. Applied Mathematics and Computer Science 11, 287–318.

Armaou, A., Christofides, P.D., 2001c. Robust control of parabolic PDE systems with time-dependent spatial domains. Automatica 37, 61–69.

Armaou, A., Christofides, P.D., 2002. Dynamic optimization of dissipative PDE systems using nonlinear order reduction. Chemical Engineering Science 57, 5083–5114.

Baker, J., Christofides, P.D., 2000. Finite-dimensional approximation and control of non-linear parabolic PDE systems. International Journal of Control 73, 439–456.

Bangia, A.K., Batcho, P.F., Kevrekidis, I.G., Karniadakis, G.E., 1997. Unsteady two-dimensional flows in complex geometries: Comparative bifurcation studies with global eigenfunction expansions. SIAM Journal on Scientific Computing 18, 775.

Bleris, L.G., Kothare, M.V., 2005. Reduced order distributed boundary control of thermal transients in microsystems. IEEE Transactions on Control Systems Technology 13, 853–867.

Chakravarti, S., Ray, W.H., 1999. Boundary identification and control of distributed parameter systems using singular functions. Chemical Engineering Science 54, 1181–1204.

Christofides, P.D., 2001. Nonlinear and robust control of PDE systems: Methods and applications to transport-reaction processes. Birkhäuser.

Deen, W.M., 1998. Analysis of transport phenomena. Oxford University Press, New York.

Fogleman, M., Lumley, J., Rempfer, D., Haworth, D., 2004. Application of the proper orthogonal decomposition to datasets of internal combustion engine flows. Journal of Turbulence 5, 023.

Gay, D.H., Ray, W.H., 1995. Identification and control of distributed parameter systems by means of the singular value decomposition. Chemical Engineering Science 50, 1519–1539.

Glavaski, S., Marsden, J.E., Murray, R.M., 1998. Model reduction, centering, and the Karhunen-Loève expansion, in: Proceedings of the 37th IEEE Conference on Decision and Control, pp. 2071–2076.

Loève, M., 1955. Probability Theory. Van Nostrand.

Mangold, M., Sheng, M., 2004. Nonlinear model reduction of a two-dimensional MCFC model with internal reforming. Fuel Cells 4, 68–77.

McPhee, J., Yeh, W., 2008. Groundwater management using model reduction via empirical orthogonal functions. Journal of Water Resources Planning and Management 134, 161–170.

Ng, J., Dubljevic, S., 2011. Optimal control of convection-diffusion process with time-varying spatial domain: Czochralski crystal growth. Journal of Process Control 21, 1361–1369.

Ng, J., Dubljevic, S., 2012. Optimal boundary control of a diffusion-convection-reaction PDE model with time-dependent spatial domain: Czochralski crystal growth process. Chemical Engineering Science 67, 111–119.

Nie, Q., Joshi, Y., 2008. Multiscale thermal modeling methodology for thermoelectrically cooled electronic cabinets. Numerical Heat Transfer, Part A: Applications 53, 225–248.

Park, H.M., Cho, D.H., 1996. The use of the Karhunen-Loève decomposition for the modeling of distributed parameter systems. Chemical Engineering Science 51, 81–98.

Park, H.M., Jung, W.S., 2001. The Karhunen-Loève-Galerkin method for the inverse natural convection problems. International Journal of Heat and Mass Transfer 44, 155–167.

Park, H.M., Lee, J.H., 1998. A method of solving inverse convection problems by means of mode reduction. Chemical engineering science 53, 1731–1744.

Park, H.M., Lee, M.W., 2000. Boundary control of the Navier-Stokes equation by empirical reduction of modes. Computer methods in applied mechanics and engineering 188, 165–186.

Park, H.M., Lim, J.Y., 2009. A reduced-order model of the low-voltage cascade electroosmotic micropump. Microfluidics and Nanofluidics 6, 509–520.

Raimondeau, S., Vlachos, D., 2000. Low-dimensional approximations of multiscale epitaxial growth models for microstructure control of materials. Journal of Computational Physics 160, 564–576.

Ray, W.H., Seinfeld, J.H., 1975. Filtering in distributed parameter systems with moving boundaries. Automatica 11, 509–515.

Reddy, J.N., Gartling, D.K., 2010. The finite element method in heat transfer and fluid dynamics. CRC.

Shvartsman, S.Y., Kevrekidis, I.G., 1998. Nonlinear model reduction for control of distributed systems: A computer-assisted study. AIChE Journal 44, 1579–1595.

Sirovich, L., 1987. Turbulence and the dynamics of coherent structures. I-Coherent structures. II-Symmetries and transformations. III-Dynamics and scaling. Quarterly of applied mathematics 45, 561–571.

Sirovich, L., Park, H., 1990. Turbulent thermal convection in a finite domain: Part I. Theory. Physics of Fluids A: Fluid Dynamics 2, 1649–1658.

Theodoropoulou, A., Zafiriou, E., Adomaitis, R.A., 1999. Inverse model-based real-time control for temperature uniformity of RTCVD. IEEE Transactions on Semiconductor Manufacturing 12, 87–101.

Wang, P.K.C., 1990. Stabilization and control of distributed systems with time-dependent spatial domains. Journal of Optimization Theory and Applications 65, 331–362.

Wang, P.K.C., 1995. Feedback control of a heat diffusion system with time-dependent spatial domain. Optimal control applications & methods 16, 305–320.

Zheng, D., Hoo, K.A., 2002. Low-order model identification for implementable control solutions of distributed parameter systems. Computers & chemical engineering 26, 1049–1076.

Zheng, D., Hoo, K.A., 2004. System identification and model-based control for distributed parameter systems. Computers & chemical engineering 28, 1361–1375.

Zhou, X.G., Zhang, X.S., Wang, X., Dai, Y.C., Yuan, W.K., 2001. Optimal control of batch electrochemical reactor using KL expansion. Chemical Engineering Science 56, 1485–1490.

Chapter 5

Low-order Optimal Regulation of Parabolic PDEs with Time-dependent Domain

5.1 Introduction

The synthesis and treatment procedures in many industrial plants including chemical, petrochemical and pharmaceutical processes, lead to changes in the shape and material properties. This change in material can be characterized by transport phenomena associated with the material deformation, phase change mechanism, generation and consumption of chemical species through chemical reactions, heat and mass transfer. Mathematically, a broad collection of these processes are modelled by application of conservation laws and yield models in the form of moving boundary parabolic partial differential equations (PDEs). Methods for control of linear parabolic PDEs have been extensively studied in the past and have mainly focused on process systems with fixed spatial domains and boundary and/or distributed actuations. Specifically, the functional analytic formulation using semigroup theory and related con-

cepts have proven to be a powerful tool for system analysis and control design (Curtain and Zwart, 1995; Luo et al., 1999). Regarding process models with moving boundaries, it is established that parabolic PDE systems with time-varying domains are inherently nonautonomous (Kloeden et al., 2008). In this context, there are several contributions which formulate the solutions to nonautonomous parabolic PDE systems with fixed spatial domain in terms of two-parameter semigroups which resemble the standard one-parameter semigroup generated by time-invariant parabolic operators (Lasiecka, 1980; Pazy, 1983; Acquistapace and Terreni, 1987). However, in general an analytic expression for the two-parameter semigroup describing the nonautonomous system behaviour can not be found, which prevents direct analysis and controller synthesis. In addition, only few contributions have reported the study of parabolic PDEs with time-varying domain, in which main results are focused on establishing existence and regularity properties of the solution. These include development of transformations to map the PDE onto a new time invariant spatial domain (Baconneau and Lunardi, 2004; Burdzy et al., 2004; Lunardi, 2004) and evolution of continuously differentiable diffeomorphisms (Kloeden et al., 2008, 2009). Among contributions along this line, a design of nonlinear distributed state observers for systems with moving boundaries using stochastic methods (Ray and Seinfeld, 1975) is notable. In particular, Wang (1990) studied stabilization and optimal control problem of such systems and later synthesized the linear optimal controller for thermal gradient regulation of crystal growth processes (Wang, 1995). Ng and Dubljevic presented the PDE on a moving boundary as an abstract evolution equation on an infinite-dimensional function space with nonautonomous parabolic opera-

tor which generates a two-parameter semigroup. With this formulation, they posed the time-varying optimal control (Ng et al., 2013) and optimal boundary control (Ng and Dubljevic, 2012) problems for regulation of a parabolic PDE. However, the setting in (Ng et al., 2013; Ng and Dubljevic, 2012) accounts only for a well-defined 1D or 2D time-varying trivial square domain while more practically motivated and physically relevant cases of irregular domain evolution are not addressed.

Another notable approach in the linear/semilinear PDE control area is the backstepping method emerging from nonlinear finite-dimensional control systems synthesis. In this methodology, a Volterra-type integral transformation is used to transform the PDE to a suitably selected stable target system. The kernel of transformation is defined by the solution of the kernel PDE that is of higher-order in space, leading to a state-feedback control law (Krstic and Smyshlyaev, 2008). This technique provides a framework to handle a large class of distributed parameter systems controlled at the boundary, however, the complexity associated with finding the solution of the kernel PDE for distributed systems described in 2D or 3D spaces prevents the use of this method for such problems.

Dissipative parabolic PDE systems have the property that the eigenspectrum of the spatial differential operator can be partitioned into a finite- dimensional slow subspace and the infinite-dimensional fast and stable complement, which implies that the dynamic behavior of such processes can be approximately described by finite-dimensional systems. Hence, if eigenfunctions of the parabolic operator can be expressed explicitly, one can use Galerkin's method to derive a reduced-order model (ROM) in terms of ordinary differen-

tial equations (ODEs) that accurately describe the dominant dynamics of the distributed parameter system and subsequently use it for the controller synthesis. Low-dimensional model identification of distributed parameter systems governed by parabolic PDEs attracted attention of a significant number of researchers in recent years. Among many, the most notable contributions came from Gay and Ray (1995); Chakravarti and Ray (1999); Park and Cho (1996); Christofides (2001); Armaou and Christofides (2002); Zheng and Hoo (2002, 2004). However, there is no analytic solution to the operator eigenvalue problem in general, the examples being the nonlinear spatial operator or problems with nontrivial geometric domain. In such cases, a well-known approach in the extraction of spatial characteristics (modes) of distributed parameter systems is the use of statistical tools, specifically the Karhunen-Loève (KL) decomposition on an ensemble of solutions of the system obtained by numerical resolution or experiments (Park and Cho, 1996). These modes, known as empirical eigenfunctions, can be adopted as the basis set of functions in the Galerkin's method to find a reduced-order model. This approach is widely used in the derivation of accurate reduced-order approximations of many distributed parameter systems, see for example Shvartsman and Kevrekidis (1998); Theodoropoulou et al. (1999); Baker and Christofides (2000) for diffusion-reaction systems, Arkun and Kayihan (1998) for sheet-forming processes, Mangold and Sheng (2004) for molten carbonate fuel cell model, Bleris and Kothare (2005) for thermal microsystem models and McPhee and Yeh (2008) for ground-water flow model.

To obtain a reduced-order model of parabolic PDE systems with a moving boundary domain, Armaou and Christofides (2001a) used a mathematical

transformation to represent the PDE on a time-invariant spatial domain and applied Karhunen-Loève decomposition to find the set of eigenfunctions on the fixed domain. In application, they used this approach in the nonlinear feedback (Armaou and Christofides, 2001b) and robust (Armaou and Christofides, 2001c) control of 1D reaction-diffusion systems based on the use of Galerkin's method. This approach cannot be used in general, since the mathematical transformation does not always have an analytical form, e.g. for nontrivial geometry. In Chapter 4 a more generalized approach to reduce the order of PDE systems with time-varying domain is proposed, in which the transformation that preserves the space-invariant properties of PDE solutions is found and the ensemble of the solution to the PDE is mapped to a selected fixed reference configuration. Subsequently, KL decomposition is applied on the mapped data to extract a low-dimensional set of eigenfunctions that contains most of the energy of the system on the fixed domain. These eigenfunctions are mapped on the time-varying domain using inverse transformation and as a result, a set of time-varying empirical eigenfunctions are obtained that can be used in Galerkin's method.

In this Chapter, a methodology is developed to design an observer and to find an optimal control law for output tracking of linear parabolic distributed systems with nontrivial time-varying domain. Since the boundary actuation of PDE systems rather than the distributed input as in Chapter 4 is more realistic in applications, the boundary input control problem is formulated as finding the appropriate state-space representation of the PDE system. Then, the proposed method of model order reduction by empirical eigenfunctions on the time-varying domain is used. Although the approach in Chapter 4

can be used for general nonlinear parabolic PDE systems, we consider the order reduction of boundary actuated linear dissipative distributed parameter systems with subsequent realization of observer to synthesize a linear optimal output tracking controller. Finally, numerical results are prepared for the 2D model of temperature distribution in the industrially relevant Czochralski (CZ) crystal growth process.

5.2 Mathematical Formulation

In this section, the mathematical aspects of the proposed method are reviewed. In particular, a general description of the parabolic PDE on the moving boundary domain and boundary actuation is presented. Then the order reduction methodology is briefly reviewed followed by the optimal control formulation. Finally, the design of the state observer is considered.

5.2.1 Model Description

We are interested in the model dynamics of an extensive property

$$G(t) = \int_{\Omega(t)} \rho(\xi, t)\sigma x(\xi, t) d\Omega$$

given by the intensive property $x(\xi, t)$ at each point $\xi \in \Omega(t) \subset \mathbb{R}^n$ at time $t \in [0, t_f]$, where $\rho(\xi, t)$ is density and σ is a constant. The body $\Omega(t)$ under consideration has the velocity $v(\xi, t)$ and its boundary is denoted by $\Gamma(t)$. With the use of the Leibniz integral rule and divergence theorem, conservation of the property $G(t)$ for continuous media ($\nabla \cdot v = 0$) is governed by the following

parabolic partial differential equation (Ng et al., 2013):

$$\rho\sigma\frac{\partial x}{\partial t} = \nabla\cdot(\kappa\nabla x) - \rho\sigma v\cdot\nabla x \tag{5.1}$$

where κ is diffusivity. This equation describes the differential form of a diffusion-convection process dynamics in terms of the property (state) $x(\xi,t)$ in the time-varying domain $\Omega(t)$. Initial conditions are given by $x(\xi,0) = x_0(\xi)$ and actuations $q_i(t)$ are applied to m portions of the domain boundary in the following form:

$$\kappa n\cdot\nabla x = q_i \text{ on } \Gamma_i^{\mathrm{a}} \text{ for } i = 1,2,\cdots,m \tag{5.2}$$

Other boundary conditions are given as Neumann or Dirichlet boundary conditions, respectively as:

$$\begin{aligned}\kappa n\cdot\nabla x &= 0 \text{ on } \Gamma^{\mathrm{n}}\\ x &= 0 \text{ on } \Gamma^{\mathrm{d}}\end{aligned} \tag{5.3}$$

In these equations n is the normal outward vector at each point on the $\Gamma(t)$.

It is assumed that the evolution of the domain $\Omega(t)$ is smooth and known *a priori*, as it can be easily measured in many chemical and material process systems. In the example of the model of industrial CZ semiconductor crystal growth, there are robust control practices in achieving a desired crystal shape by manipulating the pulling rate of the crystal from the melt and other control inputs (see Abdollahi et al. (2014) and series of studies by Gevelber and Stephanopoulos (1987); Gevelber et al. (1988); Gevelber (1994a,b) for more details). Hence, the PDE domain evolution is considered independent of the

thermal field and the mentioned assumption is valid in this case. Furthermore, we assume that the solution of the PDE (5.1) is unique and sufficiently smooth.

5.2.2 Boundary control formulation

In many relevant control applications, boundary actuation is more realistic than distributed control within spatial domain. The following formulation, motivated by Fattorini (1968); Curtain (1985); Park and Cho (1996), converts the boundary control problem to a distributed control problem. In particular, the transformation:

$$x(\xi,t) = p(\xi,t) + \sum_{i=1}^{m} b_i(\xi,t) q_i(t) \tag{5.4}$$

introduces the new state variable $p(\xi,t)$ along with m functions $b_i(\xi,t)$ that determine the spatial contribution of each actuation $q_i(t)$, where m is the number of actuators on the boundary, see (5.2). Rewriting (5.1-5.3) leads to the following PDE with initial and boundary conditions:

$$\begin{aligned}
\rho\sigma\frac{\partial p}{\partial t} &= \nabla\cdot(\kappa\nabla p) - \rho\sigma v\cdot\nabla p - \rho\sigma\sum_{i=1}^{m} b_i\dot{q}_i \\
p(\xi,0) &= x_0(\xi) \\
\kappa n\cdot\nabla p &= 0 \text{ on } \Gamma^{\mathrm{n}}\bigcup_{i=1}^{m}\Gamma_i^{\mathrm{a}} \\
p &= 0 \text{ on } \Gamma^{\mathrm{d}}
\end{aligned} \tag{5.5}$$

providing that the function $b_i(\xi, t)$ satisfies

$$\begin{aligned}
\rho\sigma\frac{\partial b_i}{\partial t} &= \nabla\cdot(\kappa\nabla b_i) - \rho\sigma v\cdot\nabla b_i \\
b_i(\xi,0) &= 0 \\
\kappa n\cdot\nabla b_i &= 1 \text{ on } \Gamma_i^{\mathrm{a}} \\
\kappa n\cdot\nabla b_i &= 0 \text{ on } \Gamma^{\mathrm{n}} \\
b_i &= 0 \text{ on } \Gamma^{\mathrm{d}}
\end{aligned} \tag{5.6}$$

for $i = 1, 2, \cdots, m$ with over dot representing differentiation with respect to time. Note that (5.5) is a distributed parameter system actuated by distributed inputs $\dot{q}_i$ and functions $b_i(\xi, t)$ are the solutions to (5.6). Equations (5.5) can be written in the state-space form as

$$\begin{aligned}
\frac{\partial p}{\partial t} &= \mathcal{A}p - \bar{B}u \\
p(\xi,0) &= x_0(\xi)
\end{aligned} \tag{5.7}$$

where $\mathcal{A}$ is the spatial differential operator with given boundary conditions, $\bar{B} = [b_1\ b_2\ \cdots\ b_m]$ and

$$u = \dot{q} = [\dot{q}_1\ \dot{q}_2\ \cdots\ \dot{q}_m]^T \tag{5.8}$$

5.2.3 Order reduction of the infinite-dimensional system

In this section the reduced-order model of the infinite-dimensional system described by (5.7) is developed. To this end, we follow the methodology proposed in Chapter 4 for the PDE given by (5.5). This approach, schematically depicted in Fig. 5.1, yields to a set of time-varying empirical eigenfunctions $\{\phi_j(\xi,t)\}, j = 1,2,\cdots,M$ that capture the most energy of the ensemble of solutions (snapshots) $\{p(\xi,t_i)\}, i = 1,2,\cdots,N \gg M$, of (5.5). The fact that eigenfunctions are inherently time-varying is due to their spatially time-dependent domain.

There exists the invertible smooth mapping $\mathcal{T}(t)$ that maps the domain $\Omega(t)$ to a fixed reference configuration $\bar{\Omega}$ as $\mathcal{T}(t) : \xi \in \Omega(t) \mapsto \bar{\xi} \in \bar{\Omega}$ at each time t as shown in Fig.5.2, with the coordinate transformation $\bar{\xi} = \bar{\xi}(\xi,t)$ and the Jacobian matrix $[J(t)] = \frac{\partial \bar{\xi}}{\partial \xi}$.

Also, the transformation $\mathcal{S}(t_i)$ given by $\bar{p}_i(\bar{\xi}) = p(\xi,t_i)J_i^{-1}$ maps the snapshot $p(\xi,t_i)$ on the moving boundary domain to $\bar{p}_i(\bar{\xi})$ on the fixed domain such that $\sigma p d\Omega = \sigma \bar{p} d\bar{\Omega}$, that is the space-invariant property $\sigma p d\Omega$ is preserved. Given the ensemble $\{\bar{p}_i(\bar{\xi})\}$ on the reference configuration, Karhunen-Loève (KL) decomposition can be applied to find the empirical eigenfunctions $\{\bar{\phi}_j(\bar{\xi})\}$ that can approximate each snapshot. KL decomposition is a procedure for representation of a stochastic field with a minimum number of degrees of freedom (Loève, 1955; Sirovich and Park, 1990).

Once the set of M eigenfunctions $\{\bar{\phi}_j(\bar{\xi})\}$ is found, they can be transformed to the time-varying domain $\Omega(t_i)$ at each time t_i using the inverse of $\mathcal{S}(t_i)$.

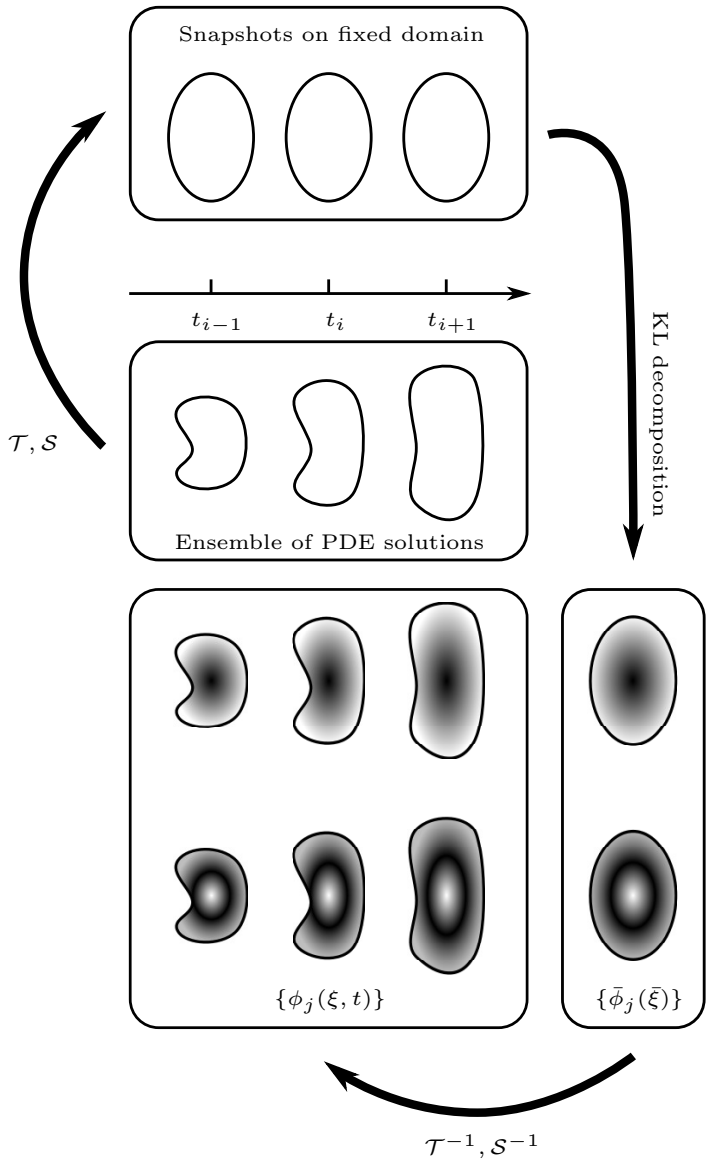

Figure 5.1: Schematics of order-reduction approach: the transformations $\mathcal{T}(t)$ and $\mathcal{S}(t)$ map geometry and state of the PDE solution to a fixed domain. Using KL decomposition, empirical eigenfunctions $\{\bar{\phi}_j(\bar{\xi})\}$ are extracted on the fixed domain and transformed to the time-varying domain by the application of $\mathcal{T}$ and $\mathcal{S}$ resulting in the time-varying basis $\{\phi_j(\xi, t)\}$.

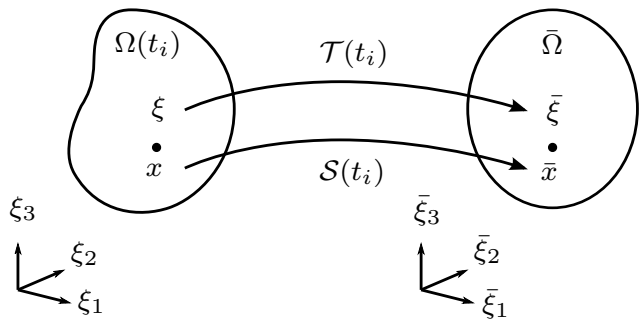

Figure 5.2: At each time instance t_i, $\mathcal{T}(t_i)$ maps moving boundary domain Ω to the fixed domain $\bar{\Omega}$ and the transformation $\mathcal{S}(t_i)$ maps the state $p(\xi, t_i)$ from time-varying domain to $\bar{p}_i(\xi)$ on the fixed domain

Therefore, one has the basis of M time-varying eigenfunctions $\{\phi_j(\xi, t)\}$ which can be used to approximate the state p on the moving boundary domain $\Omega(t)$ as

$$p(\xi, t) = \sum_{i=1}^{M} a_i(t)\phi_i(\xi, t) \tag{5.9}$$

Finally, Galerkin's method is used to obtain the reduced-order model by replacing (5.9) in (5.7) and projecting on the basis ϕ_j to get:

$$\begin{aligned} \dot{a}(t) &= A(t)a(t) + B(t)u(t) \\ a(0) &= D^{-1}(0)y^0 \end{aligned} \tag{5.10}$$

with terms defined as follows:

$$
\begin{aligned}
a(t) &= [a_1(t)\ a_2(t)\ \cdots a_M(t)]^T \\
A(t) &= D^{-1}(t)H(t), \\
B(t) &= D^{-1}(t)F(t) \\
D_{ij}(t) &= \langle \phi_i, \phi_j \rangle \\
H_{ij}(t) &= \left\langle \mathcal{A}\phi_i - \dot{\phi}_i, \phi_j \right\rangle \\
F_{ij}(t) &= -\langle b_i, \phi_j \rangle \\
y_i^0 &= \langle x_0, \phi_i(\xi, 0) \rangle
\end{aligned}
$$

Equations (5.10) represent the reduced-order form of (5.7), which is a linear time-varying model of the process.

5.2.4 Optimal output tracking formulation

The control objective is to find a control law $u(t)$ based on the reduced-order model (5.10), for which the state of the PDE system $x(\xi_i, t) = y_i$ at arbitrary points ξ_i, $i = 1, 2, \cdots, s$, track desired reference trajectories $y_i^r = x^r(\xi_i, t)$. Since the state $x(\xi, t)$ is described by $p(\xi, t)$ and boundary actuations $q_i(t)$ (see (5.4)), the extended state is introduced as $a^e = \left[a^T\ q^T\right]^T$ and the boundary control problem is given by

$$\dot{a}^e(t) = A^e(t)a^e(t) + B^e(t)u(t) \tag{5.11}$$

$$a^e(0) = \left[a^T(0)\ q^T(0)\right]^T \tag{5.12}$$

where

$$A^e(t) = \begin{bmatrix} A(t) & 0 \\ 0 & 0 \end{bmatrix}, \quad B^e(t) = \begin{bmatrix} B(t) \\ I \end{bmatrix}$$

and I is the identity matrix. Now one may evaluate the state (5.4) at points ξ_j to get:

$$y(t) = C(t)a^e(t) \tag{5.13}$$

which is considered as the system output equation, with

$$C(t) = \begin{bmatrix} \Phi(t) \ \bar{C}(t) \end{bmatrix}$$
$$\Phi_{ij}(t) = \phi_i(\xi_j, t) \quad \bar{C}_{ij}(t) = b_i(\xi_j, t)$$

Equations (5.11,5.13) describe the extended system with an initial condition (5.12).

One can formulate the control problem as classical linear optimal output tracking control problem for the process described by equations (5.11-5.13) by minimizing the finite time linear quadratic cost functional

$$J = \frac{1}{2}\tilde{y}^T(t_f)P\tilde{y}(t_f) + \frac{1}{2}\int_0^{t_f} \left(\tilde{y}(t)^T Q\tilde{y}(t) + u(t)^T Ru(t)\right) dt$$

where $\tilde{y} = y - y^r$. The optimal control is a time-varying linear state-feedback control law given by (Lewis et al., 2012):

$$u(t) = -\kappa(t)a^e(t) + \omega(t) \tag{5.14}$$

where $\kappa(t) = R^{-1}B^{eT}(t)S(t)$, $\omega(t) = R^{-1}B^{eT}(t)w(t)$, the real symmetric and

positive-definite matrix S is the solution of the differential Riccati equation

$$\begin{aligned} -\dot{S}(t) =& A^{eT}(t)S(t) + S(t)A^{e}(t) - S(t)B^{e}(t)R^{-1}B^{eT}(t)S(t) + C^{T}(t)QC(t), \\ S(t_f) =& C^{T}(t_f)PC(t_f) \end{aligned}$$

and the vector $w(t)$ is the solution of the linear vector differential equation

$$\begin{aligned} -\dot{w}(t) =& \left[A^{e}(t) - B^{e}(t)R^{-1}B^{eT}(t)S(t)\right]^{T} w(t) + C^{T}(t)Qy^{r}(t) \\ w(t_f) =& C^{T}(t_f)Py^{r}(t_f) \end{aligned}$$

Replacing (5.14) into (5.11) yields the following:

$$\dot{a}^{e}(t) = (A^{e}(t) - B^{e}(t)\kappa(t))a^{e}(t) + B^{e}(t)\omega(t)$$

Let $\bar{A}(t) = A^{e}(t) - B^{e}(t)\kappa(t)$, the controllability of the process results in exponential stability of $\dot{a}^{e}(t) = \bar{A}(t)a^{e}(t)$ which guarantees the existence of a continuously differentiable symmetric bounded positive definite matrix $\Pi_1(t)$ that satisfies the differential Lyapunov equation

$$-\dot{\Pi}_1(t) = \Pi_1(t)\bar{A}(t) + \bar{A}^{T}(t)\Pi_1(t) + \chi_1(t)$$

where $\chi_1(t)$ is continuous, symmetric, and positive definite. Hence, the candidate $V_1(a^e, t) = a^{eT}\Pi_1 a^e$ is a Lyapunov function with time-derivative $\dot{V}_1 = -a^{eT}\chi_1 a^e$.

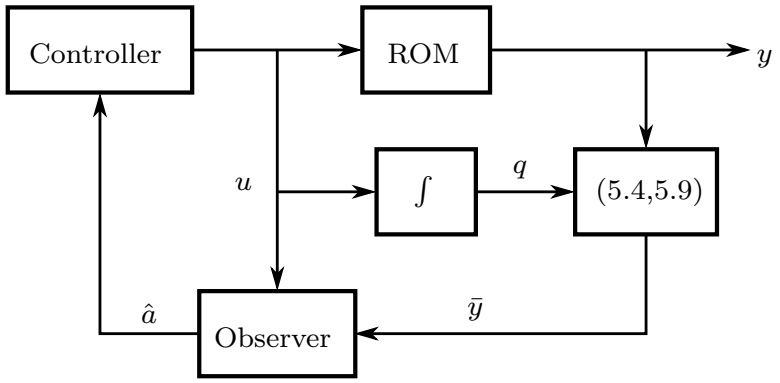

Figure 5.3: Block diagram representation of the controller-observer setup.

5.2.5 Observer Design

In practice, state variables may not be accessible for the application of state-feedback control (5.14), specifically, the ROM state $a(t)$ cannot be measured or physically interpreted. However, the finite-dimensional representation (5.10) provides tools for state estimation where the measurements of physical properties are usually available at domain boundaries in applications. In this section, a state observer is designed to be used in the closed-loop setup depicted in Fig. 5.3. This controller-observer configuration is chosen due to the fact that the PDE deriving signal $q(t)$ can be determined by integration of input signal $u(t)$ from (5.8), hence, there is no need to estimate $q(t)$ in the extended state $a^e(t)$. Also, having the measurement $y(t)$ and the knowledge of $q(t)$, one can determine the new output variable $\bar{y}(t) = \Phi(t)a(t)$ from (5.4,5.9).

Now the open-loop Luenberger-type observer with time-varying gain $\lambda(t)$ is introduced as:

$$\dot{\hat{a}}(t) = A(t)\hat{a}(t) + B(t)u(t) + \lambda(t)(\bar{y}(t) - \Phi(t)\hat{a}(t))$$

with the estimation error $e(t) = a(t) - \hat{a}(t)$. It can be readily shown that the error dynamics is given by

$$\dot{e}(t) = (A(t) - \lambda(t)\Phi(t))e(t) \tag{5.15}$$

Although the matrices A and Φ are time-dependent, the continuous observer gain $\lambda(t)$ can be evaluated at each time instance t such that $A(t) - \lambda(t)\Phi(t)$ becomes time-independent with (stable) eigenvalues placed at desired pre-specified values. Therefore, there exists symmetric positive definite time-independent matrices Π_2 and χ_2 that satisfy Lyapunov equation

$$\Pi_2(A(t) - \lambda(t)\Phi(t)) + (A(t) - \lambda(t)\Phi(t))^T\Pi_2 + \chi_2 = 0$$

and the Lyapunov function $V_2(a) = a^T\Pi_2 a$ with time-derivative $\dot{V}_1 = -a^T\chi_2 a$ implies the exponential stability of (5.15).

Now, the state-feedback gain $\kappa(t)$ is partitioned as

$$u(t) = -\begin{bmatrix} \kappa_1(t) & \kappa_2(t) \end{bmatrix}\begin{bmatrix} \hat{a}(t) \\ q(t) \end{bmatrix} + \omega(t)$$

which develops the following state-equation for the overall system shown in Fig. 5.3:

$$\begin{bmatrix} \dot{a} \\ \dot{q} \\ \dot{e} \end{bmatrix} = \begin{bmatrix} A - B\kappa_1 & -B\kappa_2 & B\kappa_1 \\ -\kappa_1 & -\kappa_2 & \kappa_1 \\ 0 & 0 & A - \lambda\Phi \end{bmatrix}\begin{bmatrix} a \\ q \\ e \end{bmatrix} + \begin{bmatrix} B \\ I \\ 0 \end{bmatrix}\omega \tag{5.16}$$

Consider the continuously differentiable function

$$V(a,q,e,t) = \begin{bmatrix} a^T & q^T & e^T \end{bmatrix} \begin{bmatrix} \Pi_1 & 0 \\ 0 & \Pi_2 \end{bmatrix} \begin{bmatrix} a \\ q \\ e \end{bmatrix}$$

which is a valid Lyapunov function candidate. It can be shown that its time derivative is given by

$$\dot{V} = -\begin{bmatrix} a^T & q^T & e^T \end{bmatrix} \chi \begin{bmatrix} a \\ q \\ e \end{bmatrix}$$

where

$$\chi = \begin{bmatrix} \chi_1 & -2\Pi_1 \begin{bmatrix} B\kappa_1 \\ \kappa_1 \end{bmatrix} \\ 0 & \chi_2 \end{bmatrix}$$

All matrices defining χ are continuous and bounded. Moreover, at each time instance the eigenvalues of χ are the union of eigenvalues of positive definite matrices χ_1 and χ_2. So χ is positive definite and V is indeed a Lyapunov function that implies the exponential stability of the dynamics of (5.16). Thus inserting the observer does not affect the original state-feedback law and it can be designed separately.

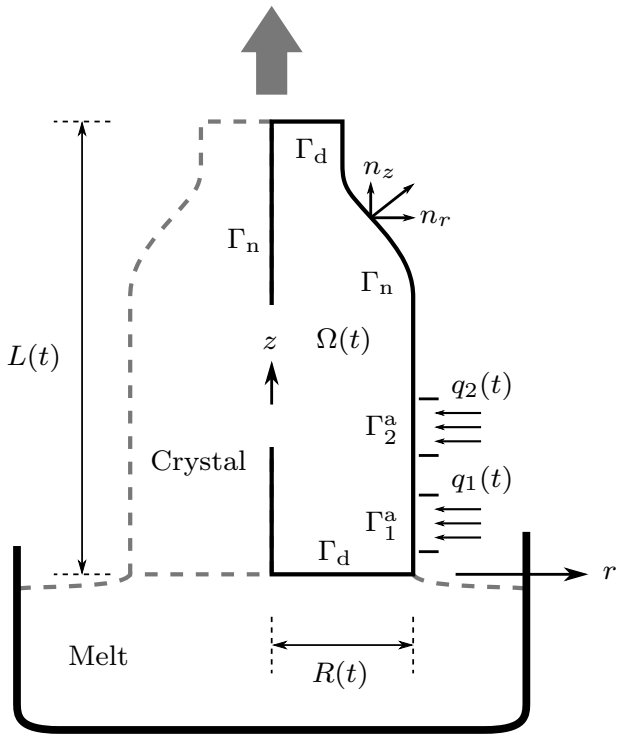

Figure 5.4: Schematic representation of axisymmetric crystal domain in Czochralski growth process where $L(t)$ and $R(t)$ are the height and radius of crystal at time t, respectively.

5.3 Numerical Simulation

In this section, the results from previous section are applied to the 2D representation of the Czochralski crystal temperature boundary control problem depicted in Fig. 5.4. CZ process is one of the main methods in the manufacturing of semiconductor materials on a large-scale for the use in the high performance electronic devices. In this process, a pulling arm drags out the crystal rod vertically from the surface ($z = 0$) of a heated pool of melt contained in a crucible. One can observe that the shape of the gradually grown crystal is nontrivial.

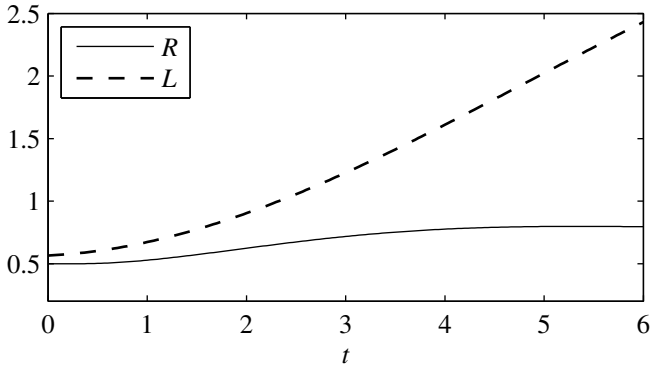

Figure 5.5: Domain evolution result from radius control strategy.

We consider the axisymmetric diffusive system described by the following nondimensionalized parabolic PDE (Derby et al., 1987; Ng et al., 2013):

$$\frac{\partial x}{\partial t} = k\left[\frac{1}{r}\frac{\partial}{\partial r}\left(r\frac{\partial x}{\partial r}\right) + \frac{\partial^2 x}{\partial z^2}\right] - \dot{L}\frac{\partial x}{\partial z} \tag{5.17}$$

for $x(r, z, t)$ being the temperature in the time-varying domain $\Omega(t)$ subject to boundary actuations $q_i(t)$ on two portions of the domain boundary Γ_i^{a}, $i = 1, 2$ and Neumann and Dirichlet boundary conditions. In (5.17), $k = 6.25$ is the dimensionless process parameter and $\dot{L}(t)$ represents the domain velocity which is the derivative of the height function $L(t)$ with respect to time. A simplified radius control strategy arising from geometric model provides the domain evolution in terms of $L(t)$ and $R(t)$ as shown in Fig. 5.5, see Abdollahi et al. (2014) for more details.

We developed a finite element model (FEM) that is used to find the solutions to the aforementioned PDE, as well as using as a process plant to apply the synthesized control. Since the geometry of the domain is time-varying and the evolution is known, the Arbitrary Lagrangian Eulerian (ALE) mesh

moving scheme is used in formulating FEM (Reddy and Gartling, 2010). The domain of interest is spatially discretized by 11×29 2D linear 4-node elements into 297 degrees of freedom. The evolution of the time-dependent set of ordinary differential equations obtained from the finite element discretization is realized by first-order implicit time integration with the time step $dt = 0.0333$. Figure 5.6 shows the schematics of moving elements and functions $b_1(r, z, t)$ and $b_2(r, z, t)$ obtained from the solutions to corresponding PDEs by FEM.

The reference configuration $\bar{\Omega}$ on which the solutions of (5.17) are mapped for the order reduction purpose is considered to be a rectangular with dimensions $\bar{R} = 0.7$ and $\bar{L} = 1.25$. We chose three empirical eigenfunctions which contains more than 99.9% of the energy of snapshots, to construct the ROM.

The temperature field in the grown crystal cannot be measured directly, however, boundary measurements are available by the use of sensing devices. To reconstruct the state of the reduced-order model of the CZ process, the temperature of a point on the outer surface of the crystal close (at the distance of 0.1) to the pulling arm (top of the crystal) is measured, this point can be considered on the crystal seed that is initially used to grow crystal on.

Thermal gradients near the melt interface in the grown crystal play a key role in the properties of the product. Structural defects in the form of dislocations can be generated by thermal stress, which is related to the thermal gradients near the interface (Jordan et al., 1984). Also, thermally induced stress can cause slip in the crystal structure. Stress analysis results have shown that thermal stress is largest at the crystal surface (Gevelber, 1994a).

We have chosen two target points close to the interface and crystal surface, namely at $z = 0.2$ and at distances 0.05 and 0.25 from the crystal surface.

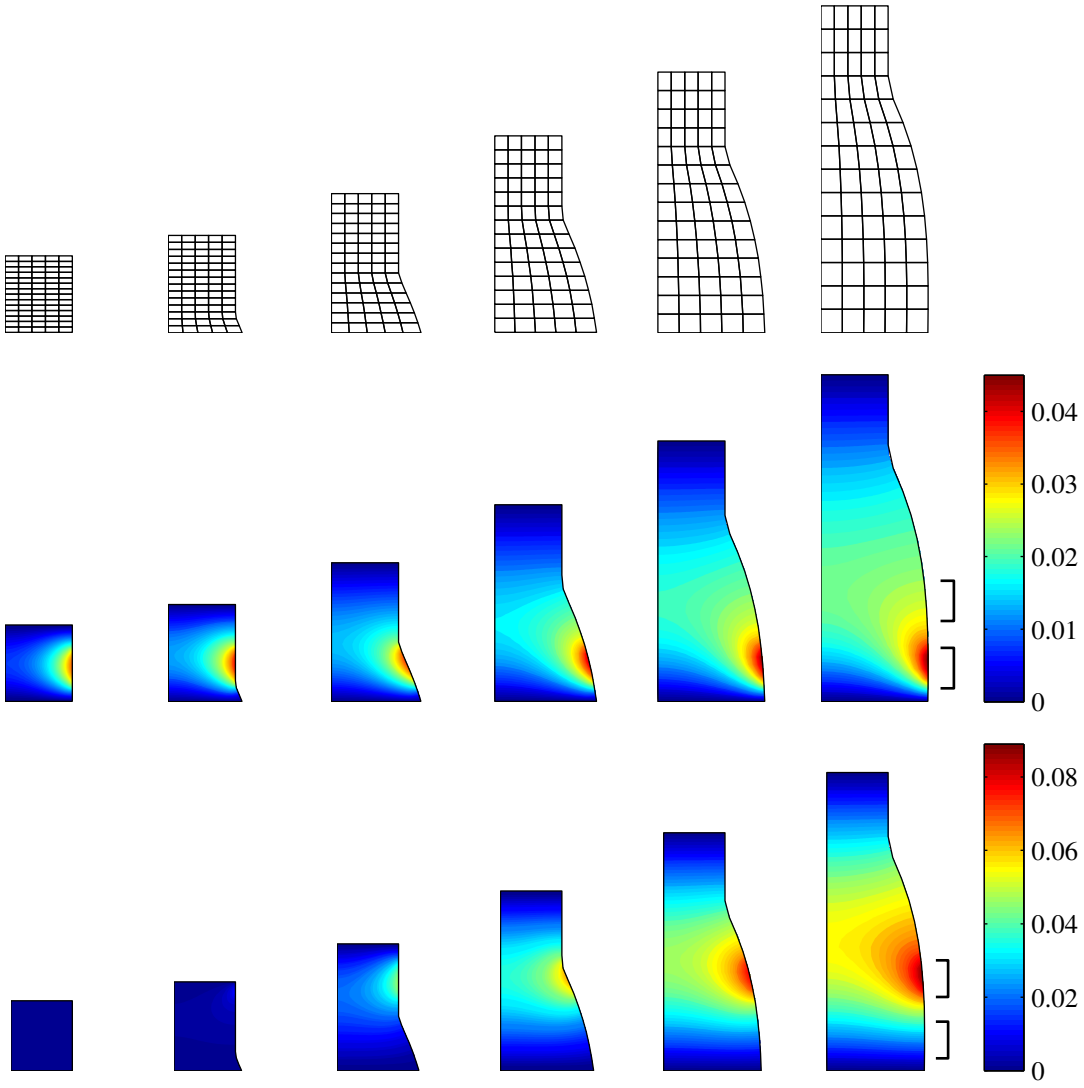

Figure 5.6: Finite element moving mesh (top) and functions $b_1(r, z, t)$ (middle) and $b_2(r, z, t)$ (bottom) at $t = 0.1, 1.27, 2.43, 3.63, 4.8,$ and 6.

The objective is to keep the dimensionless temperature at these target points $y(t)$ to track reference value of $y^r = \begin{bmatrix} -0.1 & -0.1 \end{bmatrix}^T$ which complies with the requirements for the thermal gradients. Hence, the optimal control problem is to find the control law to track the reference temperature at the target points. The input profiles $u(t)$ generated as the time-varying linear state-feedback

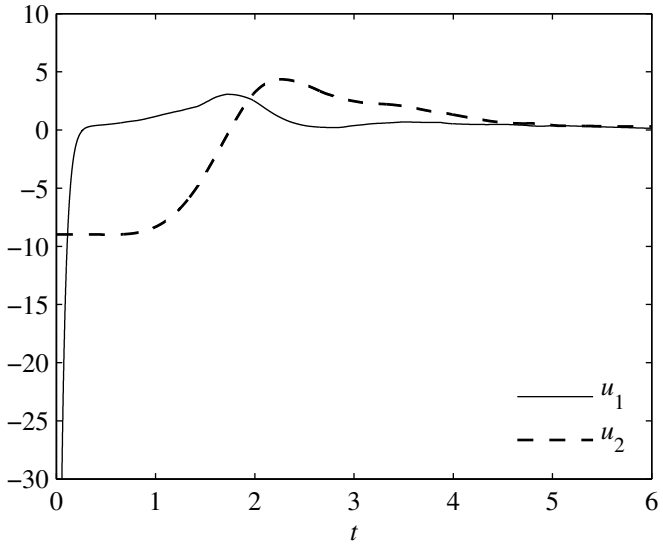

Figure 5.7: Optimal boundary inputs applied to the crystal.

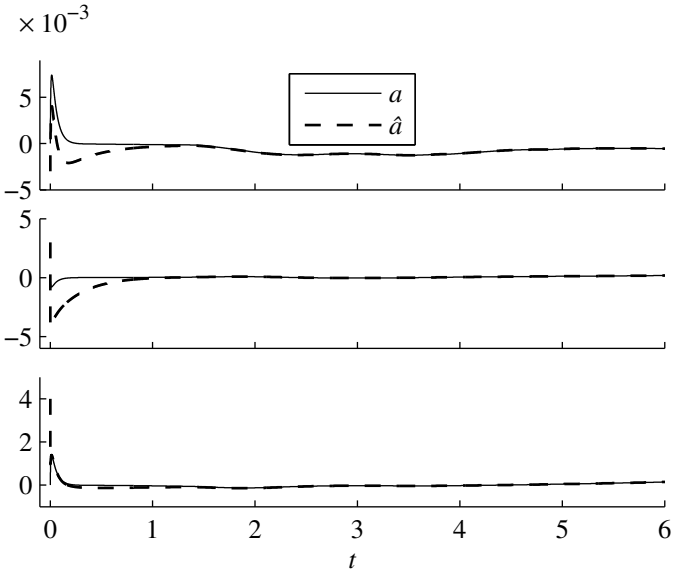

Figure 5.8: Evolution of the states of ROM and corresponding estimates.

control using the estimated state for the reduced-order system is shown in Fig. 5.7. Figure 5.8 shows the convergence of the estimated states to ROM

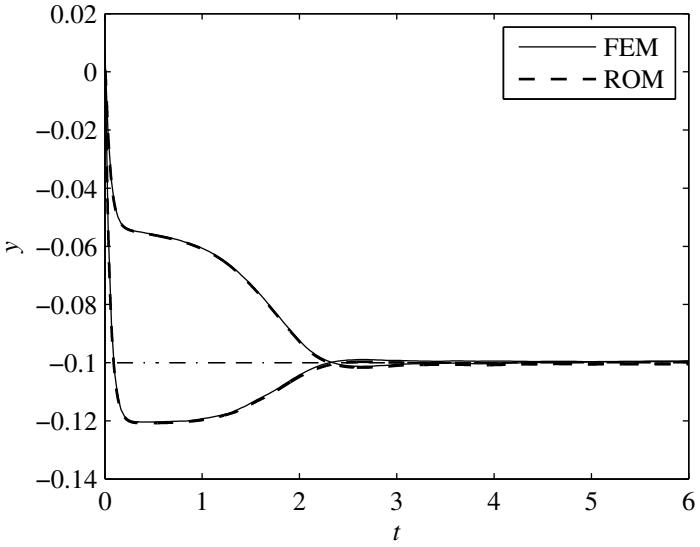

Figure 5.9: Outputs of the reduced-order model and finite element plant.

states when state-feedback control is applied to the system.

Figure 5.9 shows the closed-loop response of the reduced-order model as well as the response of the finite element. As it can be seen, the response of the system converges to the reference value. Also, there is a perfect match between the profiles of the two models showing the capability of the ROM to be used for controller design. Finally, the overall temperature profile of the crystal and target points are captured in Fig. 5.10 showing the evolution of the state $x(r, z, t)$ of the finite element plant.

5.4 Summary

This Chapter considers the state estimation and optimal control problem with boundary actuation for linear parabolic PDEs defined on time-dependent spatial domains. The formulation of time-varying parabolic system as a bound-

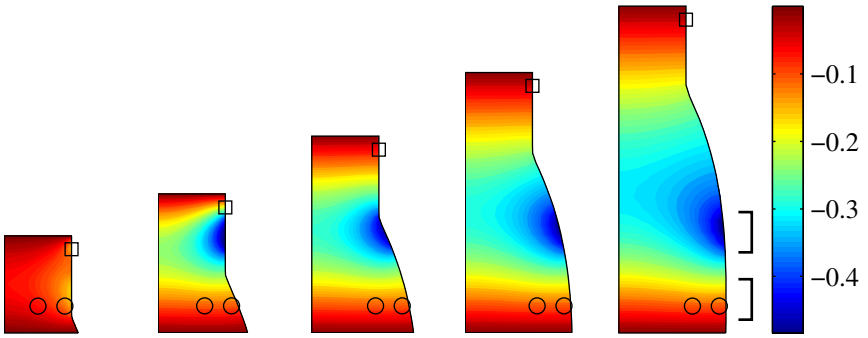

Figure 5.10: Dimensionless crystal temperature distribution from the FEM at $t = 1.27, 2.43, 3.63, 4.8,$ and 6. Temperature measurement is taken at the point indicated by square on the boundary and target points are shown by circles.

ary control problem enabled order reduction of the system by extracting the set of time-varying empirical eigenfunctions that capture the most energy of PDE snapshots and the utilization of Galerkin's method. The reduced-order model which is in the form of a linear time-varying system facilitated the Luenberger-type observer design and synthesis of a time-varying linear feedback controller based on a quadratic cost minimization. As an illustrative example, the Czochralski crystal growth process with the 2D crystal temperature distribution was considered and the proposed controller formulation was applied. The numerical results of the simulated system demonstrated the output tracking of the system in the time-dependent crystal by the optimal feedback controller through boundary actuation.

References

Abdollahi, J., Izadi, M., Dubljevic, S., 2014. Temperature distribution reconstruction in Czochralski crystal growth process. AIChE Journal 60, 2839–2852.

Acquistapace, P., Terreni, B., 1987. A unified approach to abstract linear nonautonomous parabolic equations, in: Rendiconti del Seminario Matematico della Universita di Padova, pp. 47–107.

Arkun, Y., Kayihan, F., 1998. A novel approach to full CD profile control of sheet-forming processes using adaptive PCA and reduced-order IMC design. Computers & Chemical Engineering 22, 945 – 962.

Armaou, A., Christofides, P.D., 2001a. Computation of empirical eigenfunctions and order reduction for nonlinear parabolic PDE systems with time-dependent spatial domains. Nonlinear Analysis: Theory, Methods and Applications 47, 2869–2874.

Armaou, A., Christofides, P.D., 2001b. Finite-dimensional control of nonlinear parabolic PDE systems with time-dependent spatial domains using empirical eigenfunctions. Applied Mathematics and Computer Science 11, 287–318.

Armaou, A., Christofides, P.D., 2001c. Robust control of parabolic PDE systems with time-dependent spatial domains. Automatica 37, 61–69.

Armaou, A., Christofides, P.D., 2002. Dynamic optimization of dissipative PDE systems using nonlinear order reduction. Chemical Engineering Science 57, 5083–5114.

Baconneau, O., Lunardi, A., 2004. Smooth solutions to a class of free boundary parabolic problems. Transactions of the American Mathematical Society 356, 987–1005.

Baker, J., Christofides, P.D., 2000. Finite-dimensional approximation and control of non-linear parabolic PDE systems. International Journal of Control 73, 439–456.

Bleris, L.G., Kothare, M.V., 2005. Reduced order distributed boundary control of thermal transients in microsystems. IEEE Transactions on Control Systems Technology 13, 853–867.

Burdzy, C., Chen, Z.Q., Sylvester, J., 2004. The heat equation in time dependent domains with insulated boundaries. Journal of mathematical analysis and applications 294, 581–595.

Chakravarti, S., Ray, W.H., 1999. Boundary identification and control of distributed parameter systems using singular functions. Chemical Engineering Science 54, 1181–1204.

Christofides, P.D., 2001. Nonlinear and robust control of PDE systems: Methods and applications to transport-reaction processes. Birkhäuser.

Curtain, R.F., 1985. On stabilizability of linear spectral systems via state boundary feedback. SIAM journal on control and optimization 23, 144–152.

Curtain, R.F., Zwart, H., 1995. An introduction to infinite-dimensional linear systems theory. Springer-Verlag.

Derby, J., Atherton, L., Thomas, P., Brown, R., 1987. Finite-element methods for analysis of the dynamics and control of Czochralski crystal growth. Journal of Scientific Computing 2, 297–343.

Fattorini, H.O., 1968. Boundary control systems. SIAM Journal on Control 6, 349–385.

Gay, D.H., Ray, W.H., 1995. Identification and control of distributed parameter systems by means of the singular value decomposition. Chemical Engineering Science 50, 1519–1539.

Gevelber, M.A., 1994a. Dynamics and control of the Czochralski process III. Interface dynamics and control requirements. Journal of crystal growth 139, 271–285.

Gevelber, M.A., 1994b. Dynamics and control of the czochralski process IV. Control structure design for interface shape control and performance evaluation. Journal of crystal growth 139, 286–301.

Gevelber, M.A., Stephanopoulos, G., 1987. Dynamics and control of the Czochralski process: I. Modelling and dynamic characterization. Journal of crystal growth 84, 647–668.

Gevelber, M.A., Stephanopoulos, G., Wargo, M.J., 1988. Dynamics and control of the czochralski process II. Objectives and control structure design. Journal of crystal growth 91, 199–217.

Jordan, A.S., Von Neida, A., Caruso, R., 1984. The theory and practice of dislocation reduction in GaAs and InP. Journal of Crystal Growth 70, 555–573.

Kloeden, P., Marín-Rubio, P., Real, J., 2008. Pullback attractors for a semilinear heat equation in a non-cylindrical domain. Journal of Differential Equations 244, 2062–2090.

Kloeden, P.E., Real, J., Sun, C., 2009. Pullback attractors for a semilinear heat equation on time-varying domains. Journal of Differential Equations 246, 4702–4730.

Krstic, M., Smyshlyaev, A., 2008. Boundary control of PDEs: A course on backstepping designs. SIAM, Philadelphia.

Lasiecka, I., 1980. Unified theory for abstract parabolic boundary problems– A semigroup approach. Applied Mathematics and Optimization 6, 287–333.

Lewis, F.L., Vrabie, D., Syrmos, V.L., 2012. Optimal control. Wiley (New York).

Loève, M., 1955. Probability Theory. Van Nostrand.

Lunardi, A., 2004. An introduction to parabolic moving boundary problems, in: Iannelli, M., Nagel, R., Piazzera, S. (Eds.), Functional analytic methods for evolution equations. Springer. volume 1855, pp. 371–399.

Luo, Z.H., Guo, B.Z., Morgül, Ö., 1999. Stability and stabilization of infinite-dimensional systems with applications. Springer.

Mangold, M., Sheng, M., 2004. Nonlinear model reduction of a two-dimensional MCFC model with internal reforming. Fuel Cells 4, 68–77.

McPhee, J., Yeh, W., 2008. Groundwater management using model reduction via empirical orthogonal functions. Journal of Water Resources Planning and Management 134, 161–170.

Ng, J., Aksikas, I., Dubljevic, S., 2013. Control of parabolic pdes with time-varying spatial domain: Czochralski crystal growth process. International Journal of Control , 1–12.

Ng, J., Dubljevic, S., 2012. Optimal boundary control of a diffusion-convection-reaction PDE model with time-dependent spatial domain: Czochralski crystal growth process. Chemical Engineering Science 67, 111–119.

Park, H.M., Cho, D.H., 1996. The use of the Karhunen-Loève decomposition for the modeling of distributed parameter systems. Chemical Engineering Science 51, 81–98.

Pazy, A., 1983. Semigroups of linear operators and applications to partial differential equations. Springer-Verlag.

Ray, W.H., Seinfeld, J.H., 1975. Filtering in distributed parameter systems with moving boundaries. Automatica 11, 509–515.

Reddy, J.N., Gartling, D.K., 2010. The finite element method in heat transfer and fluid dynamics. CRC.

Shvartsman, S.Y., Kevrekidis, I.G., 1998. Nonlinear model reduction for control of distributed systems: A computer-assisted study. AIChE Journal 44, 1579–1595.

Sirovich, L., Park, H., 1990. Turbulent thermal convection in a finite domain: Part I. Theory. Physics of Fluids A: Fluid Dynamics 2, 1649–1658.

Theodoropoulou, A., Zafiriou, E., Adomaitis, R.A., 1999. Inverse model-based real-time control for temperature uniformity of RTCVD. IEEE Transactions on Semiconductor Manufacturing 12, 87–101.

Wang, P.K.C., 1990. Stabilization and control of distributed systems with time-dependent spatial domains. Journal of Optimization Theory and Applications 65, 331–362.

Wang, P.K.C., 1995. Feedback control of a heat diffusion system with time-dependent spatial domain. Optimal control applications & methods 16, 305–320.

Zheng, D., Hoo, K.A., 2002. Low-order model identification for implementable control solutions of distributed parameter systems. Computers & chemical engineering 26, 1049–1076.

Zheng, D., Hoo, K.A., 2004. System identification and model-based control for distributed parameter systems. Computers & chemical engineering 28, 1361–1375.

Chapter 6

Conclusions and Future work

Moving boundary parabolic PDEs are models of a class of transport-reaction phenomena in a variety of processes and they describe the temporal and spatial profiles of state variables. Two systematic treatments are developed in this thesis for the general boundary control problem of such processes: PDE backstepping method and empirical order-reduction approach.

6.1 Conclusions

The PDE backstepping boundary control synthesis of one-dimensional heat equation on a time-varying domain is formulated in Chapter 2. The PDE system is transformed to an exponentially stable target system through the invertible Volterra-type integral transformation resulting in the two-dimensional time-varying PDE with time-dependant domain describing the transformation kernel. Then, a numerical solution to the kernel PDE is provided and simulated to demonstrate stabilization of the moving boundary unstable system.

In Chapter 3 the observer design of one-dimensional unstable parabolic PDE on a time-varying domain is formulated, where the observer gains are

determined by the use of backstepping methodology. This includes a Volterra integral transformation to transform the estimation error PDE to a prescribed exponentially stable target system. The kernel function of this transformation is described by a two-dimensional time-varying PDE on a moving boundary domain. Then, the designed observer is incorporated with the backstepping control in an output-feedback controller and the exponential stability of the closed-loop system is shown by Lyapunov theorem. Finally, numerical solutions to the kernel PDEs are provided and the output-feedback boundary stabilization of the unstable system is simulated to demonstrate the successful performance of the state observer.

Chapters 4 and 5 consider optimal boundary control of parabolic PDEs with nontrivial time-dependent domain using empirical modes. The method to obtain a set of time-varying empirical eigenfunctions of data given on the spatially time-dependent domain is proposed in Chapter 4 where the solutions of the PDE system are mapped to a fixed reference configuration in such a way that invariant properties of the data are preserved. Then, KL decomposition is applied on the mapped solutions to extract a small set of eigenfunctions that contains most of the energy of system on the fixed domain. These eigenfunctions are mapped back on the time-varying domain yielding a set of time-varying empirical eigenfunctions that can be used to find the reduced-order representation of the main PDE system.

Chapter 5 formulates the boundary control problem of moving boundary parabolic system to be suitable for the order-reduction technique introduced in Chapter 4 by the use of Galerkin's method. Then, the state reconstruction and optimal control problem for the boundary actuated linear parabolic

PDE is considered. The reduced-order model which is in the form of a linear time-varying system facilitated the Luenberger-type observer design and synthesis of a time-varying linear feedback controller based on a quadratic cost minimization. As an illustrative example, the Czochralski crystal growth process with the two-dimensional crystal temperature distribution is studied and the proposed controller formulation is applied. The numerical results of the simulated system demonstrate the output tracking of the system in the time-dependent crystal by the optimal feedback controller through boundary actuation.

6.2 Future work

This thesis developed PDE backstepping and order-reduction methodologies to address the control problem of moving boundary parabolic PDE systems. There remain many open questions regarding this subject and a number of them are briefly mentioned here.

The coupling of moving boundary PDEs with ODE systems or other transport phenomena is an open research area that can be addressed in future. For the CZ process, there are many other important process dynamics, e.g. heat transport in the melt, pulling dynamics and dislocation formation, that can be considered in a more realistic model investigated by backstepping method or order-reduction. This is of more interest in the backstepping approach since the knowledge of domain evolution is not required *a priori*.

Although PDE backstepping is mainly formulated for one-dimensional problems and this is due the high dimensionality of the kernel PDE, there are cases

of problems in two- or three-dimensional space for which backstepping method can be used. Another possibility is to extend these special cases to moving boundary problems.

Another promising area is the development of advanced control strategies such as Model Predictive Control (MPC) for parabolic PDEs with time-varying domain. This is of special interest because there are state and input constraints in many industrial applications.

References

Abdollahi, J., Izadi, M., Dubljevic, S., 2014. Temperature distribution reconstruction in Czochralski crystal growth process. AIChE Journal 60, 2839–2852.

Acquistapace, P., Terreni, B., 1987. A unified approach to abstract linear nonautonomous parabolic equations, in: Rendiconti del Seminario Matematico della Universita di Padova, pp. 47–107.

Antonio Susto, G., Krstic, M., 2010. Control of PDE-ODE cascades with Neumann interconnections. Journal of the Franklin Institute 347, 284–314.

Arkun, Y., Kayihan, F., 1998. A novel approach to full CD profile control of sheet-forming processes using adaptive PCA and reduced-order IMC design. Computers & Chemical Engineering 22, 945 – 962.

Armaou, A., Christofides, P.D., 2001a. Computation of empirical eigenfunctions and order reduction for nonlinear parabolic PDE systems with time-dependent spatial domains. Nonlinear Analysis: Theory, Methods and Applications 47, 2869–2874.

Armaou, A., Christofides, P.D., 2001b. Finite-dimensional control of nonlinear parabolic PDE systems with time-dependent spatial domains using empirical eigenfunctions. Applied Mathematics and Computer Science 11, 287–318.

Armaou, A., Christofides, P.D., 2001c. Robust control of parabolic PDE systems with time-dependent spatial domains. Automatica 37, 61–69.

Armaou, A., Christofides, P.D., 2002. Dynamic optimization of dissipative PDE systems using nonlinear order reduction. Chemical Engineering Science 57, 5083–5114.

Baconneau, O., Lunardi, A., 2004. Smooth solutions to a class of free boundary parabolic problems. Transactions of the American Mathematical Society 356, 987–1005.

Baker, J., Christofides, P.D., 2000. Finite-dimensional approximation and control of non-linear parabolic PDE systems. International Journal of Control 73, 439–456.

Balas, M.J., 1978. Active control of flexible systems. Journal of Optimization theory and Applications 25, 415–436.

Bangia, A.K., Batcho, P.F., Kevrekidis, I.G., Karniadakis, G.E., 1997. Unsteady two-dimensional flows in complex geometries: Comparative bifurcation studies with global eigenfunction expansions. SIAM Journal on Scientific Computing 18, 775.

Bekiaris-Liberis, N., Krstic, M., 2012. Compensation of time-varying input and state delays for nonlinear systems. Journal of Dynamic Systems, Measurement, and Control 134, 011009.

Bleris, L.G., Kothare, M.V., 2005. Reduced order distributed boundary control of thermal transients in microsystems. IEEE Transactions on Control Systems Technology 13, 853–867.

Burdzy, C., Chen, Z.Q., Sylvester, J., 2004. The heat equation in time dependent domains with insulated boundaries. Journal of mathematical analysis and applications 294, 581–595.

Chakravarti, S., Ray, W.H., 1999. Boundary identification and control of distributed parameter systems using singular functions. Chemical Engineering Science 54, 1181–1204.

Christofides, P.D., 2001. Nonlinear and robust control of PDE systems: Methods and applications to transport-reaction processes. Birkhäuser.

Curtain, R.F., 1985. On stabilizability of linear spectral systems via state boundary feedback. SIAM journal on control and optimization 23, 144–152.

Curtain, R.F., Zwart, H., 1995. An introduction to infinite-dimensional linear systems theory. Springer-Verlag.

Deen, W.M., 1998. Analysis of transport phenomena. Oxford University Press, New York.

Demetriou, M.A., 2004. Natural second-order observers for second-order distributed parameter systems. Systems & control letters 51, 225–234.

Derby, J., Atherton, L., Thomas, P., Brown, R., 1987. Finite-element methods for analysis of the dynamics and control of Czochralski crystal growth. Journal of Scientific Computing 2, 297–343.

El Jai, A., Amouroux, M., 1988. Sensors and observers in distributed parameter systems. International Journal of Control 47, 333–347.

Fattorini, H.O., 1968. Boundary control systems. SIAM Journal on Control 6, 349–385.

Fogleman, M., Lumley, J., Rempfer, D., Haworth, D., 2004. Application of the proper orthogonal decomposition to datasets of internal combustion engine flows. Journal of Turbulence 5, 023.

Gay, D.H., Ray, W.H., 1995. Identification and control of distributed parameter systems by means of the singular value decomposition. Chemical Engineering Science 50, 1519–1539.

Gevelber, M.A., 1994a. Dynamics and control of the Czochralski process III. Interface dynamics and control requirements. Journal of crystal growth 139, 271–285.

Gevelber, M.A., 1994b. Dynamics and control of the czochralski process IV. Control structure design for interface shape control and performance evaluation. Journal of crystal growth 139, 286–301.

Gevelber, M.A., Stephanopoulos, G., 1987. Dynamics and control of the Czochralski process: I. Modelling and dynamic characterization. Journal of crystal growth 84, 647–668.

Gevelber, M.A., Stephanopoulos, G., Wargo, M.J., 1988. Dynamics and control of the czochralski process II. Objectives and control structure design. Journal of crystal growth 91, 199–217.

Glavaski, S., Marsden, J.E., Murray, R.M., 1998. Model reduction, centering, and the Karhunen-Loève expansion, in: Proceedings of the 37th IEEE Conference on Decision and Control, pp. 2071–2076.

Gressang, R.v., Lamont, G., 1975. Observers for systems characterized by semigroups. IEEE Transactions on Automatic Control 20, 523–528.

Izadi, M., Dubljevic, S., 2013. Order-reduction of parabolic PDEs with time-varying domain using empirical eigenfunctions. AIChE Journal 59, 4142–4150.

Jadachowski, L., Meurer, T., Kugi, A., 2012. An efficient implementation of backstepping observers for time-varying parabolic PDEs, in: The Proceedings of 7th International Conference on Mathematical Modelling, pp. 798–803.

Jadachowski, L., Meurer, T., Kugi, A., 2013. State estimation for parabolic pdes with reactive-convective non-linearities, in: The Proceedings of 12th European Control Conference (ECC), pp. 1603–1608.

Jordan, A.S., Von Neida, A., Caruso, R., 1984. The theory and practice of dislocation reduction in GaAs and InP. Journal of Crystal Growth 70, 555–573.

Katō, T., 1995. Perturbation theory for linear operators. Springer-Verlag.

Kitamura, S., Sakairi, S., Nishimura, M., 1972. Observer for distributed-parameter diffusion systems. Electrical engineering in Japan 92, 142–149.

Kloeden, P., Marín-Rubio, P., Real, J., 2008. Pullback attractors for a semi-linear heat equation in a non-cylindrical domain. Journal of Differential Equations 244, 2062–2090.

Kloeden, P.E., Real, J., Sun, C., 2009. Pullback attractors for a semilinear heat equation on time-varying domains. Journal of Differential Equations 246, 4702–4730.

Kobayashi, T., Hitotsuya, S., 1981. Observers and parameter determination for distributed parameter systems. International Journal of Control 33, 31–50.

Krstic, M., 2009a. Compensating a string PDE in the actuation or sensing path of an unstable ODE. IEEE Transactions on Automatic Control 54, 1362–1368.

Krstic, M., 2009b. Compensating actuator and sensor dynamics governed by diffusion PDEs. Systems & Control Letters 58, 372–377.

Krstic, M., 2010. Lyapunov stability of linear predictor feedback for time-varying input delay. IEEE Transactions on Automatic Control 55, 554–559.

Krstic, M., Guo, B.Z., Balogh, A., Smyshlyaev, A., 2008. Output-feedback stabilization of an unstable wave equation. Automatica 44, 63–74.

Krstic, M., Smyshlyaev, A., 2008. Boundary control of PDEs: A course on backstepping designs. SIAM, Philadelphia.

Lasiecka, I., 1980. Unified theory for abstract parabolic boundary problems–A semigroup approach. Applied Mathematics and Optimization 6, 287–333.

Lewis, F.L., Vrabie, D., Syrmos, V.L., 2012. Optimal control. Wiley (New York).

Liu, W., 2003. Boundary feedback stabilization of an unstable heat equation. SIAM journal on control and optimization 42, 1033–1043.

Liu, Y., Lapdus, L., 1976. Observer theory for distributed-parameter systems. International Journal of Systems Science 7, 731–742.

Loève, M., 1955. Probability Theory. Van Nostrand.

Lunardi, A., 2004. An introduction to parabolic moving boundary problems, in: Iannelli, M., Nagel, R., Piazzera, S. (Eds.), Functional analytic methods for evolution equations. Springer. volume 1855, pp. 371–399.

Luo, Z.H., Guo, B.Z., Morgül, Ö., 1999. Stability and stabilization of infinite-dimensional systems with applications. Springer.

Mangold, M., Sheng, M., 2004. Nonlinear model reduction of a two-dimensional MCFC model with internal reforming. Fuel Cells 4, 68–77.

McPhee, J., Yeh, W., 2008. Groundwater management using model reduction via empirical orthogonal functions. Journal of Water Resources Planning and Management 134, 161–170.

Meurer, T., 2013. On the extended Luenberger-type observer for semilinear distributed-parameter systems. IEEE Transactions on Automatic Control 58, 1732–1743.

Meurer, T., Kugi, A., 2009. Tracking control for boundary controlled parabolic PDEs with varying parameters: Combining backstepping and differential flatness. Automatica 45, 1182–1194.

Nambu, T., 1984. On the stabilization of diffusion equations: boundary observation and feedback. Journal of differential equations 52, 204–233.

Ng, J., Aksikas, I., Dubljevic, S., 2013. Control of parabolic pdes with time-varying spatial domain: Czochralski crystal growth process. International Journal of Control , 1–12.

Ng, J., Dubljevic, S., 2011. Optimal control of convection-diffusion process with time-varying spatial domain: Czochralski crystal growth. Journal of Process Control 21, 1361–1369.

Ng, J., Dubljevic, S., 2012. Optimal boundary control of a diffusion-convection-reaction PDE model with time-dependent spatial domain: Czochralski crystal growth process. Chemical Engineering Science 67, 111–119.

Nguyen, T.D., 2008. Second-order observers for second-order distributed parameter systems in R^2. Systems & Control Letters 57, 787–795.

Nie, Q., Joshi, Y., 2008. Multiscale thermal modeling methodology for thermoelectrically cooled electronic cabinets. Numerical Heat Transfer, Part A: Applications 53, 225–248.

Orner, P.A., Foster, A.M., 1971. A design procedure for a class of distributed parameter control systems. Journal of Dynamic Systems, Measurement, and Control 93, 86–92.

Park, H.M., Cho, D.H., 1996. The use of the Karhunen-Loève decomposition for the modeling of distributed parameter systems. Chemical Engineering Science 51, 81–98.

Park, H.M., Jung, W.S., 2001. The Karhunen-Loève-Galerkin method for the inverse natural convection problems. International Journal of Heat and Mass Transfer 44, 155–167.

Park, H.M., Lee, J.H., 1998. A method of solving inverse convection problems by means of mode reduction. Chemical engineering science 53, 1731–1744.

Park, H.M., Lee, M.W., 2000. Boundary control of the Navier-Stokes equation by empirical reduction of modes. Computer methods in applied mechanics and engineering 188, 165–186.

Park, H.M., Lim, J.Y., 2009. A reduced-order model of the low-voltage cascade electroosmotic micropump. Microfluidics and Nanofluidics 6, 509–520.

Pazy, A., 1983. Semigroups of linear operators and applications to partial differential equations. Springer-Verlag.

Raimondeau, S., Vlachos, D., 2000. Low-dimensional approximations of multiscale epitaxial growth models for microstructure control of materials. Journal of Computational Physics 160, 564–576.

Ray, W.H., 1981. Advanced process control. McGraw-Hill New York.

Ray, W.H., Seinfeld, J.H., 1975. Filtering in distributed parameter systems with moving boundaries. Automatica 11, 509–515.

Reddy, J.N., Gartling, D.K., 2010. The finite element method in heat transfer and fluid dynamics. CRC.

Sackinger, P., Brown, R., Derby, J., 1989. A finite element method for analysis of fluid flow, heat transfer and free interfaces in Czochralski crystal growth. International journal for numerical methods in fluids 9, 453–492.

Sakawa, Y., Matsushita, T., 1975. Feedback stabilization of a class of distributed systems and construction of a state estimator. IEEE Transactions on Automatic Control 20, 748–753.

Shvartsman, S.Y., Kevrekidis, I.G., 1998. Nonlinear model reduction for control of distributed systems: A computer-assisted study. AIChE Journal 44, 1579–1595.

Sirovich, L., 1987. Turbulence and the dynamics of coherent structures. I-Coherent structures. II-Symmetries and transformations. III-Dynamics and scaling. Quarterly of applied mathematics 45, 561–571.

Sirovich, L., Park, H., 1990. Turbulent thermal convection in a finite domain: Part I. Theory. Physics of Fluids A: Fluid Dynamics 2, 1649–1658.

Smyshlyaev, A., Krstic, M., 2004. Closed-form boundary state feedbacks for a class of 1-D partial integro-differential equations. IEEE Transactions on Automatic Control 49, 2185–2202.

Smyshlyaev, A., Krstic, M., 2005. On control design for PDEs with space-dependent diffusivity or time-dependent reactivity. Automatica 41, 1601–1608.

Tang, S., Xie, C., 2011. State and output-feedback boundary control for a coupled PDE-ODE system. Systems & Control Letters 60, 540–545.

Theodoropoulou, A., Zafiriou, E., Adomaitis, R.A., 1999. Inverse model-based real-time control for temperature uniformity of RTCVD. IEEE Transactions on Semiconductor Manufacturing 12, 87–101.

Wang, P.K.C., 1990. Stabilization and control of distributed systems with time-dependent spatial domains. Journal of Optimization Theory and Applications 65, 331–362.

Wang, P.K.C., 1995. Feedback control of a heat diffusion system with time-dependent spatial domain. Optimal control applications & methods 16, 305–320.

Zheng, D., Hoo, K.A., 2002. Low-order model identification for implementable control solutions of distributed parameter systems. Computers & chemical engineering 26, 1049–1076.